Satellite Application Facility on Climae Monitoring

Visiting Scientist Report

Andreas Will and Michael Woldt

BTU Cottbus, Environmental Meteorology

Comparison of COSMO-CLM results with CM-SAF products: Radiation components ToA, at the Surface and Cloud Properties

IOP VS Study No 16

Corresponding Author: Andreas Will, Umweltmeteorologie, BTU Cottbus
Address: Brandenburgische Technische Universität Cottbus
Burger Chaussee 2, Haus 4/3, Campus Nord, EG, Raum 1.21
D-03044 Cottbus
Tel.: +49-355-69-1171
Fax: +49-355-69-1128
e-mail: will@tu-cottbus.de

Contents

1 Introduction

The main idea of the study was to compare the quality proved CM-SAF products derived from Satellite measurements with simulation results of the regional climate model COSMO-CLM. At the beginning of the study the relevant variables of the CMSAF data set have been available for the years 2005 to 2006 at top of the atmosphere and for the year 2006 at the surface. The simulation period was chosen to be 2001-2007. This ensures a spin up time 2001-2004 long enough (here 4 to 5 years) to ensure for independence of the evaluation-period 2005-2006 on the initial conditions.

It was decided to use the new unified model version cosmo_4.2_clm_1, which is not an evaluated model version instead of the evaluated clm_3 model version for three reasons. First, it is a first study and all following studies in this direction are expected to be of relevance for the unified COSMO-CLM model versions. Second, this opens the opportunity to compare the results directly with the results of numerical weather prediction. Third, additional work was necessary to make the output variables available. A substantial part of this work has already been done for the COSMO-CLM (CCLM) model version.

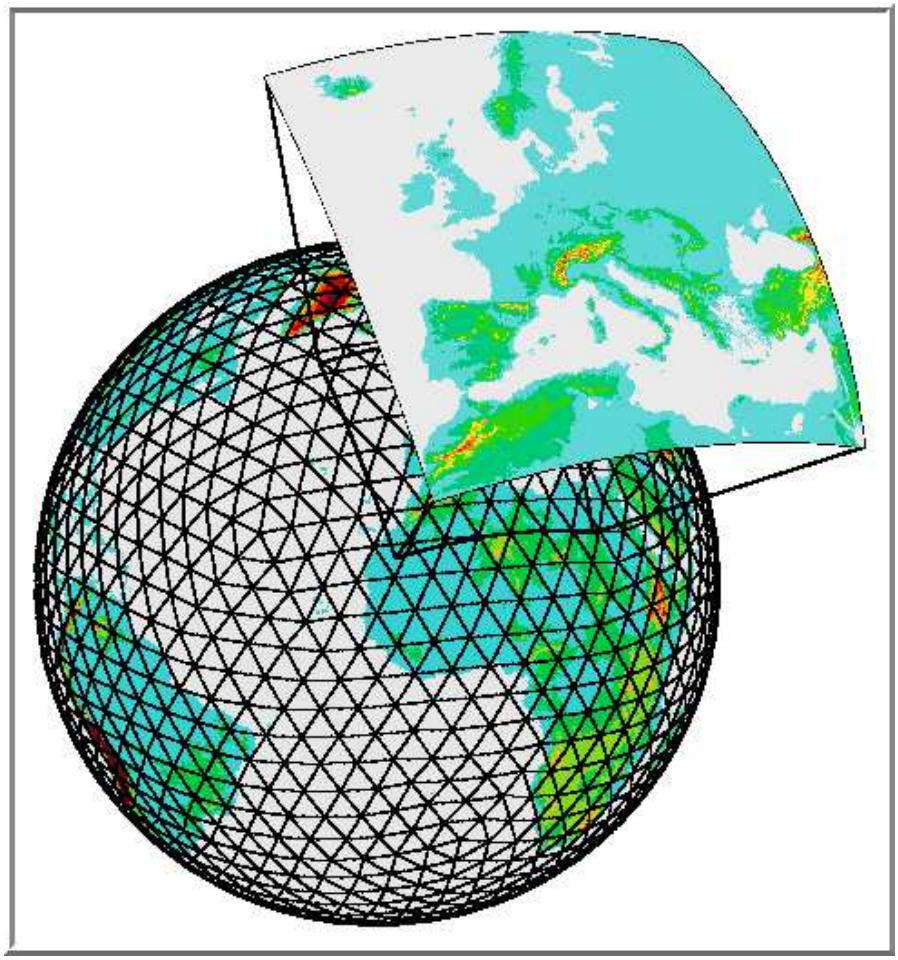

Figure 1 Concept of limited area simulations: The limited area model COSMO-CLM simulates the dynamics within the highlighted area on the globe. The dynamics on the globe is simulated by the GME model using the observations for correction of the weather state. The 6 hour forecast (analysis) of GME is used as initial and boundary conditions of the COSMO-CLM.

Therefore it can not be expected to obtain results, which may be called optimal, because the climatological behaviour of the new model version was unknown. In this sense, it is a preliminary study. On the other hand the systematic comparison of all radiation components opens the opportunity to provide a new quality of evaluation results: to identify reasons for possible deficiencies of the model, the model configuration and/or the satellite data products. This, however is possible only for differences higher than the internal model variability and the data accuracy.

The internal variability is estimated by comparison of the results of two model simulations, which differ in their initial conditions. The accuracy of the CMSAF products is estimated from different types of verifications using ground based observations and consistency tests. The accuracies of all variables investigated are specified in the [*Satellite Application Facility on Climate Monitoring*(2008)].

The following subsections provide a description of the CCLM configuration GME008 and GME010 (section 2), of the CMSAF data used and selected results of the comparison between CMSAF products and CCLM simulation results. The time period is 2005-2006 for top of the atmosphere (TOA) results and 2006 for near surface variables. Details of the comparison are described in section 4. The results are illustrated by different types of presentation as described in section 4.3. The discussion is restricted to the sub-region water (WAS), land (LND), south-west Europe (SWE) and Scandinavia (SCA) of table 8 and figure 3). In some few cases other regions have been selected to illustrate the quantitative results. All comparisons are performed on the grid of the regional model. Due to the fact, that the CMSAF-results have a coarser grid definition and a different rotation of the grid spurious differences originating in the interpolation are visible in some of the surface difference plots, if the differences have the magnitude of the interpolation errors.

2 Specification of the COSMO-CLM simulations

In the following the COSMO-CLM configuration and the data used are described. The model physics and dynamics is described in [*Will et al.*(2008), *Helmert et al.*(2008)]. An extended model documentation is available. The most important parts are [*Doms and Schättler*(2002), *Doms et al.*(2005), *Schättler*(2008)] and [*Schättler et al.*(2008)].
The model input is described in section 2.1 consisting of the fields describing the physical properties of the earths surface, the fields necessary to initialise the simulation and the fields used as boundary conditions at the lateral, the lower and upper boundaries of the model domain. In section 2.2 the definition of the model grid is given followed by the choice of the other steering parameters (namelist parameters) affecting the model dynamics and model physics. Finally, the initialisation of the runs is described.

2.1 COSMO-CLM input fields

The standard interpolation program INT2LM version *int2lm_1.7.2* is used to generate the initial and boundary fields of the COCMO-CLM grid from the original grid of the GME analysed data. The *int2lm_1.7.2* program is a unified version of the *int2lm* of the German Weather Service (see [*Schättler et al.*(2008)] for details) and the *int2clm* containing the extensions introduced by the CLM-Community for climate simulations into a previous *int2lm* model version..

DWD external fields	**GME sim. results**		
2D Initial & Boundary	**3D Initial & Boundary**	**2D Initial & Boundary**	**2D Initial 2D Initial**
FRLAND	T	SST	T_S
HSURF	U,V	T_SNOW	
Z0	P	W_SNOW	
LAI	QV		
PLCOV	QC		
ROOTDP			
STYPE			
T_CL			

Table 1 Data used for CLM simulations. Land surface and soil data from DWD data set: land fraction (FRLAND), surface height above sea level (HSURF), surface roughness length (Z0), leaf area index (LAI), plant cover (PLCOV), root depth (ROOTDP), soil type (STYPE) and the temperature of the deepest soil layer (T_CL). **GME fields:** used as initial and/or boundary conditions: temperature (T), horizontal wind (U,V), pressure (P), specific humidity (QV), liquid water content (QC), land surface temperature (T_S), sea surface temperature (SST), snow water content (W_SNOW), snow surface temperature (T_SNOW).

2.1.1 Constant input fields

The constant input (external) fields, characterising the properties of earth's surface and of the deep soil, are taken from the DWD global data set. The fields are listed in Table 1.

One specific modification of the external fields has been performed. The root depth has been stretched in order to obtain the same mean root depth as in the ECOCLIMAP data set in order to avoid the drying of the upper soil layers due to strong transpiration.

2.1.2 The GME initial and boundary conditions

The operational initialised GME analysis of the DWD (IA-GME) has been used for calculation of the initial and boundary conditions (forcing data). The IA-GME are the initialised A-GME data. The A-GME data result from an optimal interpolation of the 6h (3h) forecast with the global circulation model GME. The IA-GME data are taken in GRIB format from the DWD database.

Name	Period/Date	Resolution
GME60	1.2001-11.2004	$60 \times 60\, km^2$ and 40 levels
	31.03.2004	GME: Introduction of a sea-ice model
	17.12.2003	GME-Ass: Pseudo-TEMPs from EZMW-fields introduced
	02.12.2003	GME-Ass: MODIS-Data introduced
	16.09.2003	GME: Prognostic cloud-ice
	09.09.2003	Ana: Modification of snow-height and SST analysis
	10.03.2003	GME-Ass: Quality control of SATEM-Data
		GME: calculation of maximal wind gust velocity for convective instable weather conditions
.	12.12.2002	Ana: PAOB-Data introduced
	18.09.2002	GME: time step reduced by 25%
	12.08.2002	Ana: SST analysis corrected
	26.11.2001	GME: Time increment for TMIN_2M, TMAX_2M, VMAX_10M changed.
	17.10.2001 12 UTC	Parametrisation of turbulent fluxes over sea
	29.08.2001 12 UTC	Ana: New swell model (MSM)
	12.06.2001 12 UTC	GME: Initialisation (IDFI) modified
	31.01.2001	Reduction of the Gravity wave drag (GWD)

Table 2 GME forcing: Time period and spatial resolution of the initialised GME analysis used as initial and boundary conditions of the COSMO-CLM simulations in 1.2001-11.2004 and the relevant GME modifications.

Table 1 gives an overview of the GME fields used as boundary and/or as initial conditions of the adequate CCLM variables. Forcing fields specified as "Initial" are needed at all grid points of the CCLM domain at initial time. The dynamical fields of the COSMO-CLM are updated every 6h (time

increment) at the lateral, upper and lower (SST's only) boundaries of the CCLM domain using the fields specified as "Boundary".

Name	Period/Date	Resolution
GME40	9.2004-12.2007	$40 \times 40 km^2$ and 40 levels
	21.12.2007 18 UTC	New external parameters
	09.05.2007	New version of operational OI
	17.01.2007	Change of interface for observations in the data assimilation for GME, LME, LMK
	10.01.2007	New Weather-Interpretation and precip. in case of fog
	29.11.2006	Modification of snow analysis for GME, LME and LMK
	16.10.2006	GME: New Version 2.11
	11.10.2006	GME-Ass: Improvement of data search in the global data assimilation
	09.08.2006	OI: Various Modifications
	27.06.2006	OI: Various Modifications
	21.06.2006	OI: Change of ASCII-Meteogramm-output for GME and LME
	12.06.2006	OI: Various Modifications
	31.05.2006	GME-Ass: Change of the global humidity analysis (PDF)
	24.05.2006	GME-Ass: Use of "Atmospheric Motion Vector (AMV)" of Meteosat 8.
	20.04.2006	GME: Introduction of 48h forecast of GME and LME based on 06 UTC analysis
	04.01.2006	GME: New Version 2.9 with technical and the subsequent changes
	04.01.2006	GME-Ass: Introduction of 1D-Var-Analysis of the radiation flux densities of the polar Satellites.
	07.12.2005	GME: operational use of GME_2.7
	24.08.2005	GME: operational use of GME_2.6
	26.07.2005	GME: operational use of GME_2.3
	26.04.2005	GME: operational use of GME_2.2
	17.02.2005	GME: use of the "Atmospheric Motion Vector Winds (AMV's)" in BUFR-Format
	07.12.2004	OI: Exclusion of humidity inform. of Pseudo-Temps in the level.
	27.09.2004	GME: New config. (GME40) with $40 \times 40\, km^2$ and 40 levels.

Table 3 GME forcing: Time period and spatial resolution of the initialised GME analysis used as initial and boundary conditions of the COSMO-CLM simulations in 12.2004-12.2007 and the relevant GME modifications.

Table 2 and 3 give an overview of the model changes relevant for the calculation of the IA-GME forcing data during the time period 2001-2007 used. The tables illustrate, to what extent the IA-

GME data are not reanalysis-data, usually used for evaluation of regional climate models. Therefore unphysical gradients in the forcing data may occur and reduce the quality of the regional climate simulations. No efforts have been done to quantify these effects.

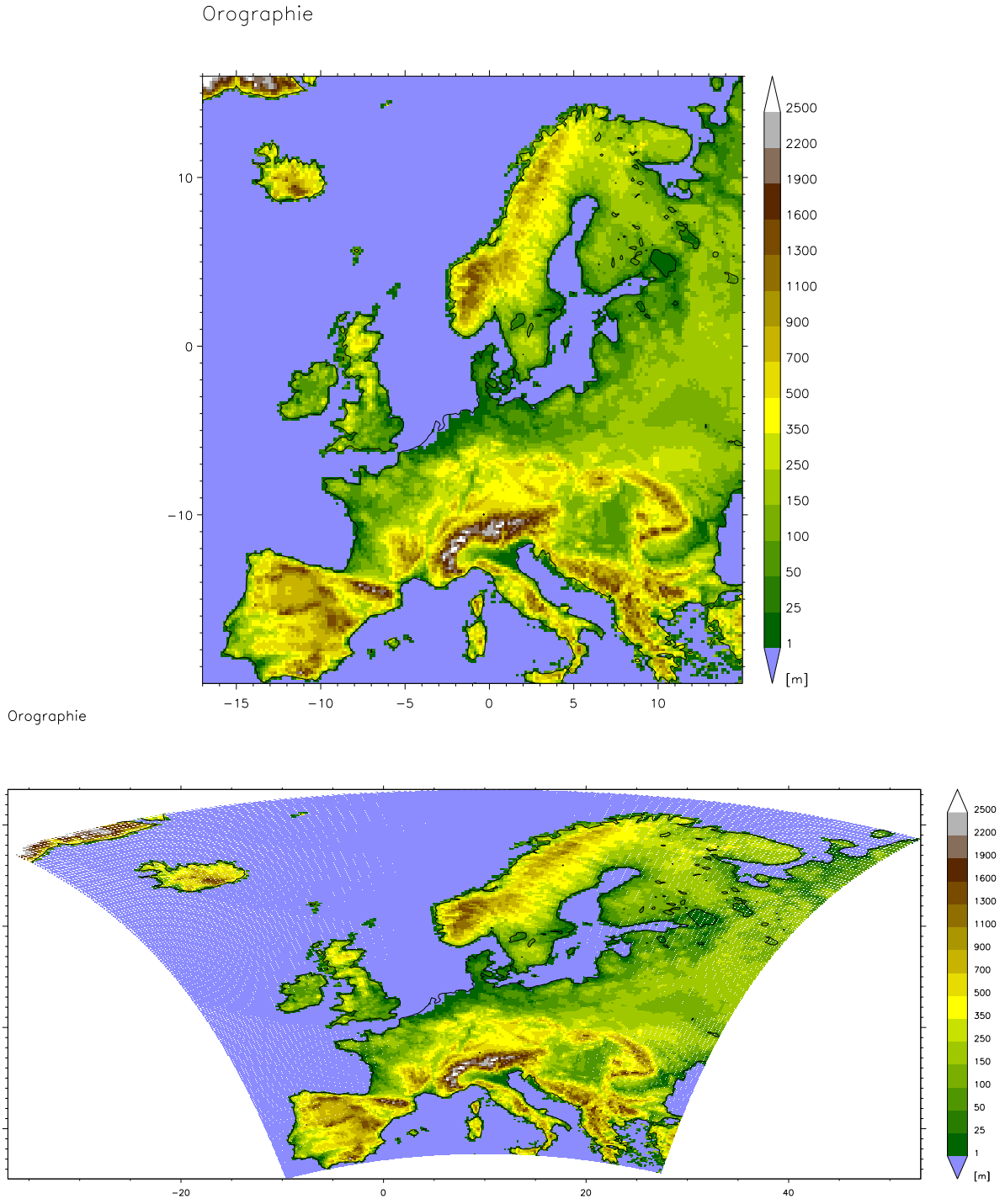

Figure 2 The orography of the experiments in the model domain in rotated model coordinates (up) and in geographical coordinates (bottom).

2.2 COSMO-CLM Configuration

The model domain used for the study was the standard evaluation domain of the COSMO-CLM, which has roughly 3500 km $\times$ 4000 km covered by 193×217 grid points resulting in a model grid resolution of approximately 18 km, which is a higher resolution than the CM-SAF data resolution. The simulation time was 2001 to 2007.

In the following the configuration GME008 of the *cosmo_4.2clm_1* model version used for the experiments is described in four paragraphs. The GME010 configuration is different in the initial conditions of the atmosphere. Instead of using the state of the cosmo-clm at 1.1.2004, the state of the GME at 1.1.2004 was used.

2.2.1 Model grid

The horizontal model domain of the experiments was decided to be the same as in the CLM evaluation simulation over Europe. It covers western and central Europe nearly entirely, including Spain, the Mediterranean European countries, the Baltic Sea, Great Britain and Scandinavia.

Horizontal Model Grid:	rlon	rlat
Rotated North-Pole's location	longitude: -170	latitude: 32.5
Extension	-17.0040 to 14.9960	- 19.996 to 18.0040
Resolution	0.16667	0.16667
Number of Grid-points	193	217

Table 4 Horizontal Model Grid: The coordinates of the COSMO-CLM are the rotated longitude (**rlon**) and latitude (**rlat**) in horizontal directions and the absolute vertical height (above the ground for the atmosphere and below the ground for the soil). The North Pole of the rotated grid is given in geographical coordinates.

The definition of the model grid is done by setting model parameters of the `LMGRID` namelist (`www.clm-community.eu` → Model System → CLM → Configuration of CLM-namelist). The model grid orography is given in Figure 2. The details of the model grid are summarised in Table 4.[1]

The CLM uses terrain-following, rotated spherical height coordinates (see [*Doms and Schättler*(2002)]). Their horizontal course is indicated by the red lines in Figure 2. One of the advantages of the grid rotation is a horizontal grid stretching close to unity. For this reason the location of the rotated North Pole is chosen in such a way that the distances between the grid cells and the equator of the rotated grid are minimised.

[1] Here the orography of the extended Europe model domain is given.

Vertical Grid :	**Atmosphere**, kmax=33			**Soil**
k	VCOORD(k)	Z(k)	P_0(k)	z
1	0.0200	23588.5	20.0000	0.01
2	0.0400	20780.5	40.0000	0.04
3	0.0604	18834.3	60.3600	0.10
4	0.0814	17289.8	81.3900	0.22
5	0.1033	15978.3	103.3200	0.46
6	0.1264	14817.2	126.3600	0.94
7	0.1506	13763.2	150.6300	1.90
8	0.1762	12789.1	176.2400	3.82
9	0.2032	11878.9	203.2300	7.66
10	0.2316	11021.9	231.6100	15.34
11	0.2614	10211.2	261.3500	
12	0.2924	9441.8	292.4000	
13	0.3246	8711.0	324.6400	
14	0.3580	8016.0	357.9700	
15	0.3922	7355.4	392.2300	
16	0.4272	6728.0	427.2500	
17	0.4629	6132.5	462.8600	
18	0.4988	5568.6	498.8400	
19	0.5350	5035.6	534.9700	
20	0.5710	4532.7	571.0500	
21	0.6068	4059.6	606.8400	
22	0.6421	3615.8	642.1100	
23	0.6766	3200.9	676.6300	
24	0.7102	2814.7	710.1700	
25	0.7425	2456.4	742.5300	
26	0.7735	2125.8	773.4900	
27	0.8029	1822.5	802.8500	
28	0.8304	1545.8	830.4500	
29	0.8561	1295.3	856.1300	
30	0.8798	1070.4	879.7600	
31	0.9012	870.5	901.2300	
32	0.9205	694.7	920.4800	
33	0.9374	542.3	937.4400	
34	0.9521	412.2	952.1400	
35	0.9646	303.3	964.5900	
36	0.9749	214.3	974.8700	
37	0.9831	143.4	983.1200	
38	0.9895	89.0	989.5000	
39	0.9942	48.7	994.2400	
40	0.9976	20.0	997.6300	
41	1.0000	0.0	1000.0000	

Table 5 Vertical Grid: The vertical grid over sea is given here for different units: k is the index, VCOORD(k) is the height in non-dimensional pressure units, Z(k) is the height in meters and P0(k) is the height in hPa. The vertical height of the levels is calculated assuming the dry-adiabatic stratification of the standard atmosphere. The height of the levels is given in [Pa/Pa], which is the factor P_f in $P(z) = P_f(z) \times P_0$ with P_0 the standard pressure at sea level, and in [m], which is the corresponding absolute height. See documentation of the model for details of the terrain following grid.

The model grid ($\Delta\lambda = \Delta\phi = 1/6°$) is chosen the same as in the CLM evaluation runs (CLM_3-E), which has 193 $\times$ 217 horizontal grid points. The down-scaling factor of the simulation, which can be calculated as the quotient of the mean grid sizes is $40km/18km \simeq 2.2$ The vertical resolution of the simulations is 40 layers, which is nearly the same as in GME. The differences occur only near surface due to different horizontal resolutions.

2.2.2 Configuration (namelist) parameters

The CCLM has more than 150 external (namelist) parameters affecting the model physics, dynamics, input and output. Overall tested configurations are given on the CLM-home-page (www.clm-community.e → Model System → CLM → Configuration of CLM-namelist). These are the evaluation configurations CLM_3-E and CLM_3-K. These configurations are based on the LME configuration, which is similar to the COSMO-EU configuration of the actual DWD operational configuration for Europe. At the time of the GME008 and GME010 simulation there was no overall tested configuration for the climate mode of the new model version cosmo-clm (cosmo_4.2_clm_1). Furthermore, it was also not possible to use the standard configuration COSMO-EU of the DWD for different technical reasons. Therefore a number of modifications of the namelist became necessary. The tests with an evaluated configuration remains for future work.

The set of roughly 150 parameters is arranged in the following 12 `NAMELIST` groups:

`LMGRID`	specifying the domain and the size of the grid
`RUNCTL`	parameters for the model run
`TUNING`	tuning parameters of the model equations
`DYNCTL`	parameters for the adiabatic model
`PHYCTL`	parameters for the diabatic model
`DIACTL`	parameters for the diagnostic calculations
`NUDGING`	controlling the data assimilation
`INICTL`	parameters for the initialisation of model variables
`IOCTL`	controlling the environment
`DATABASE`	specification of database job
`GRIBIN`	controlling the model input
`GRIBOUT`	controlling the model output

The `LMGRID` parameters define the model grid and have been discussed in the previous paragraph. The `DATABASE` and the `NUDGING` namelist groups are needed for operational weather prediction

only. The parameters contained in the remaining 9 namelist groups can not be discussed in detail here. The meaning of the single settings is explained shortly in the online documentation mentioned above and in more detail in the model external documentation (see [*Schättler et al.*(2008)], and the other parts of the documentation).

The settings in the GME010 configuration affecting the results in comparison with the COSMO-EU (1.1.2009) configuration are a different version of the preprocessor for interpolation of the input and boundary conditions and the following settings of the namelist parameters:

Parameter	Value
dlon	0.1667
dlat	0.1667
dt	120
ldiabf_lh	.TRUE.
l2tls	.TRUE.
lsl_adv_qx	.FALSE.
lhdiff_mask	.TRUE.
ldyn_bbc	.TRUE.
rlwidth	208000
nrdtau	5
hd_corr_u	0.75
lforest	.FALSE.
ke_soil	9
czbot_w_so	4.0
itype_wcld	1
ico2_rad	2
icldm_turb	1
yncglob_source	cosmo_4.2_clm_1
lbdclim	.TRUE.
lana_qi	.FALSE.
llb_qi	.FALSE.
lana_qr_qs	.FALSE.
lana_rho_snow	.FALSE.
hincbound	6.0

Table 6 Configuration of GME010 simulation: Values of the namelist parameters different from COSMO-EU (1.1.2009) and of dynamical relevance. The complete namelist COSMO-EU is available from the COSMO and from the CLM-Community home-page www.clm-community.eu.

2.2.3 Initialisation of the simulations

The simulation GME008 started at 1 January 2001 00:00 UTC. The model results are made available from 1 January 2005 00:00 UTC. The first 4 years of the simulation are the spin-up phase.

Climatological initial condition has been used for the soil. The CCLM soil model TERRA_ML ([*Helmert et al.*(2008), *Heise*(2002)]) is a deep soil model with a lower boundary condition of constant temperature (see Table 4 for the soils configuration). The GME uses the same deep soil model. However, the distribution of the soil model layers in the model domain is different in the evaluated CLM runs and the equilibrium state in the CCLM-simulation is different from the GME-simulation. Therefore, an initialisation of the CCLM soil using the GME profile was not useful. The soil temperature has been initialised as solution of the heat conduction equation between the land surface temperature at initial time and the prescribed temperature of the deepest soil layer (T_{CL}). The latter has been calculated as the 1961-1990 mean of the 2 m temperature of the ERA40 2 m temperature. The lower boundary condition T_{CL} was kept constant over the whole simulation period, which is a reasonable assumption, as shown by [*Smerdon and Stieglitz*(2006)]. The soil water content was initialised as 75% of the soil layers pore volume, which of course depends on the soil type.
In order to avoid an influence of this unphysical initial conditions on model results, a 4 year long spin-up phase between 2001 and 2004 was introduced for the development of the vertical soil temperature and soil water content profile at each grid point consistent with the model physics and dynamics.

The second simulation GME010 was initialised on 1.1.2004 using the GME008 results for this date.

2.3 Execution of experiments with IMDI

The GME0xx dynamical down-scaling experiments with CCLM described here have been conducted by A.Will, BTU Cottbus. They have been running within the modelling environment IMDI [*Legutke et al.*(2007)] on NEC SX-6 machines at German Climate Computing Centre (DKRZ). This standard compile and running environment is a toolkit that can be used to compile (Standard Compile Environment 'SCE') and execute (Standard Run Environment 'SRE') Earth System models. It also includes data aspects (postprocessing, archiving, WDCC data base filling facilities) (`www.mad.zmaw.de/imdi/`).

It was initially developed by M&D in the European FP5 PRISM project (Project for Integrated Earth System Modelling). Developments since the end of PRISM concentrate on data management aspects. Emphasis is on efficient use of resources, in this case of the DKRZ and HLRS infrastructures.

The modelling environment toolkit and the model source code, as well as some input data, can be downloaded from the SVN repository of M&D, provided one has the right access authorisation and authentification is recognised. In practice, this means that a person interested in downloading the model and tools should contact M&D (model@dkrz.de) to obtain an SVN user account and required access rights. Due to the license conditions for COSMO-CLM, access can only be provided to persons authorised to use COSMO-CLM as laid down in the 'CLM Community Agreement' (`www.clm-community.eu`).

3 CMSAF data

The CM-SAF-datasets for the top of the atmosphere (SAF120) and the surface (SAF150 and SAF210) were obtained from the CM-SAF web ordering interface. The vertical humidity datasets (SAFH30) were provided for this comparison by CM-SAF.
The datasets in the BTU-database have six character names. For the CM-SAF-datasets the following names have been chosen: SAF120 for version 120 of the top of the atmosphere data, SAF150 for version 150 of the surface and cloud data, SAF210 for version 210 of the surface and cloud data and SAFH30 for version 300 of the atmospheric humidity.
The data are processed from different sources as given in table 7. The CM-SAF products used in this study are derived from the following satellites and instruments:

- Geostationary Meteosat Second Generation (MSG1 and MSG2) Satellite (Meteosat-8 onwards) with the instruments
  - SEVIRI, the Spinning Enhanced Visible and Infrared Image and
  - GERB, the Geostationary Earth Radiation Budget Experiment radiometer

  .
- polar orbiting NOAA (15 onwards) Satellite with the instruments
  - AVHRR, the Advanced Very High Resolution Radiometer,
  - ATOVS, the Advanced TIROS Operational Vertical Sounder instrument suite consisting of HIRS/3, MHS, AMSU-A and AMSU-B.
- polar orbiting satellite AQUA with the instruments
  - CERES, the Clouds and the Earths Radiant Energy System radiometer
- polar orbiting satellite TERRA with the instruments
  - CERES, the Clouds and the Earths Radiant Energy System radiometer

The original datasets are in HDF5-format. To use them with our evaluation tools, the data had to be converted into our internal data format (BTU-format). It has been done in the following way. First, by extracting them as ASCII-data from the HDF5-files and second, by converting them into BTU-format. To avoid problems with some visualisation tools only data north of the equator were transfered to the BTU-archive.
The CM-SAF datasets have different resolutions and grids. For the evaluation tools three new grids had to be defined (SAF150 and SAF210 use the same grid) and conversion datasets to the CCLM-grid had to be calculated.
Our evaluation tools need for each grid the dependence of the fields longitude, latitude and height on geographical coordinates and a land/sea-mask. They were partly available from the CM-SAF web user interface, the missing datasets were provided for this comparison by the CM-SAF unit.

One problem occured with the longitude data in the northern parts of the CM-SAF-domain. Since SAF120, SAF150 and SAF210 are provided on a regular grid in a sinusoidal projection,which has fixed spatial distances (and not fixed longitude/latitude distances), in high northern regions redundant informations for overlapping regions are contained in the data. This caused problems with grid transformation and evaluation tools in use. 'Missing data' for the grid-points in the overlaping areas have been introduced and the longitudinal coordinates in these areas have been redefined in such a way that they donÂ´t overlap anymore.

CM-SAF data set and source	Resolution	Parameter (P)	Physical descr.	Accuracy of P Bias (ΔP)
SAF150/ SAF210 polar orbiting / MSG1	$(15\,km)^2$	SIS	Surf.incoming solar	10 [W/m^2] >10 [W/m^2] (ALP)
		SRS	Surf.refl.solar	18* [W/m^2]
		SNS	Surf.net solar	15 [W/m^2]
		SDL	Surf.down longw.	10 [W/m^2] >10 [W/m^2] (ALP)
		SOL	Surf.outg.longw.	10 [W/m^2] >10 [W/m^2](ALP)
		SNL	Surf. net longw.	15 [W/m^2]
		SRB	Surf. rad. budget	20 [W/m^2]
		CFC	Cloud fr. cover	10% LND 15% WAS
		CTH	Cloud top height	1000 [m]
		SAL	Surf. albedo	25%
SAF120 MSG1	$(45\,km)^2$	TIS	ToA incom. solar	1 [W/m^2]
		TRS	ToA refl.solar	12%
		TES	ToA emitted solar	10* [W/m^2] >10 [W/m^2] (ALP)
		TET	ToA emit. thermal	0.06%
		TER	ToA emit. rad.	14* [W/m^2]
SAFH30 ATOVS	$(90\,km)^2$	HTW_TPW	Vert.integr.wat.vap.	1 [mm] $\sigma_P = 4.5$ [mm]

Table 7 CMSAF data The CMSAF data sets used, their horizontal resolution and the variables used in this study as given in [*Satellite Application Facility on Climate Monitoring*(2008)]. * Additionally calculated parameters are TES=TIS-TRS, TER=TES-TET and SRS=SIS-SNS.

4 Strategy for quality control

The quantitative comparison of the evaluation runs GME008 and GME010 with different reference datasets determines the quality of the regional climate model itself. Such an examination also considers deviations between different reference data of the same climatological quantity (if available), i.e. the data uncertainty of the actual climate state.

Usually data sets for the standard near surface parameters T_2m and precipitation are used for regional climate model evaluation. These quantities integrate the model dynamics. In general different sources of model errors contribute to these model errors and they can not be identified any more one by one. In this study all radiation components TOA and at the surface and properties of humidity and clouds are compared independently. This opens the opportunity to identify the possible sources of model deficiencies and/or inconsistencies of the reference data. An extensive discussion of the quality control of regional climate model simulations can be found in [*Hollweg et al.*(2008)].

The study is based on the comparison of the GME008 and GME010 simulation results with reference data (SAF, ECAD [*Haylock et al.*(2008)], GPCP [*Adler et al.*(2003)]) derived from observations and with each other in order to identify the internal model variability, the model deficiencies and/or limits of accuracy of the data used for comparison.

However, the quality of the regional climate simulation results essentially depends on three factors:

- the quality of the regional model itself,
- the quality of the input data (global simulation results, soil and vegetation parameter fields) and
- the internal variability (uncertainty originating in the dependence on initial conditions).

A limitation of the study is the length of the SAF products available. Assuming statistical independence of monthly means, the ensemble is very small and has 24 members TOA and 12 members else. The ensemble of specific monthly means has 2 members TOA and only one ensemble member else.
It is similar for the internal variability. Two simulations only have been conducted to estimate it. The internal variability originating in imperfect knowledge of initial conditions is investigated by comparison of two regional simulations initialised with different states of the soil at 1.1.2004 (GME008, GME010).
The spatial averaging does not solve the ensemble size problem, if the values at different grid points are not statistically independent. This question has not been investigated in detail and remains for future work. However, many regions exhibit a systematic stationary bias and it has been assumed, that the bias in time is not stochastic in space.

The uncertainty originating in the uncertainty of global simulation results has not been investigated.

The quality of the model itself and of the SAF data is being investigated within this study. Hereto the uncertainty ΔA of SAF product A and the internal model variability ΔB of model output variable B is combined to the accuracy of the difference $\Delta(B - A)$ (see section 4.2 for details). Significant differences $B - A$ are identified, if $B - A > \Delta(B - A)$, i.e. if the difference between model and observations exceeds the accuracy of the difference

This strategy can not clarify whether the differences originate in the regional model or in insufficient quality of the input data.

The main aim of this study is to analyse, which of the significant differences originates in the model output and which in the SAF data used for comparison. This is done on the basis of physical understanding of the model physics and of the procedure of calculation of the SAF products. The hypotheses resulting from this analysis need to be proved independently. The basis of this analysis is the investigation of all radiation components and of cloud and humidity quantities.

The statistical quantities calculated are the means, the second moments and its differences. Additionally quality measures like pattern correlations have been calculated. In this report the discussion is limited to the means and mean differences.

4.1 Comparisons

Usually data sets for the standard near surface parameters T_2m and precipitation are used for regional climate model evaluation. These quantities integrate the model dynamics. In general different sources of model errors contribute to these model errors and they can not be identified any more. In this study all radiation components TOA and at the surface and properties of humidity and clouds are used. This opens the opportunity to identify the possible sources of model deficiencies and/or inconsistencies of the reference data.

4.2 Calculation of the accuracy

An important aspect of the CMSAF products is the specification of the quality of the products in terms of absolute accuracy Δ (absolute bias) or δ (relative bias) for all variables A and additionally of the precision σ (RMS error) for some variables. The accuracy given in tables 9 and 7 is derived from comparisons of the SAF products with ground based observations (e.g. station data and radiosonde data) and gives the mean absolute bias of all grid point comparisons.
Additional assumptions have to be made with the interpretation of the CMSAF-accuracy as bias of monthly means of spatial averages. The assumption of a representative distribution of the reference stations with respect to the model domain allows to relate the accuracy Δ given for each CMSAF product to the bias of the monthly mean of spatial averages over a number of grid points larger than the number of stations used for calculation of the CMSAF-accuracy. Typically about 200 stations are used. Therefore regions larger than 15x15 grid points ($\simeq 250x250\,km^2$) can be assumed as large enough. Most of the sub-regions investigated are substantially larger as can be seen from table 8.
The assumption is not valid for water surfaces and for mountaineous regions. Therefore, the accuracy limits might be substantially larger for such regions.
The detailed investigation of the nature of the accuracy of spatial averages remains for future work (7).

Within this study the linear error analysis based on the assumption of Gaussian distribution is applied and the corresponding ΔA values for annual means and the derived variables are calculated. The main

formulas used are:

$$\Delta_N A = \frac{1}{\sqrt{N}} \Delta A \tag{1}$$

and $$\Delta B = \sqrt{(\Delta A_1)^2 + (\Delta A_2)^2} \quad \text{if} \quad B = A_1 \pm A_2 \tag{2}$$

and $$\delta B = \sqrt{(\delta A_1)^2 + (\delta A_2)^2} \quad \text{if} \quad B = A_1 \times A_2 \tag{3}$$

(4)

The formulas assume the statistical independence of the monthly mean accuracies and of the accuracies of independent variables A_1 and A_2. Relative accuracies are calculated as $\delta A = \Delta A / A$

Sub-regions of the model domain investigated		
Labelling	Number of grid-points	Description
Level 1		
LND	19925	Land area (NEL+SEL)
WAS	21956	Water area (NEW+SEW)
NEU	22270	Northern Europe (NEL+NEW)
NEL	12488	Northern Europe land area
NEW	9782	Northern Europe water area
SEU	11443	Southern Europa (SEL+SEW)
SEL	6231	Southern Europe land area
SEW	5212	Southern Europe water area

Table 8 (first part) Labelling of sub-regions on size level 1 and the number of associated grid-points on the regional model grid. (See Figure 3 for size and location).

4.3 Types of analysis and of presentations

The analysis of the comparisons illustrated above is essentially based on three different types of presentation: absolute plots, difference plots, and mean annual cycles of spatial averages for selected regions. The reference grid of the results presented is the model grid.

The absolute plots show the spatial distribution of the monthly and annual means of the model results and reference data sets. The difference plots show the spatial distribution of the differences between the mean of the simulation and a reference data set for the model domain. They are calculated for the annual means and the monthly means. The figures show the annual mean, January, April, July and October. In order to obtain a more detailed and quantitative regional analysis, the model domain is subdivided into a number of sub-areas (see Table 8) representing different geographical and climatological regions on different spatial scales. For every sub-region, the difference of the area averages is calculated for all pairs of compared means of the year 2005,2006 and 2005-2006 for ToA variables and 2006 for all others. Additional figures show the annual cycles of the monthly means and the difference between the reference simulation GME008 and all other data (GME010, SAFXXX etc.).

The ranges between the smallest and the largest difference of all comparisons are given in the BIAS-tables for the annual values and for the mid-season months January, April, July, and October (not shown here) on request.

Sub-regions of the model domain investigated		
Labelling Level 2	Number of grid-points	Description
SCA	3352	Scandinavia
NWE	1277	Northwestern Europe
MEU	2041	Central Europe
SWE	2264	Southwestern Europe
EEU	3451	Eastern Europe
SUE	3771	Southern Europe
NEE	1021	Northeastern Europe
RUS	1343	Western Russia
VAS	195	Southwestern Asia
MED	3753	Mediterranean Sea
OSS	1403	Baltic Sea
NOS	1495	North Sea
SWM	274	Black Sea
NOA	3189	North Atlantic
BIS	2344	Bay of Biscay
Level 3		
NSK	777	Northern Scandinavia
SSK	2575	Southern Scandinavia
ALP	619	Alpine region (grid-points above 500 m)
POE	135	Poe valley (grid-points below 300 m)
UNG	665	Pannonian Basin (grid-points below 300 m)
DTL	1045	Germany
SLW	49	Region around Schleswig
ESS	49	Region around Essen
LIN	49	Region around Lindenberg
MEI	49	Region around Meiningen
MUN	49	Region around Munich
STU	49	Region around Stuttgart
SAX	50	Saxonia

Table 8 (**Second part**) Labelling of sub-regions on size levels 2 and3 and the number of associated grid-points on the regional model grid. (See Figure 3 for size and location)..

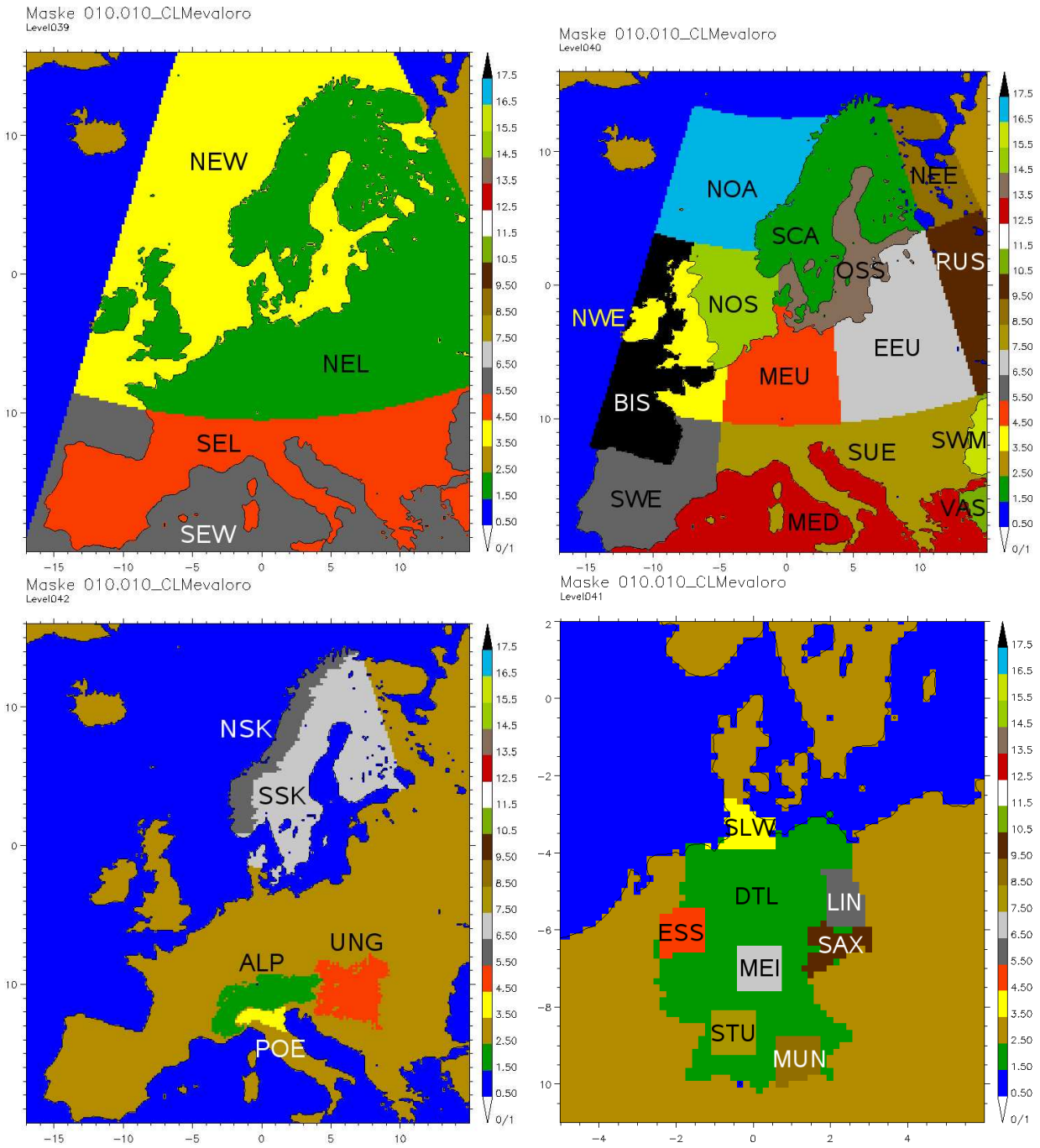

Figure 3 Location and size of the sub-regions being used for the comparisons on the regional model grid (for meaning of labels see Table 8).

The comparisons are executed for 36 different subregions listed in Table 8 and defined on the regional model grid. On the first level, the model domain is subdivided into Northern and Southern Europe as well as land and water surfaces. These regions are further subdivided into smaller sub-continental areas (level 2). The third level includes sub-regions, which are either characterised by special geographical features (Poe valley, Alps, etc.) or which have been used as sub-national areas in previous studies so that substantial experiences are available for these regions regarding the quality of regional climate simulations.

All comparisons are executed for the subsequently listed climate parameters:

Nr.	Variable long name	Acronym		Δ (δ)
		CCLM	**CM-SAF**	**CM-SAF**
1. TOA				
1.1	TOA down SW	**ASODT**	**TIS**	$1\,W/m^2$
1.2	TOA up SW	**ASOU_T**	**TRS**	$10\,W/m^2$
1.3	TOA net SW	**ASOB_T**	**TES**	($\delta = 0.12$)
1.4	TOA net LW	**ATHB_T**	**-TET**	($\delta = 0.06$)
1.5	TOA net radiation	**ANRB_T**	**TER**	$15\,W/m^2$
2. VERTICALLY INTEGRATED HUMIDITY AND CLOUD PROPERTIES				
1.1	Total cloud cover	**CLCT**	**CFC**	($\delta = 0.10$ (0.15))
1.2	Cloud top height	**HTOP_CON**	**CTH**	$1000\,m$
1.3	Vertic. integr. water vapour	**TQV**	**HTW_TPW**	$1\,mm$
3. NEAR SURFACE				
3.1	surface down SW	**ASWG_S**	**SIS**	$10\,W/m^2$
3.2	surface albedo	**ALB_RAD**	**SAL** ($\delta = 0.25$)	
3.3	surface up SW	**ASWDIFU_S**	**SRS**	$10\,W/m^2$
3.4	surface net SW	**ASOB_S**	**SNS**	$15\,W/m^2$
3.5	surface down LW	**ALWD_S**	**SDL**	$10\,W/m^2$
3.6	surface up LW	**ALWU_S**	**SOL**	$10\,W/m^2$
3.7	surface net LW	**ATHB_S**	**SNL**	$15\,W/m^2$
3.8	surface net radiation	**ANRB_S**	**SRB**	$21\,W/m^2$
			Ref.	
4. METEOROLOGICAL NEAR SURFACE VARIABLES				
4.1	2 meter Temperature	**T_2M**	**T2M**	
4.2	Total Precipitation	**TOT_PREC**	**PRECIP**	

Table 9 **Variables** investigated, their naming conventions in CCLM and reference data base (CM-SAF, ECAD01 (ECAD) or GPCP) and the absolute Δ or relative (δ) accuracy (bias) of the monthly means of CMSAF products.
The derived variables are calculated as follows: ASOU_T=ASODT-ASOB_T, ANRB_T=ASOB_T+ATHB_T, ASWG_S= ASWDIR_S+ASWDIFD_S, TES=TIS-TRS, TER=TES-TET, SRS=SIS+SNS.

Altogether, a detailed analysis for all radiation components TOA and at the surface and vertically integrated properties of clouds and humidity for many sub-regions has been carried out. In the following sections selected results of the comparison described above are presented. They summarise the essential results and give an impression of the potential of a systematic evaluation of a large number of variables.

A complete presentation of all aspects of quality for different regions is not feasible within such a report. The variety of interests of potential users of these data may require additional and more specific investigations which have to be executed with adequate care in the future. In order to support this work, the authors provide systematic data preparations in form of tables and plots in addition to the results presented in this report for other regions. The complete analysis with presentations of all executed comparisons for all parameters and sub-regions will be made available on request.

The Results are discussed in section 5 to section 7. The discussion is focused on water surface (WAS), land surface (LND), Iberian Peninsula (South-West Europe, SWE) and Scandinavia (SCA).

5 Radiation Top of the Atmosphere (ToA)

It has to be noticed, that the definition of TOA is different for the CMSAF products, and for the CCLM. The satellites measure outside of the atmosphere. The CCLMs top of the models atmosphere (TOM) is at 25 km height which corresponds to 10 hPa. Strictly speaking the following comparisons are not correct, because the CMSAFs values TOA are compared with TOM values of the CCLM. The TOA downward LW component in CCLM has a nonzero value $< 5W/m^2$ which has not been taken into account in this first comparison.

5.1 ToA down SW, 2005-2006, 2005, 2006

The down solar radiation (TIS) is the most accurate observation available from satellite born measurements. It's accuracy ΔTIS is given by CMSAF as $\Delta TIS = \pm 1$ W for monthly means. The corresponding COSMO-CLM variable is named $ASODT$. The values are climatologically prescribed in the model.

Figures 4 A to C show the annual means 2005-2006 of the GME008 simulation (A), of SAF120 (B) and their difference GME008-SAF120 (C). The results are consistent everywhere and mainly caused by the interpolation from the coarser SAF120 grid onto the CCLM grid.

Figures 5 A to D show the monthly mean differences at all grid points for January (A), April (B), July (C) and October (D) 2005-2006. Fig.6 shows the annual cycle of the monthly means averaged over the regions LND (A), WAT (B), SWE (C) and SCA (D) for the time period 2005-2006, 2005 and 2006. Additionally Fig. 7 shows the annual cycle of the regional monthly mean differences for all data sets available and for 2005-2006. On the monthly time scale spatial and temporal structures of deviations GME008-SAF120 occur with significant values $\Delta(ASODT - TIS) \geq 0.7\,W/m^2$:

- The deviations exhibit an annual cycle of approx. $2\,W/m^2$.
- The differences exhibit a spatial wave structure with a wave length of approx. 1000 km.
- The difference SAF120-GME008 has a significant inter-annual variability. It is $1\,W/m^2$ smaller for 2006 than for 2005-2006.

The result for CCLM is not surprising since the annual cycle of the down solar radiation is prescribed. The quantitative differences between the differences for 2005-2006 and 2006 show the inter-annual variability as observed by the satellites. However, the climatological relevance of the significant annual cycle of the deviations can not be answered using the present day models due to much higher uncertainties for other components.

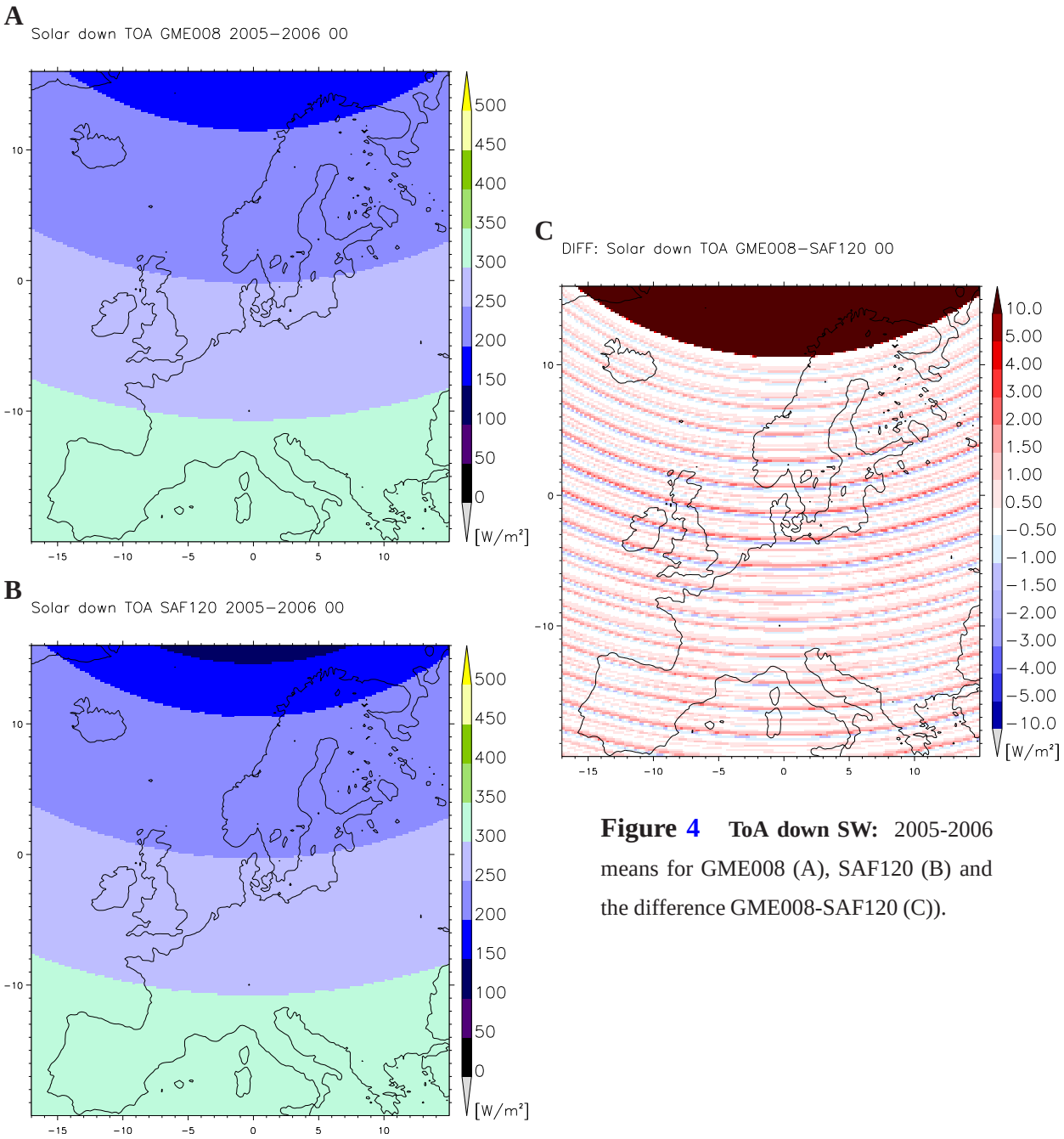

Figure 4 **ToA down SW:** 2005-2006 means for GME008 (A), SAF120 (B) and the difference GME008-SAF120 (C)).

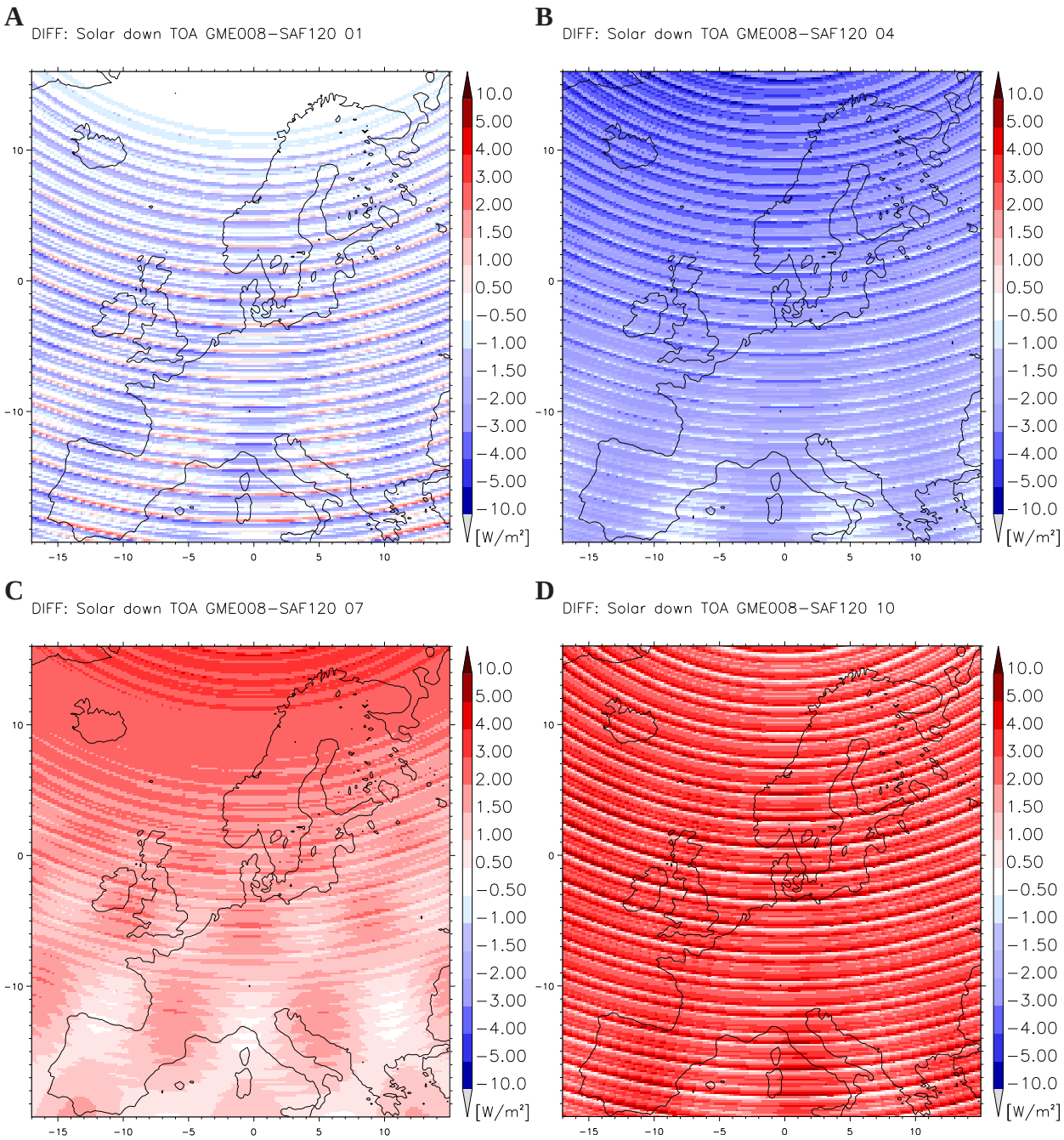

Figure 5 **ToA down SW:** monthly means of the differences GME008-SAF120 for January (A), April (B), July (C) and October (D) of the time period 2005-2006.

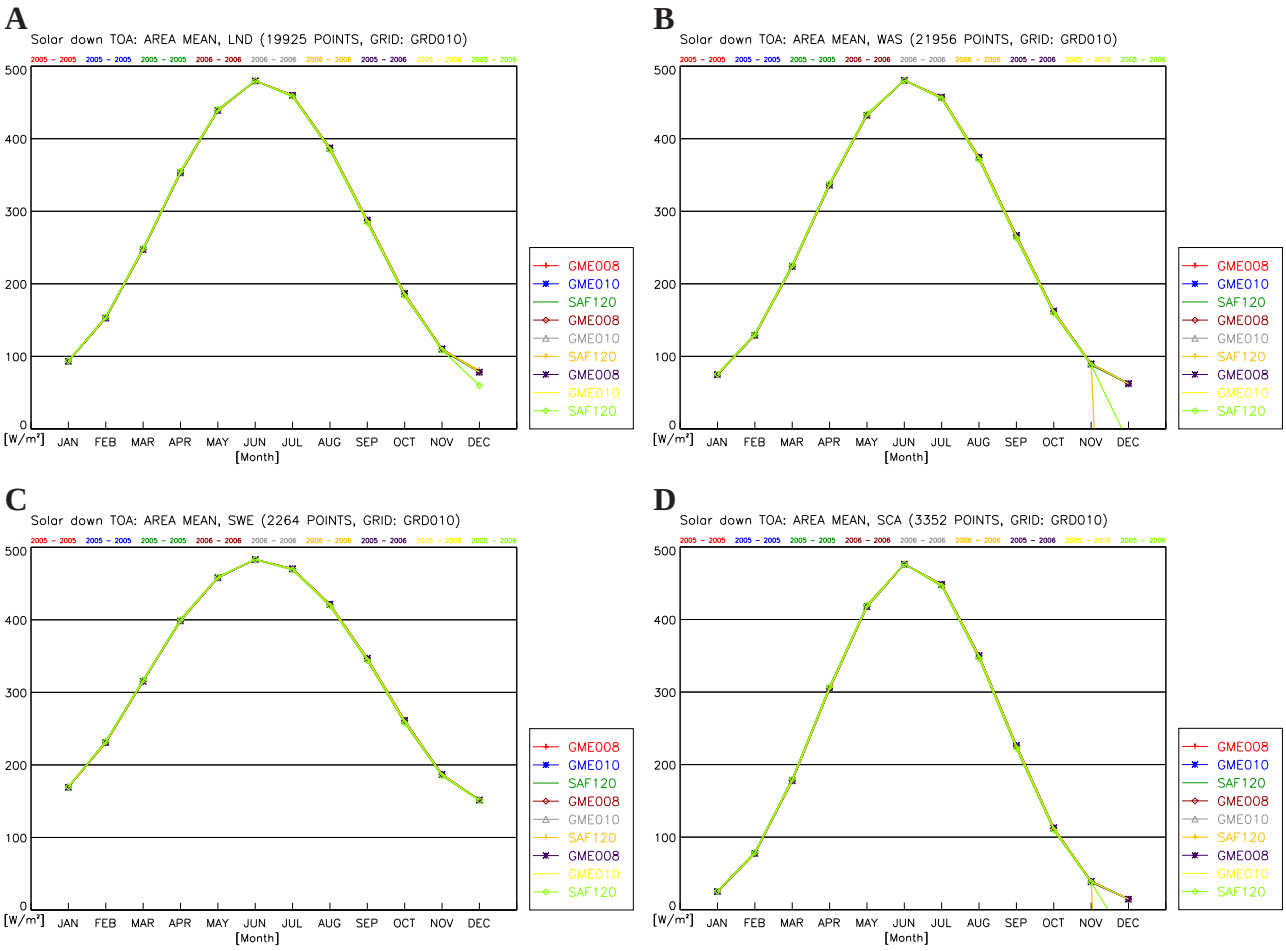

Figure 6 **ToA down SW:** annual cycle of the monthly means GME008, GME010 and SAF120 for LND (A), WAS (B), SWE (C) and SCA (D) for the years 2005, 2006 and 2005-2006.

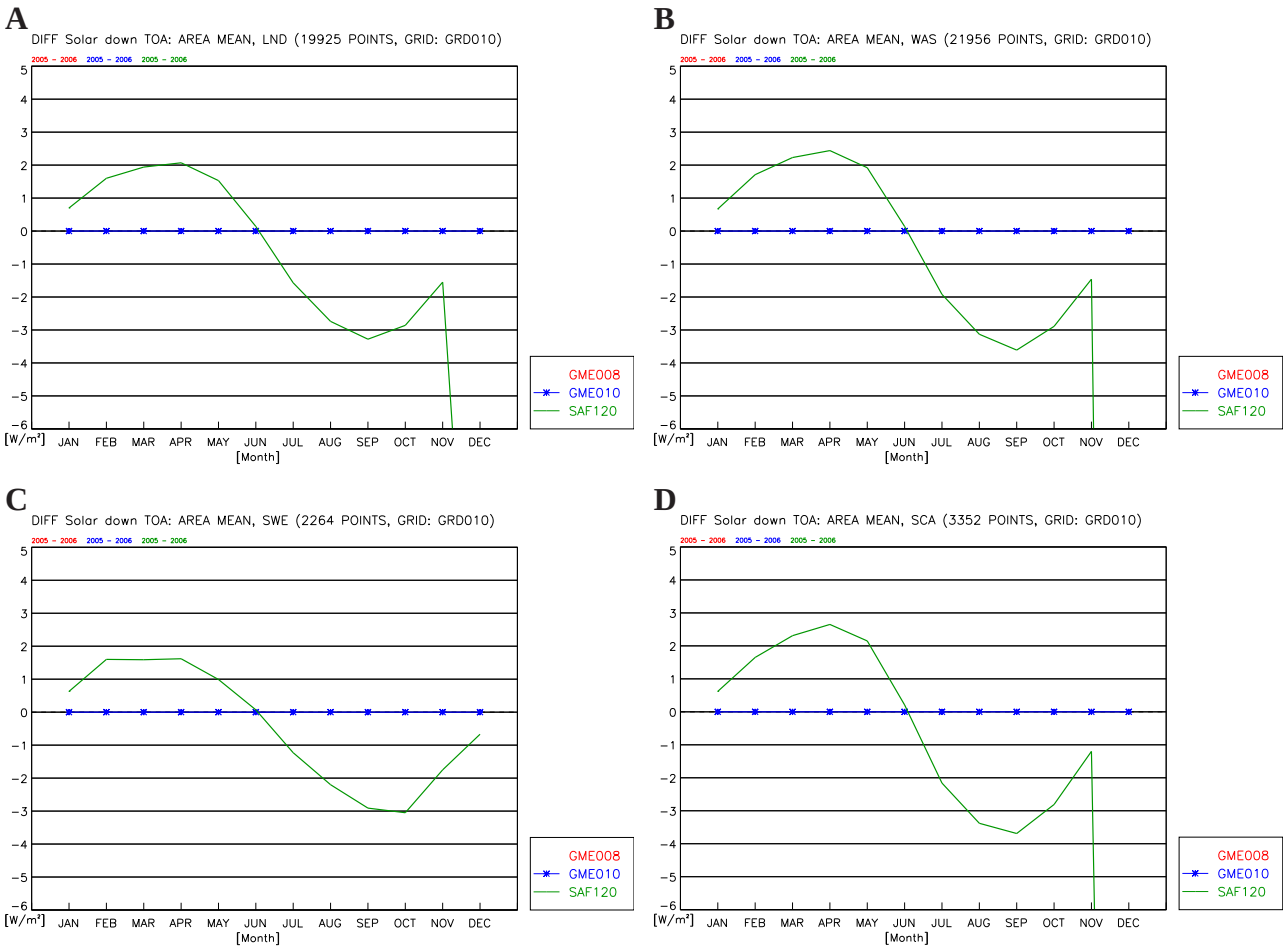

Figure 7 **ToA down SW:** annual cycle of the monthly mean differences Data-GME008 for LND (A), WAS (B), SWE (C) and SCA (D) for the time period 2005-2006.

5.2 ToA up SW, 2005-2006, 2005, 2006

The satellite derived top of the atmosphere outgoing solar radiation is denoted by TRS (top reflected solar). The corresponding CCLM quantity is denoted by $ASOU\_T$ (solar up ToA). The accuracy of TRS is given to be $\Delta TRS = 0.12TRS \simeq 12\,W/m^2$ by CMSAF for monthly means. The internal CCLM variability $\Delta ASOU\_T$ can be derived from Fig.11. It is up to $5\,W/m^2$ for all regions except for Scandinavia (SCA) and up to $\Delta ASOU\_T = 10\,W/m^2$ in SCA for the summer months.

Figure 8 A to C shows the annual mean 2005-2006 of the GME008 simulation (A), of SAF120 (B) and their difference GME008-SAF120 (C). The differences GME008-SAF120 are smaller than the accuracy $\Delta_{24}TRS = 3W/m^2$ over most parts of Europe. However,

- the mean deviations over SCA (+20W) are strongly significant,
- the mean deviations over SUE (- 3 W) and
- the mean deviations at the eastern and western boundary (- 4 W) are weakly significant.

Figures 9 A to D show the monthly mean differences at all grid points for January (A), April (B), July (C) and October (D) 2005-2006. Additionally Fig.10 exhibits the annual cycle of the monthly means for the selected regions LND (A), WAS (B), SWE (C) and SCA (D) and the time periods 2005-2006, 2005 and 2006. It allows to relate the inter-annual variability and the differences between model and CMSAF data. Additionally Fig.11 shows the annual cycle of monthly mean differences for all data sets available and for the time period 2005-2006 and the same selected regions.

On the monthly time scale the deviations GME008-SAF120 exhibit a complex spatial and temporal structure. Three different patterns can be identified exhibiting significant deviations of $(ASOU\_T - TRS) \geq 14\,W/m^2$. Fig. 10B exhibits a significantly higher model values over water in the months February to July. Fig.10D shows a significant overestimation of the outgoing short wave radiation in the model.

- Fig.9B shows significant negative values of $17\,W/m^2$ in SUE in April.
- In April and July a significant negative deviation of $20\,W/m^2$ and more occurs in the boundary zone. It is extended into the model domain over water surfaces of the North Sea.
- A strong positive deviation of up to $50\,W/m^2$ in July occurs in SCA.

All significant patterns of deviation are hypothesised to have different origins.

- The negative deviation in SUE in April (Italy, Balkan and Greece) may be an exception of the year 2006.
- The negative deviation in the boundary zone may be caused by inappropriate boundary conditions for humidity quantities causing lower cloud cover. The extension of this effect over water surfaces in April to July may be supported by too small evaporation over water surfaces.

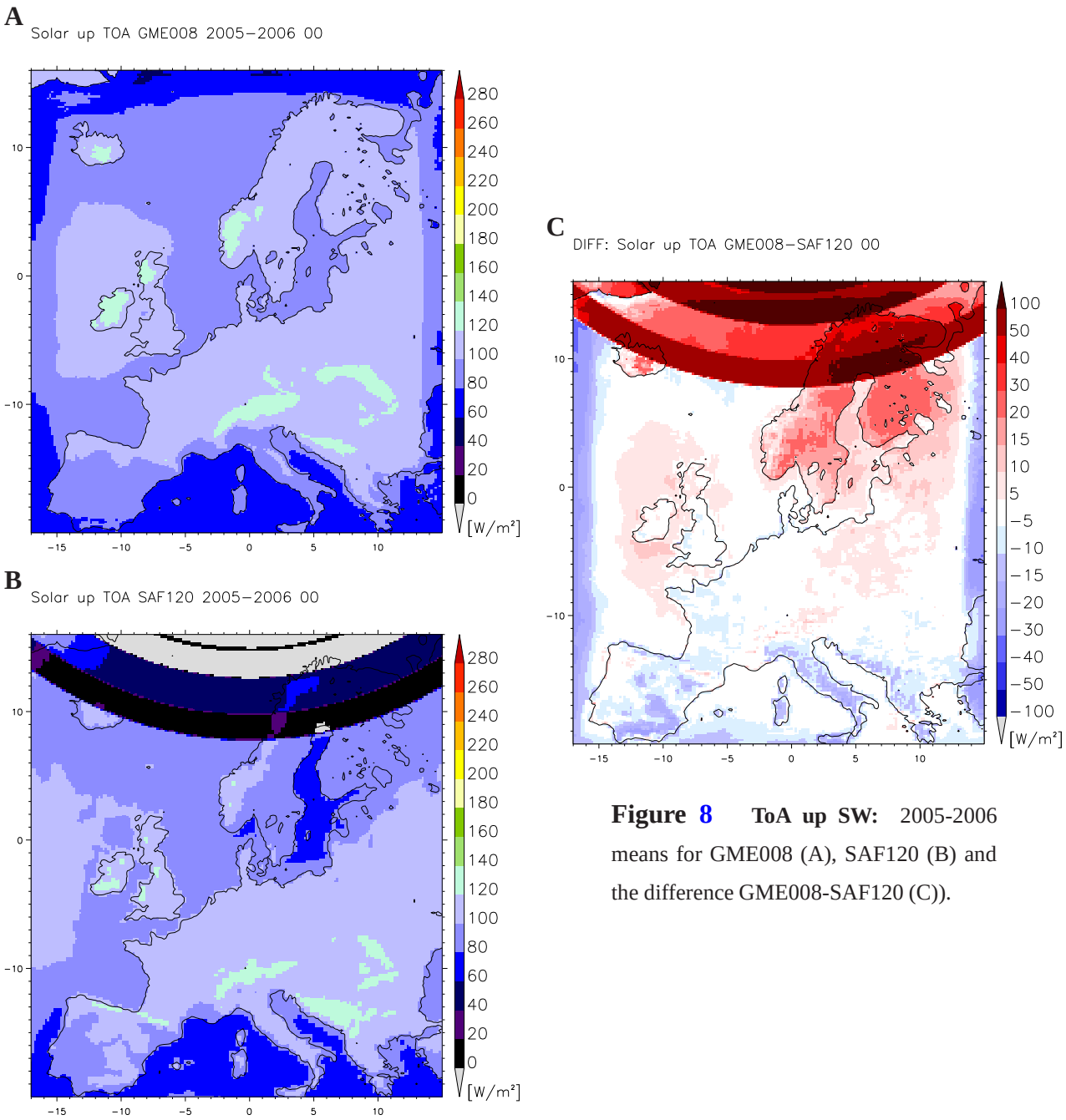

Figure 8 **ToA up SW:** 2005-2006 means for GME008 (A), SAF120 (B) and the difference GME008-SAF120 (C)).

- The strong positive deviation over Scandinavia in April and over the northern model domain in July with peak values over Scandinavia comes along with too high cloud cover (see Fig. 25) and too high relative humidity (not shown here).

A not significant south-north gradient of up to $10\,W/m^2$ occurs in the January difference of Figure 9, which is nearly free of the effects discussed above. This may be caused by inappropriate adjustment of the satellite measurements.

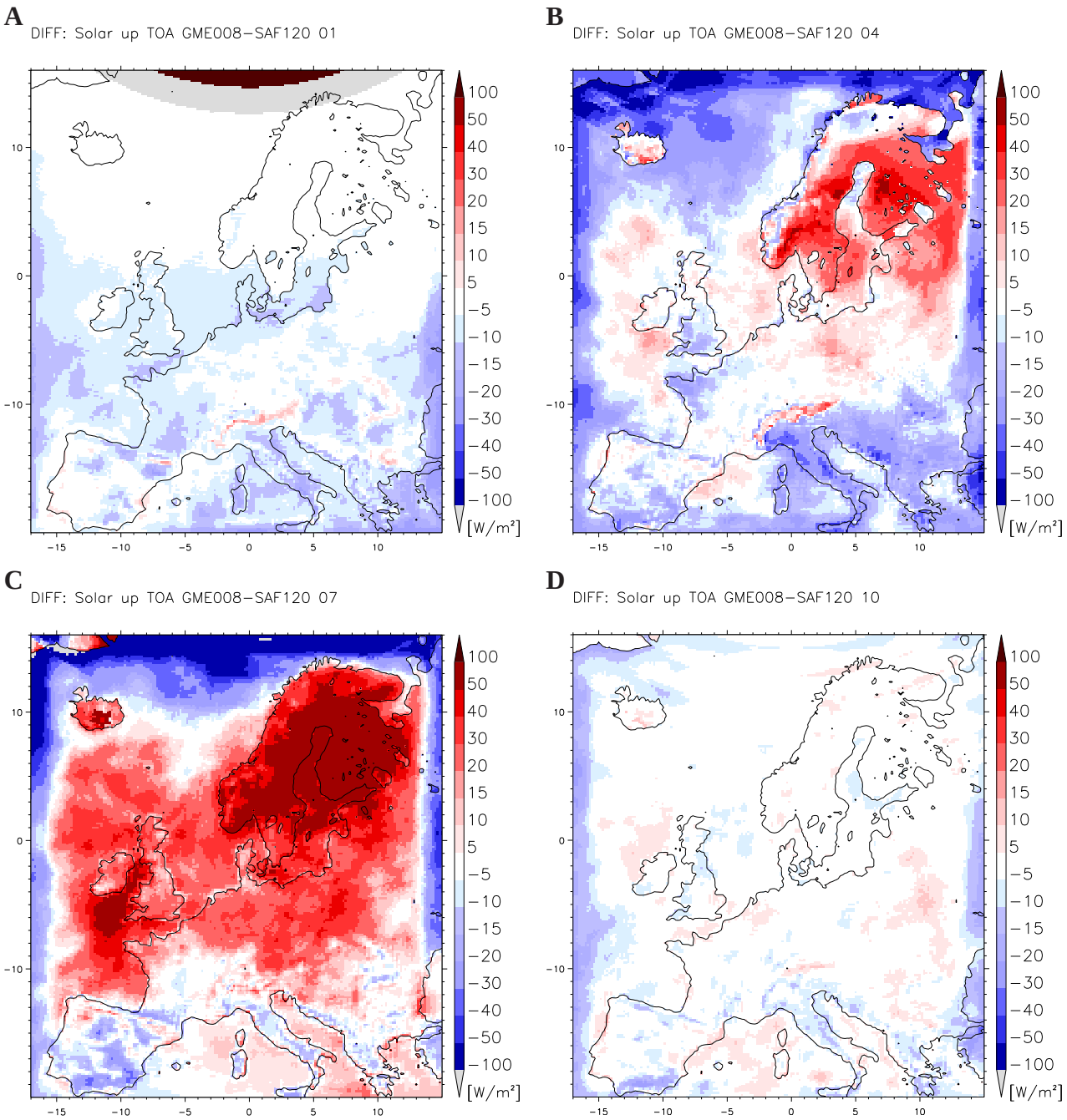

Figure 9 **ToA up SW:** monthly means of the differences GME008-SAF120 for January (A), April (B), July (C) and October (D) of the time period 2005-2006.

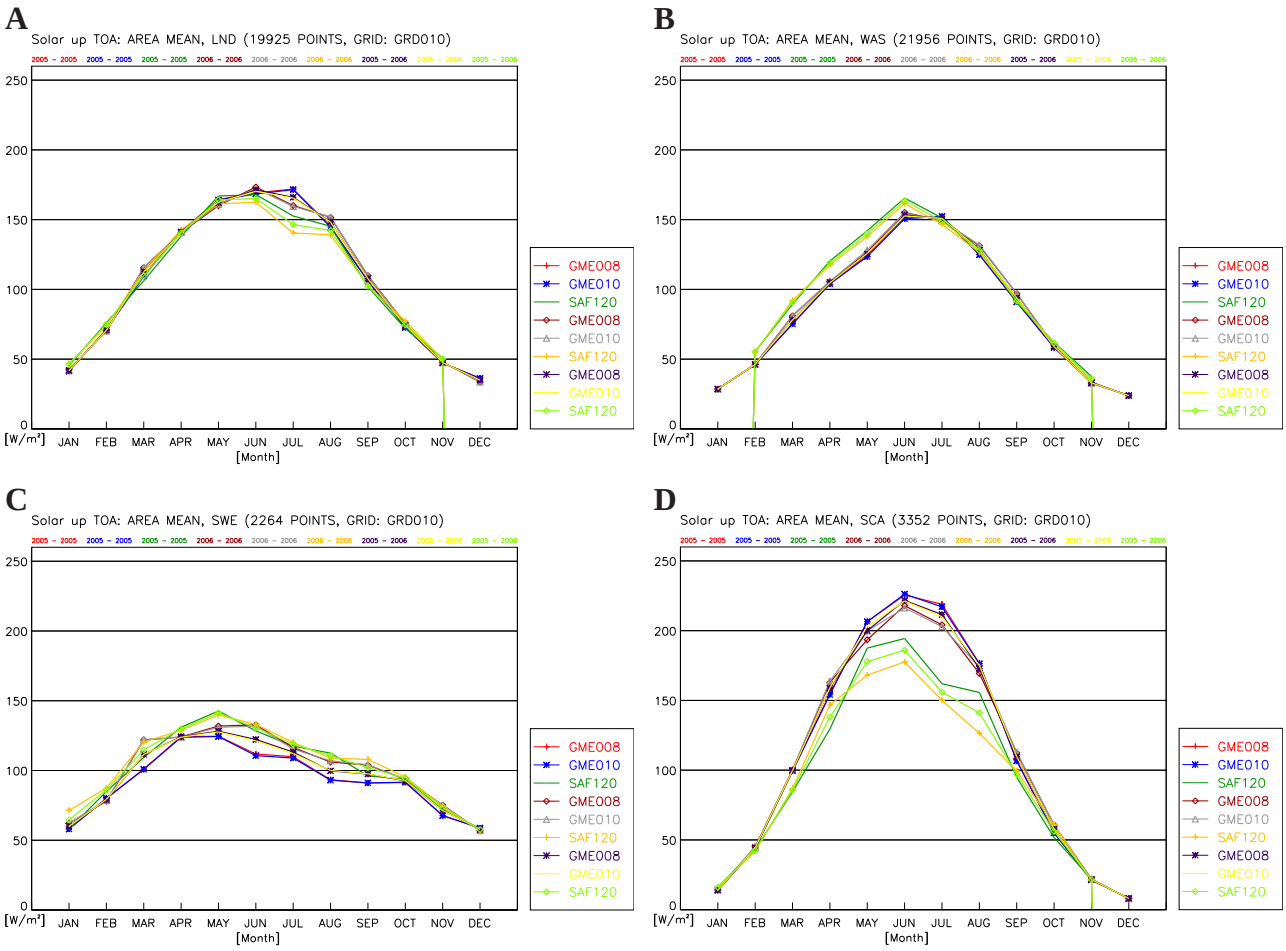

Figure 10 **ToA up SW:** annual cycle of the monthly means GME008, GME010 and SAF120 for LND (A), WAS (B), SWE (C) and SCA (D) for the years 2005, 2006 and 2005-2006.

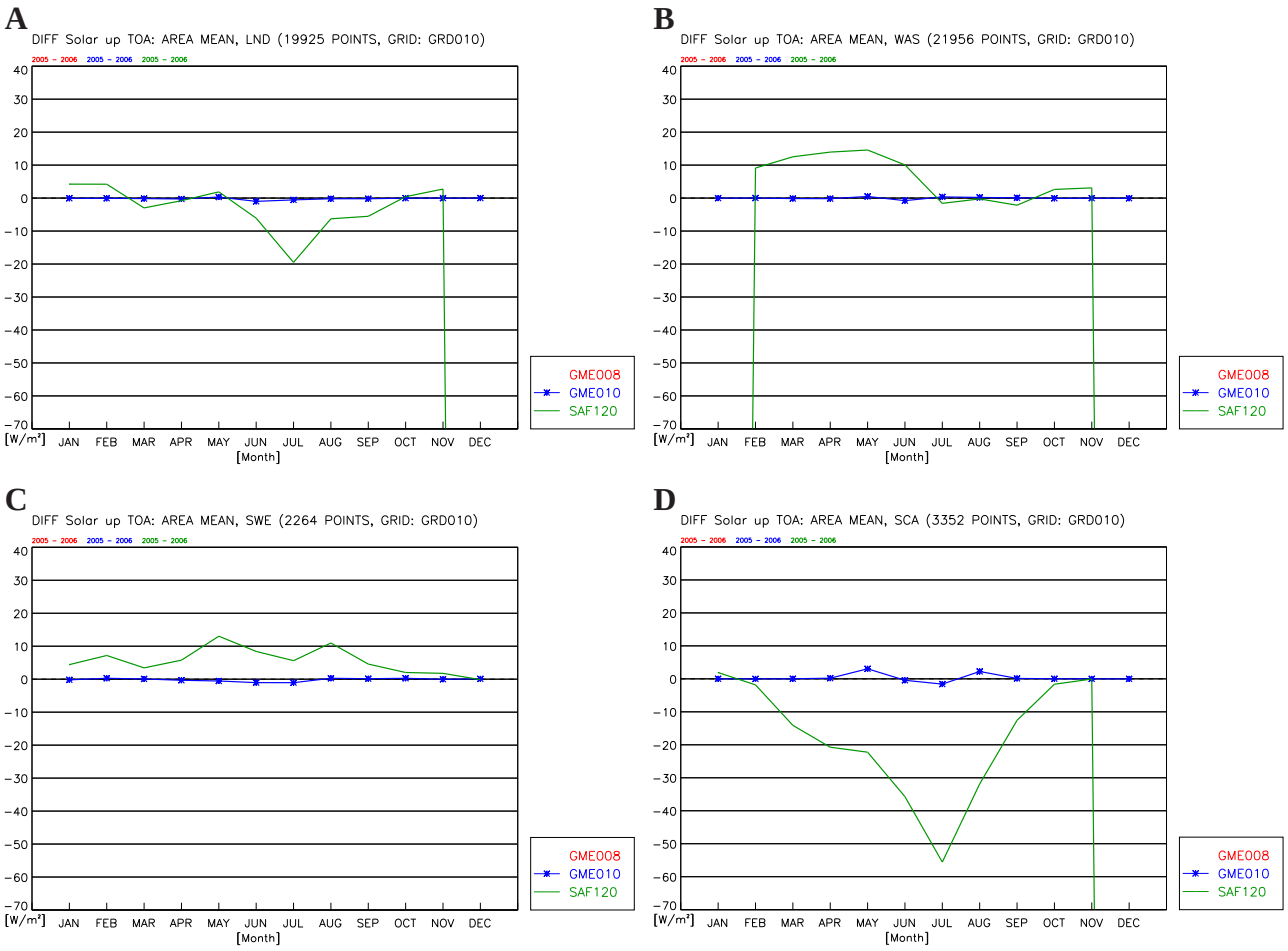

Figure 11 **ToA up SW:** annual cycle of the monthly mean differences Data-GME008 for LND (A), WAS (B), SWE (C) and SCA (D) for the time period 2005-2006.

5.3 ToA net SW, 2005-2006, 2005, 2006

The satellite derived top of the atmosphere net solar radiation is denoted by TES. The corresponding CCLM quantity is denoted by $ASOB\_T$ (solar budget). The sign convention of the net radiation is downward positive.

The results for the deviations $ASOB\_T - TES$ are dominated by the deviations of $(ASOU\_T - TRS)$, which are substantially higher than $(ASOD\_T - TIS)$. Due to the sign convention all deviations have the opposite sign.

Figure 12 to 15 show the same quantities as the corresponding figures for ToA down and up SW radiation.

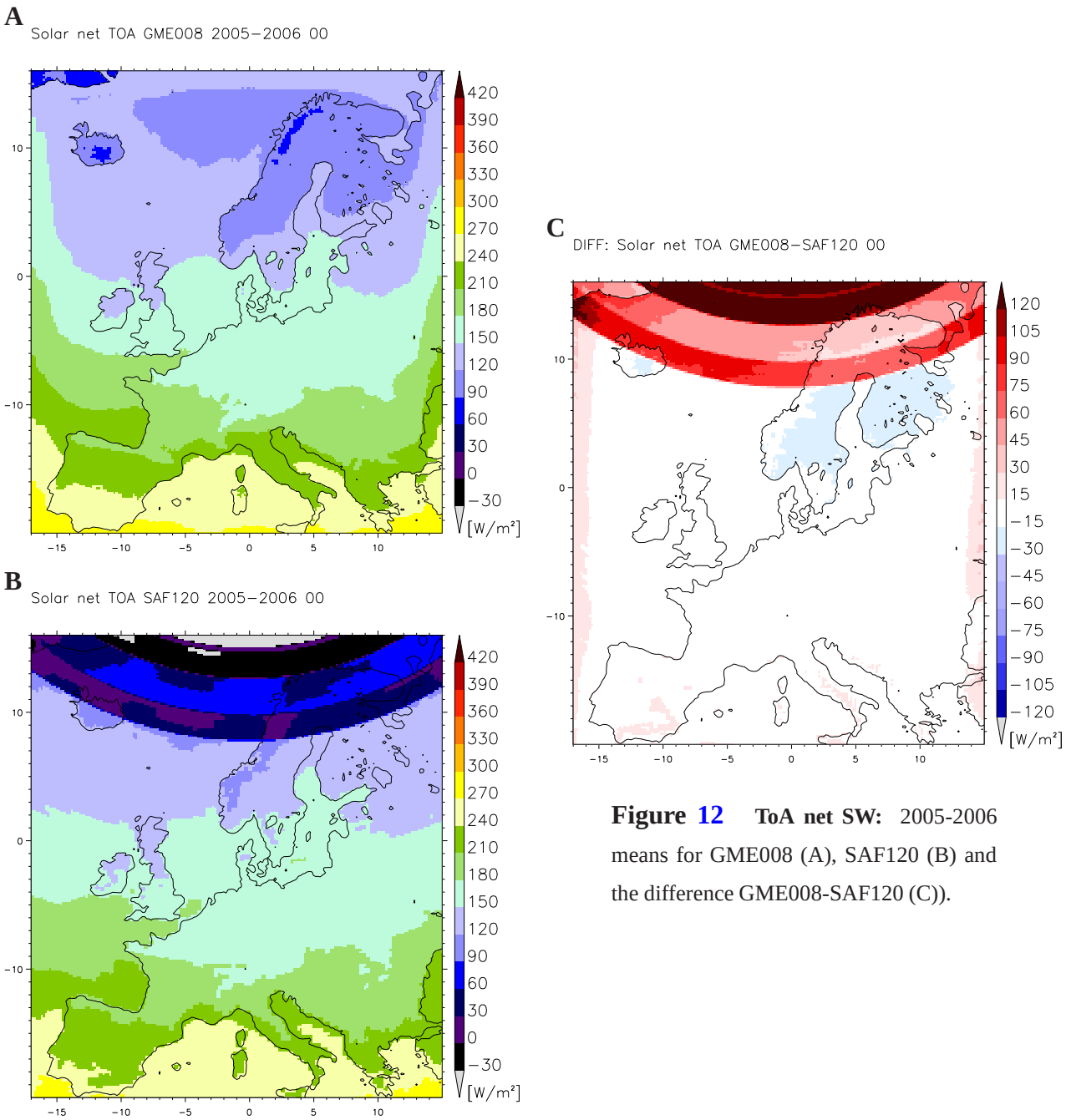

Figure 12 **ToA net SW:** 2005-2006 means for GME008 (A), SAF120 (B) and the difference GME008-SAF120 (C)).

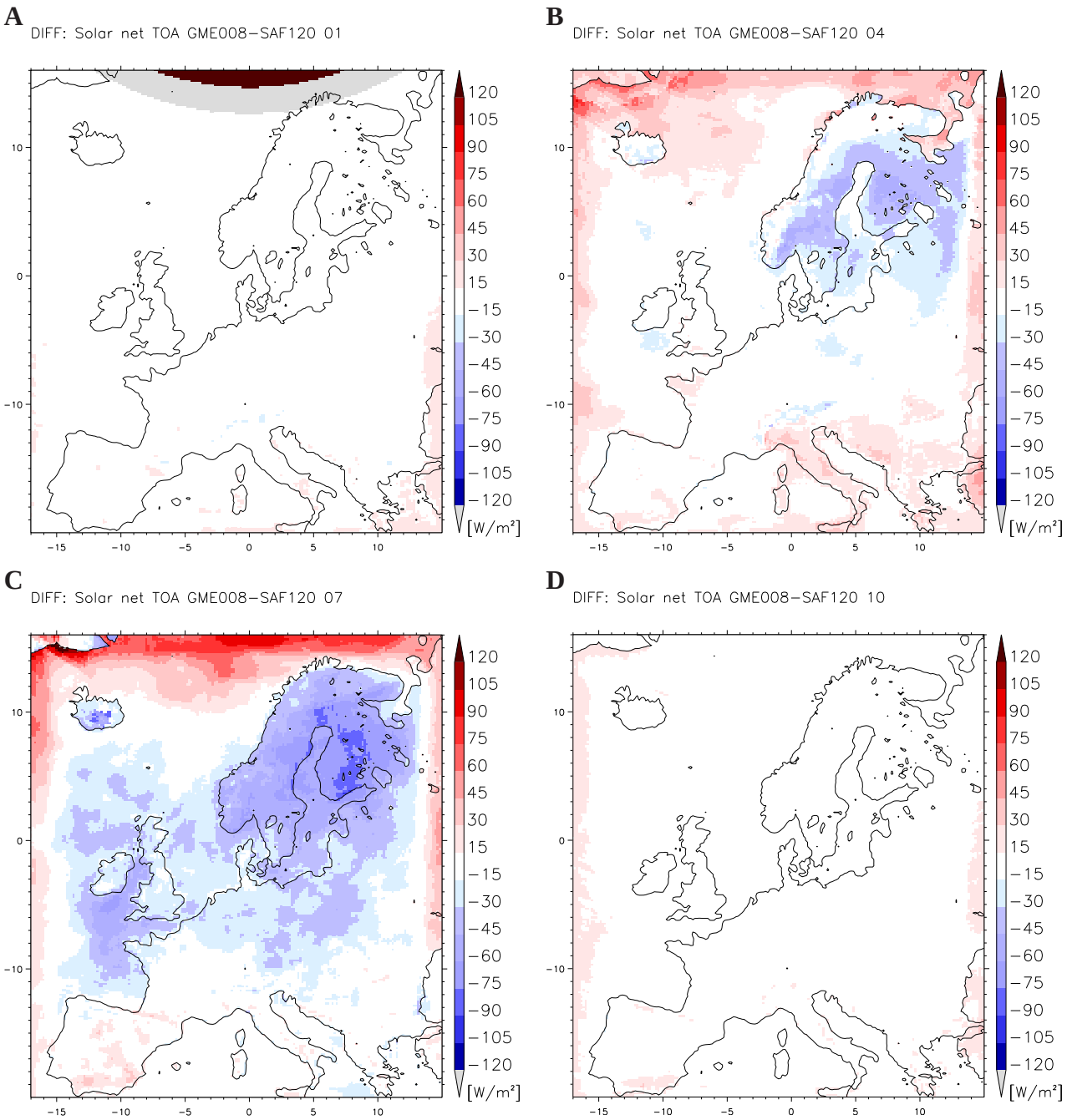

Figure 13 **ToA net SW:** monthly means of the differences GME008-SAF120 for January (A), April (B), July (C) and October (D) of the time period 2005-2006.

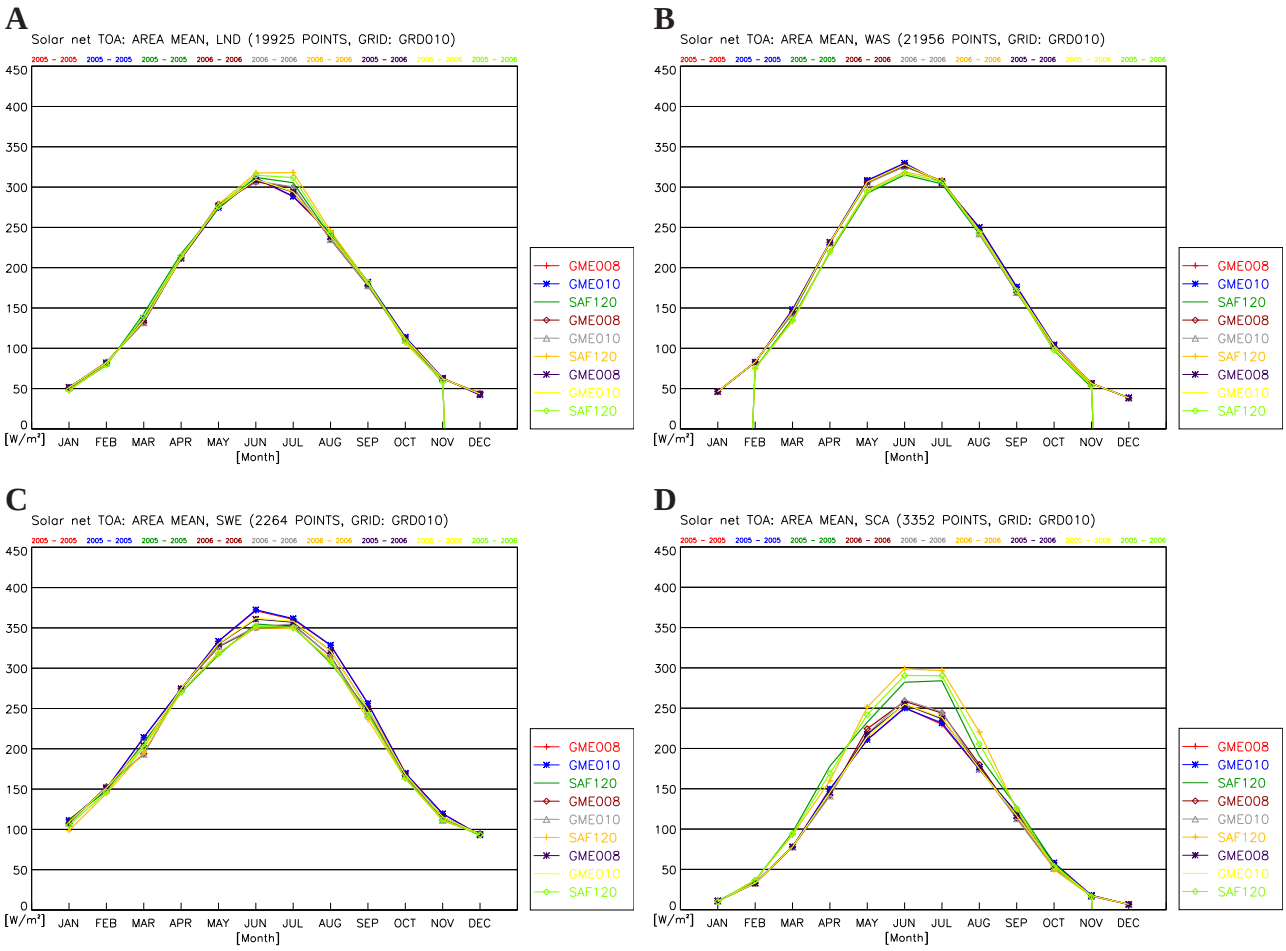

Figure 14 **ToA net SW:** annual cycle of the monthly means GME008, GME010 and SAF120 for LND (A), WAS (B), SWE (C) and SCA (D) for the years 2005, 2006 and 2005-2006.

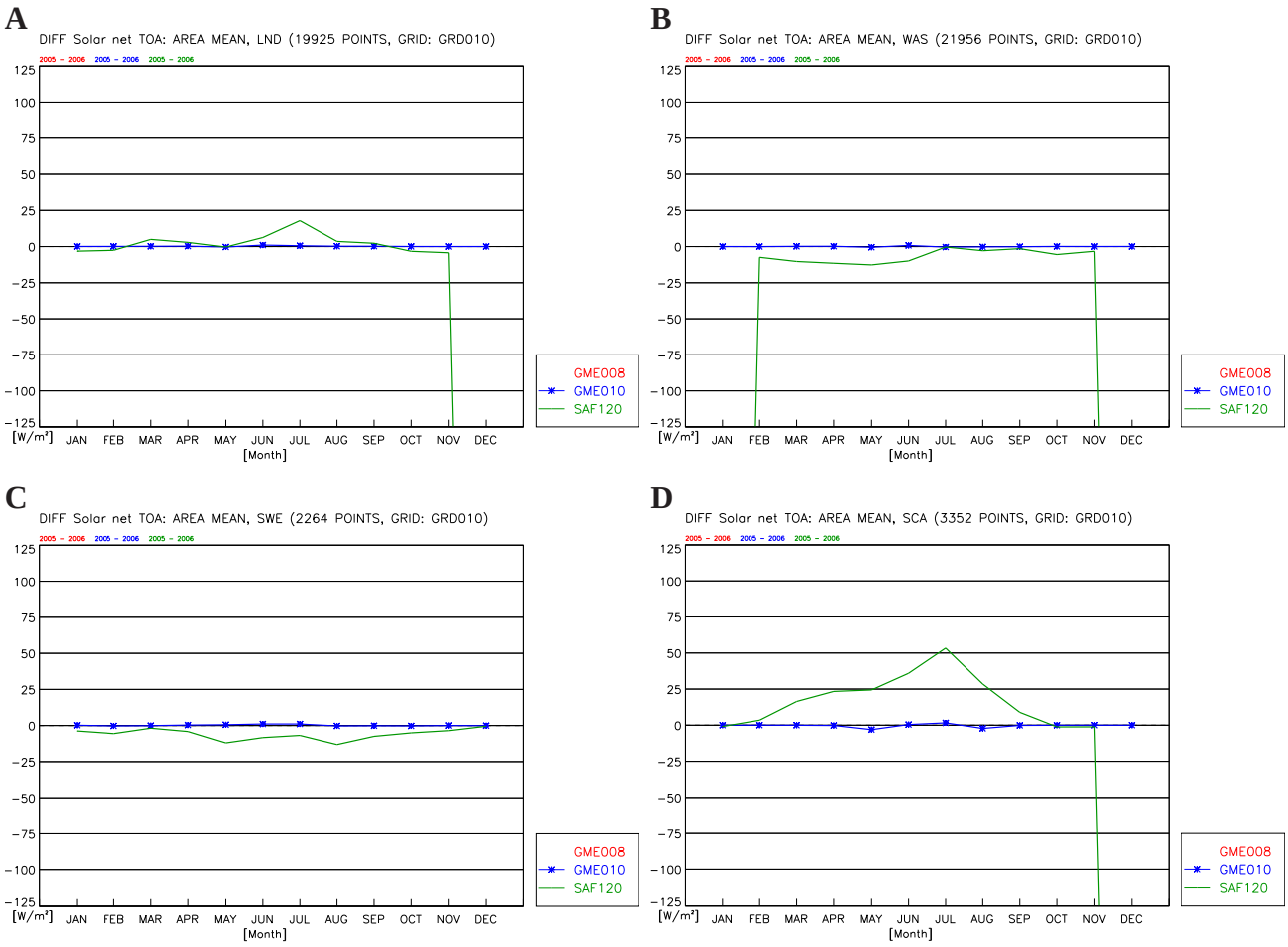

Figure 15 **ToA net SW:** annual cycle of the monthly mean differences Data-GME008 for LND (A), WAS (B), SWE (C) and SCA (D) for the time period 2005-2006.

5.4 ToA net LW, 2005-2006, 2005, 2006

The satellite derived top of the atmosphere net long wave radiation is denoted by TET (top emitted thermal). The corresponding CCLM quantity is the net long-wave radiation at the model top denoted by $ATHB\_T$ (thermal budget ToA). In this study TET and $ATHB\_T$ are directly compared with each other. Hereby the differences in the emission ToA and at the model top (25 km) are neglected. This will be taken into account later on.
Furthermore, the down long-wave radiation at model top is neglected in this study. It is estimated to be about $5W/m^2$ and will be taken into account in the forthcoming study.

The accuracy of the CMSAF variable TET is given to be $\Delta TET = 0.06TET \simeq 14\,W/m^2$ for monthly means. The internal CCLM variability $\Delta ATHB\_T$ can be derived from Fig.19. It is up to $3\,W/m^2$ for all regions except for Scandinavia (SCA) and up to $\Delta ATHB\_T = 5\,W/m^2$ in SCA for the summer months. The resulting accuracy of the monthly mean differences is $\Delta(ATHB_S - TET) = 15W/m^2$.

Figure 16 A to C shows the annual mean 2005-2006 of the GME008 simulation (A), of SAF120 (B) and their difference GME008-SAF120 (C). The differences GME008-SAF120 are smaller than the accuracy $\Delta_{24}(ATHB\_T - TET) = 4W/m^2$ over most parts of Europe. However,

- the mean deviations over WAS ($-7.6\,W/m^2$),
- the mean deviations over SWE ($-6.9\,W/m^2$) and
- the mean deviations over MED ($-10.6\,W/m^2$) are significant.
- A strongly significant gradient of the deviations can be found perpendicular to the boundaries.
- At the inflow boundaries the gradient is much weaker indicating a strong effect of the inflow conditions on the formation of clouds, especially over water surfaces.
- The land-sea contrast is also different in CMSAF and GME008. It can be seen from the significant difference MED-SWE, which is about $9W/m^2$ for TET and $12.5W/m^2$ for $ATHB\_T$

Figures 17 A to D show the monthly mean differences at all grid points for January (A), April (B), July (C) and October (D) 2005-2006. Additionally Fig. 18 exhibits the annual cycle monthly means averaged over a limited area for the selected regions LND (A), WAS (B), SWE (C) and SCA (D) for the time periods 2005, 2006 and 2005-2006. This allows to separate the internal model and/or data variability and the systematic differences between model results and CMSAF data. Additionally Fig. 19 exhibits the mean deviations for the selected regions for all data sets available and the period 2005-2006 in a more quantitative manner.
On the monthly time scale the deviations GME008-SAF120 exhibit two patterns with opposite signs of deviations. These patterns exhibit significant deviations of $(ATHB\_T - TET) \geq 15\,W/m^2$.

- First, Fig.19A shows weakly significant negative deviation of up to $-16.1\,W/m^2$ over WAS and of up to $-6.9\,W/m^2$ over LND in the winter months.

- Over SCA positive deviations of $9.4\,W/m^2$ occur in July and negative deviations of $-11\,W/m^2$ in January.
- Fig.19 exhibits an annual cycle of the differences of $7W/m^2$ over LND, $11W/m^2$ over WAS, $23W/m^2$ over SCA and no annual cycle over SWE.

The annual mean results indicate, that the cloud cover is significantly smaller and/or the cloud top higher in GME008 and that the cloud formation is also significantly disturbed over water surfaces. The suggestion of too low evaporation ($rat\_sea = 20$) in this simulation seems not to be correct due to relatively good agreement of TQV (see section 6.3). This has to be investigated in more detail.
The higher values of up long-wave radiation in the model over water surfaces, especially visible in winter, seems to be an additional effect, different from the two effects identified in the up short-wave radiation. Here the question arises, to which extent this effect originates in model deficiencies and to which extent in a data bias. One suggestion is that the land-sea contrast may have not the correct value in the CMSAF data. The results have to be investigated together with the cloud top height and/or the total cloud cover, which requires additional investigation. The comparison presented in 6.2 between CMSAF cloud top height and model convective cloud top height can not be used to answer this question. In summer the opposite effect seems to be present over LND, especially over SCA.

To clarify the origin of the land sea contrast in the differences additional comparisons and longer time series of CMSAF data are required.

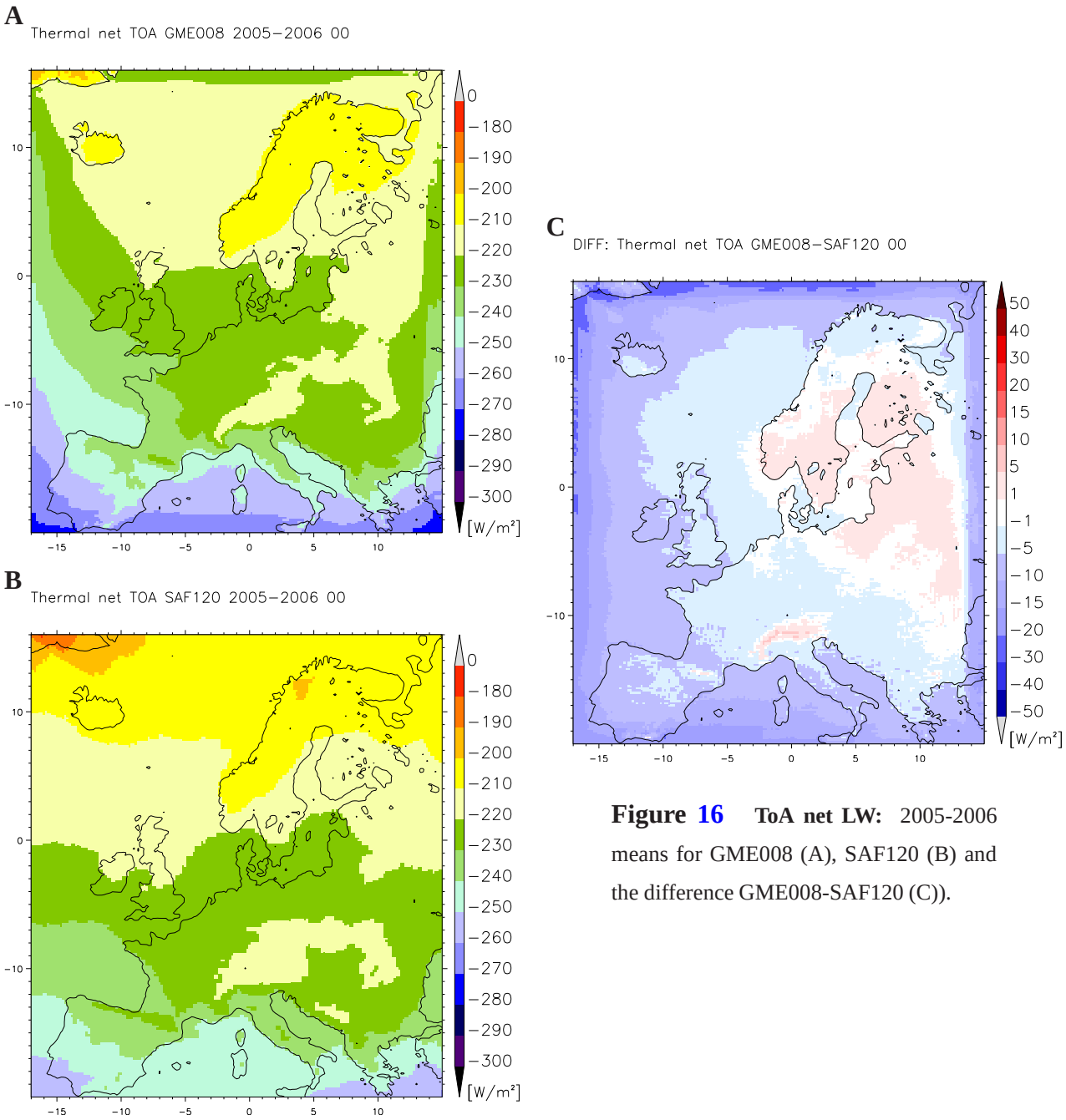

Figure 16 **ToA net LW:** 2005-2006 means for GME008 (A), SAF120 (B) and the difference GME008-SAF120 (C)).

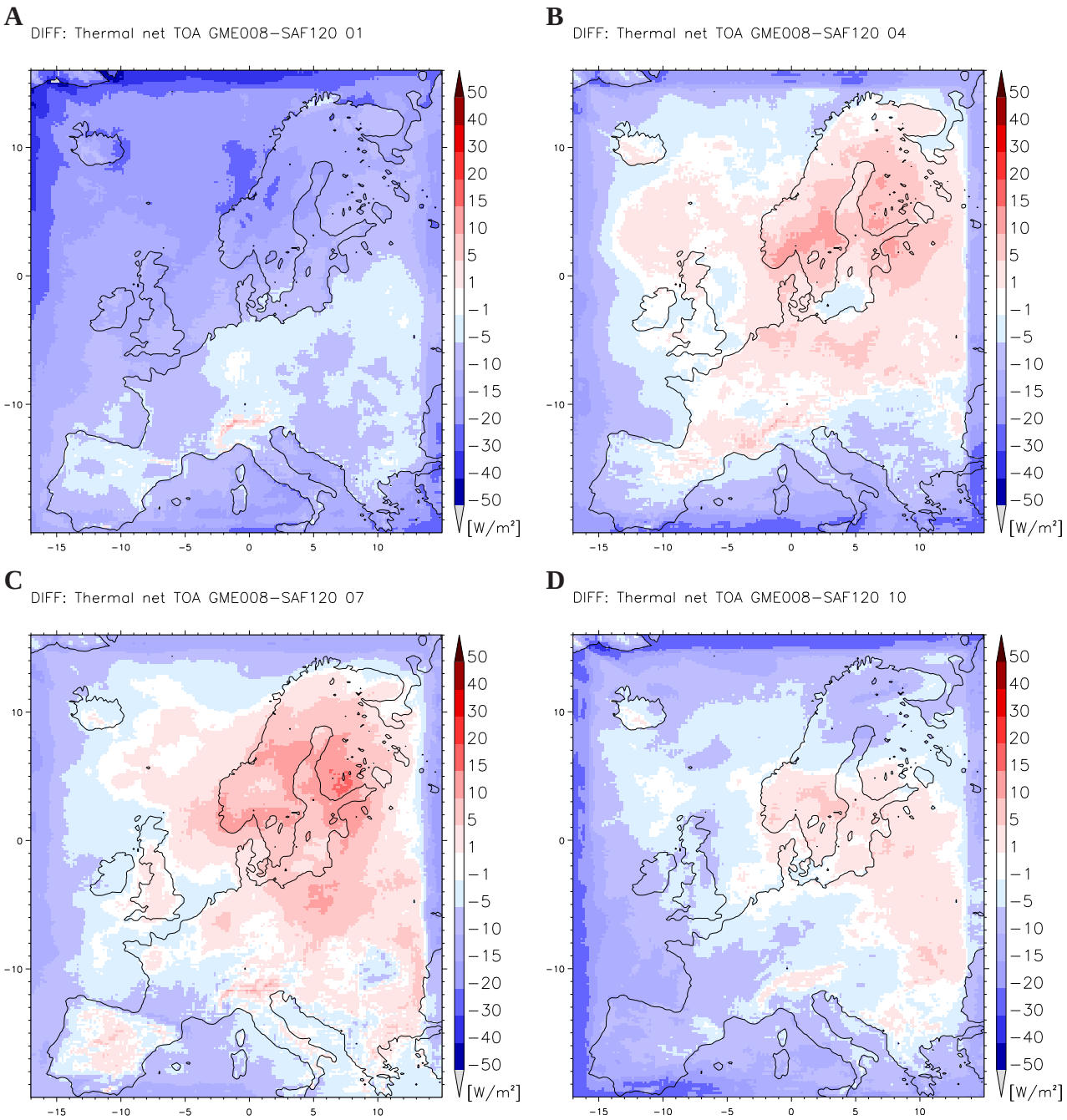

Figure 17 **ToA net LW:** monthly means of the differences GME008-SAF120 for January (A), April (B), July (C) and October (D) of the time period 2005-2006.

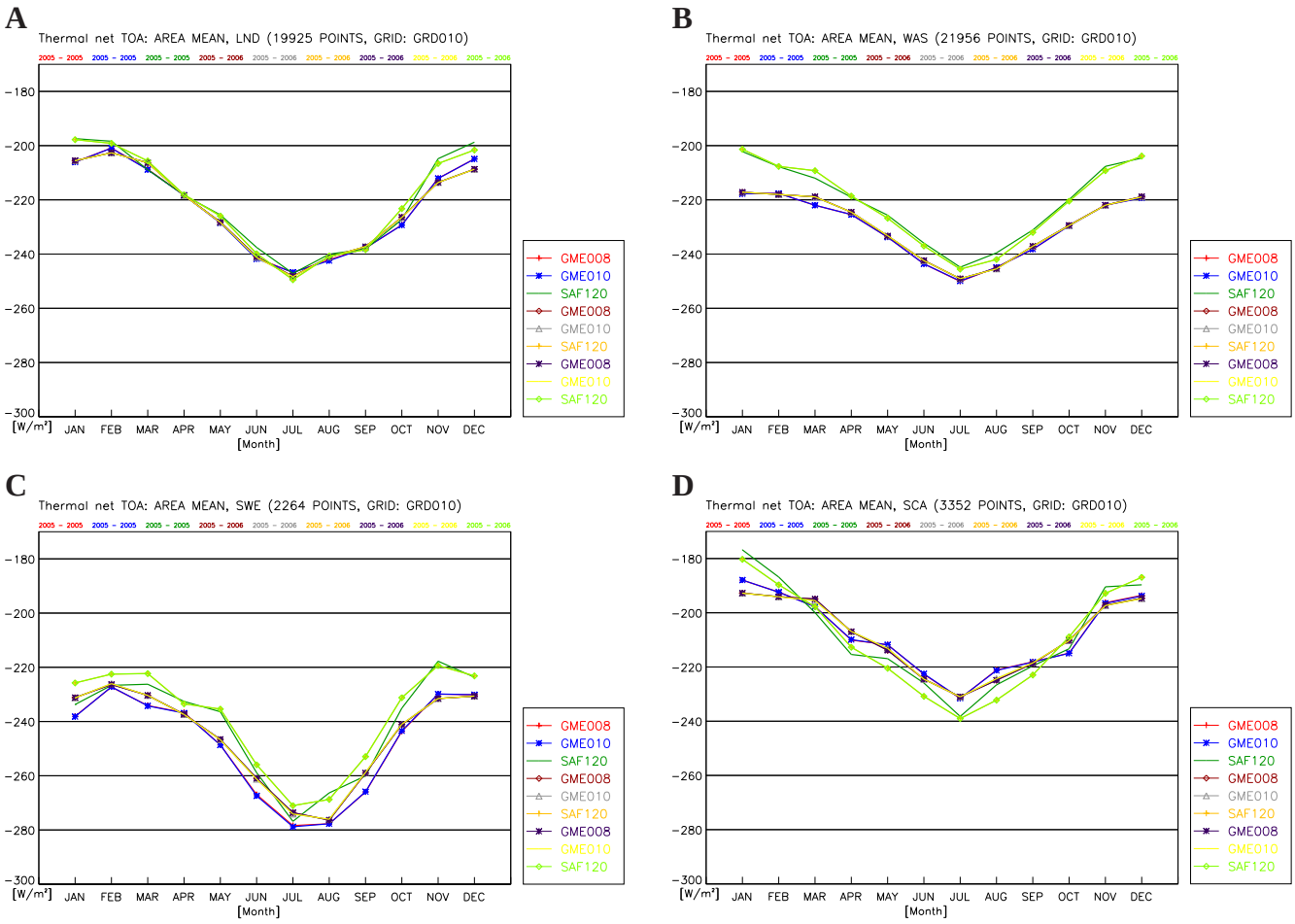

Figure 18 **ToA net LW:** Annual cycle of the monthly means of GME008, GME010 and SAF120 for LND (A), WAS (B), SWE (C) and SCA (D) for the years 2005, 2006 and 2005-2006.

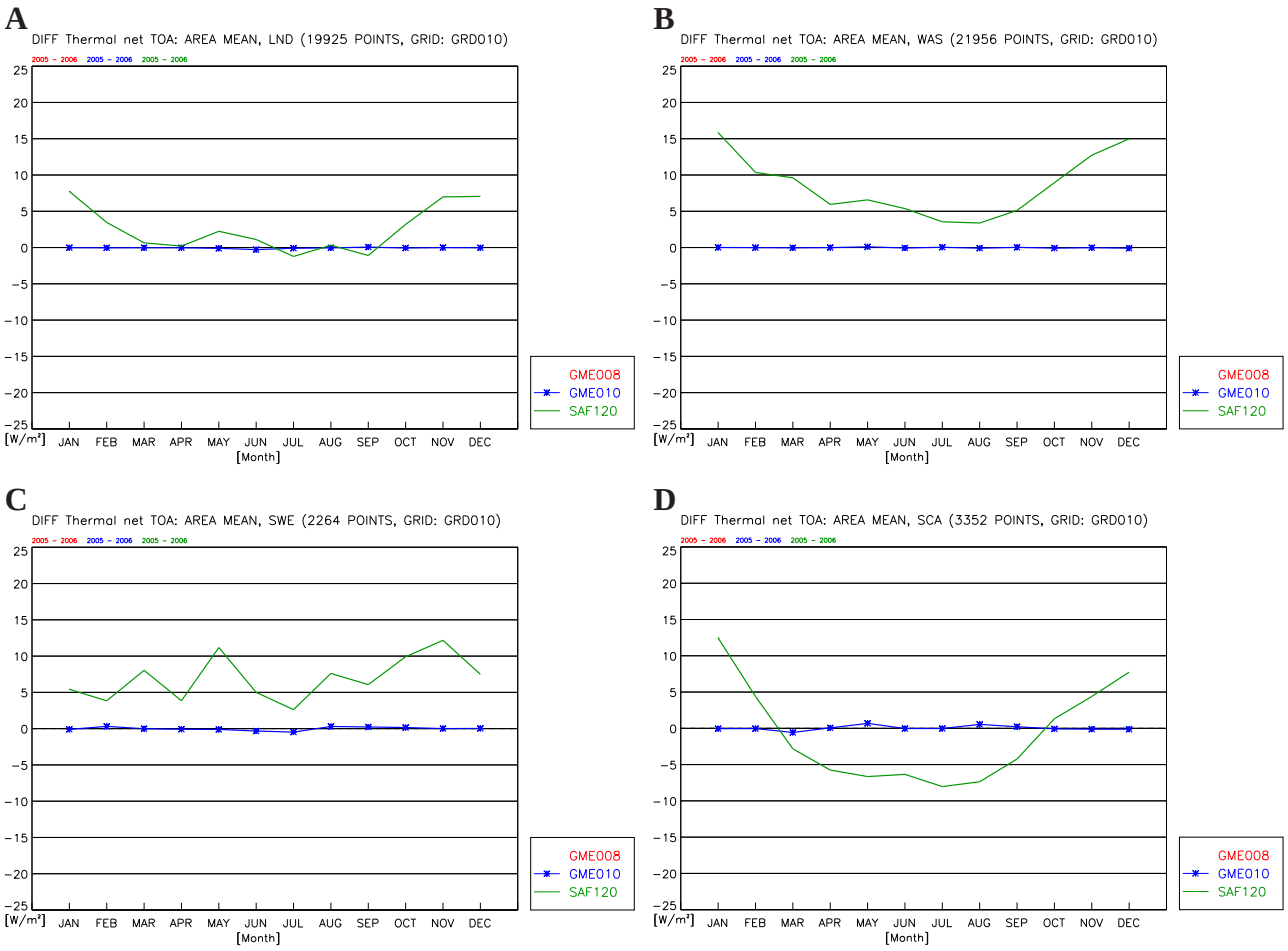

Figure 19 **ToA net LW:** annual cycle of the monthly mean differences Data-GME008 for LND (A), WAS (B), SWE (C) and SCA (D) for the time period 2005-2006.

5.5 ToA net radiation, 2005-2006, 2005, 2006

The satellite derived top of the atmosphere net radiation is denoted by TER (top emitted radiation). The corresponding CCLM quantity is the net radiation at the model top denoted by $ANRB\_T$ (net radiation budget ToA).

The accuracy of the CMSAF variable TER is given to be $\Delta TER = 14\,W/m^2$ for monthly means. The internal CCLM variability $\Delta ANRB\_T$ can be derived from Fig.23. It is up to $5\,W/m^2$ for different regions for monthly means.

Figure 20 A to C shows the ToA net radiation mean 2005-2006 of the GME008 simulation (A), of SAF120 (B) and their difference $ANRB\_S_{GME008} - TER_{SAF120}$ (C). The differences are smaller than the accuracy $\Delta_{24}(ANRB\_T - TER) = 4W/m^2$ over most parts of Europe. It exhibits the cancellation of the deviations for the SW and the LW net radiation components. Significant differences are found for

- the mean deviations in the West of the British Islands (BIS,$-12.8\,W/m^2$),
- over the Mediterranean Sea (MED, $-7.7\,W/m^2$) and
- over Scandinavia (SCA, $-12\,W/m^2$).
- All together, the model is emitting about $5W/m^2$ more energy ToA in comparison with CMSAF products.

Figures 21 A to D show the monthly mean differences at all grid points for January (A), April (B), July (C) and October (D) 2005-2006. Additionally Fig. 22 exhibits the spatial averages of the monthly means and Fig.23 the differences $XXX - ANRB\_S_{GME008}$ for the selected regions LND (A), WAS (B), SWE (C) and SCA (D), all data sets available and the time period 2005-2006.
On the monthly time scale the summer up SW radiation difference pattern dominates the results. This means

- a strongly significant down solar radiation deficit in GME008 in northern Europe ranging from $-25.6W/m^2$ over NWE to $-43.2W/m^2$ over SCA, which is about 15% of the solar radiative forcing of the atmosphere.

The patterns identified in the single ToA radiation components are hardly detectable in the radiation budget.

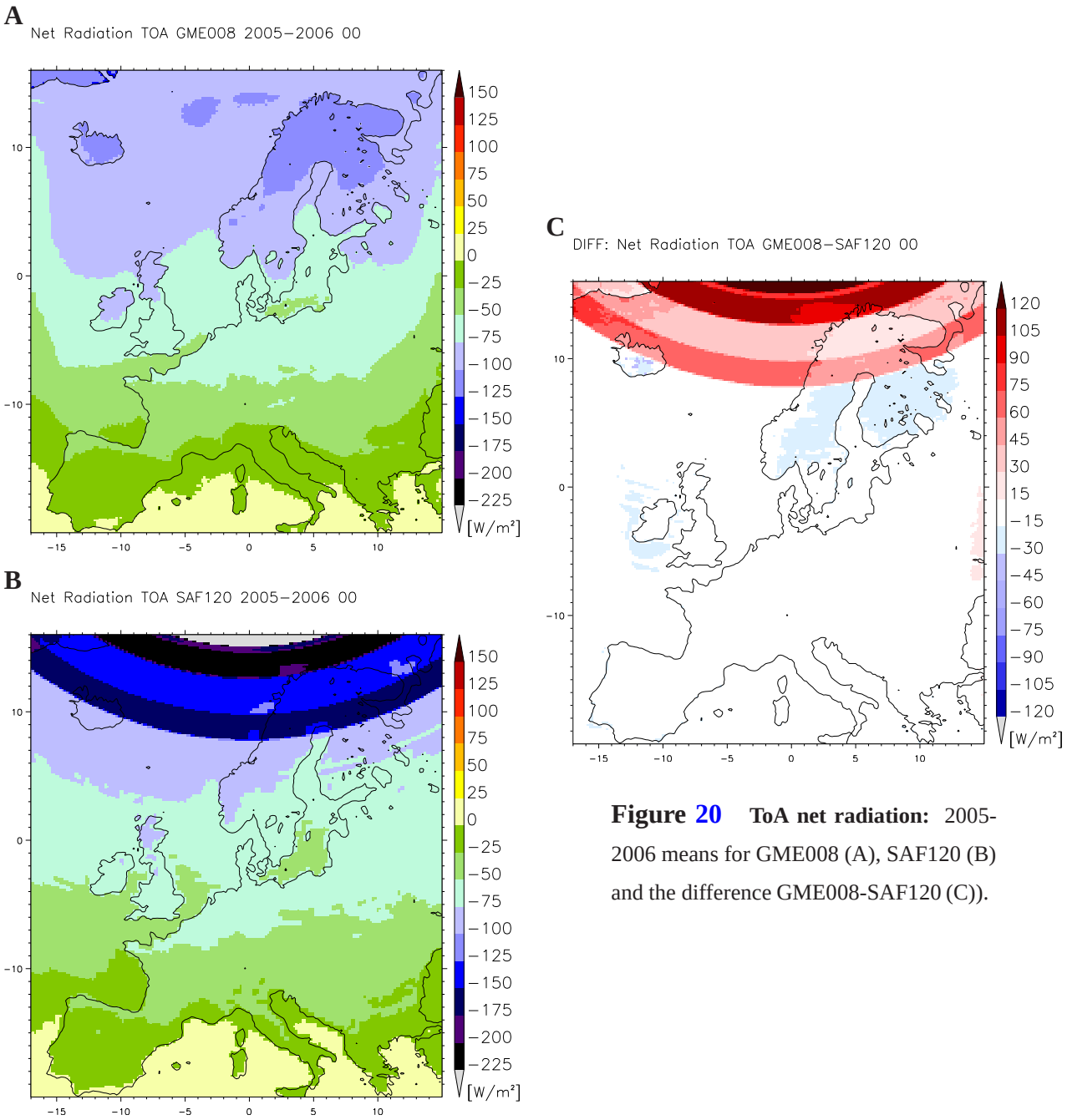

Figure 20 **ToA net radiation:** 2005-2006 means for GME008 (A), SAF120 (B) and the difference GME008-SAF120 (C)).

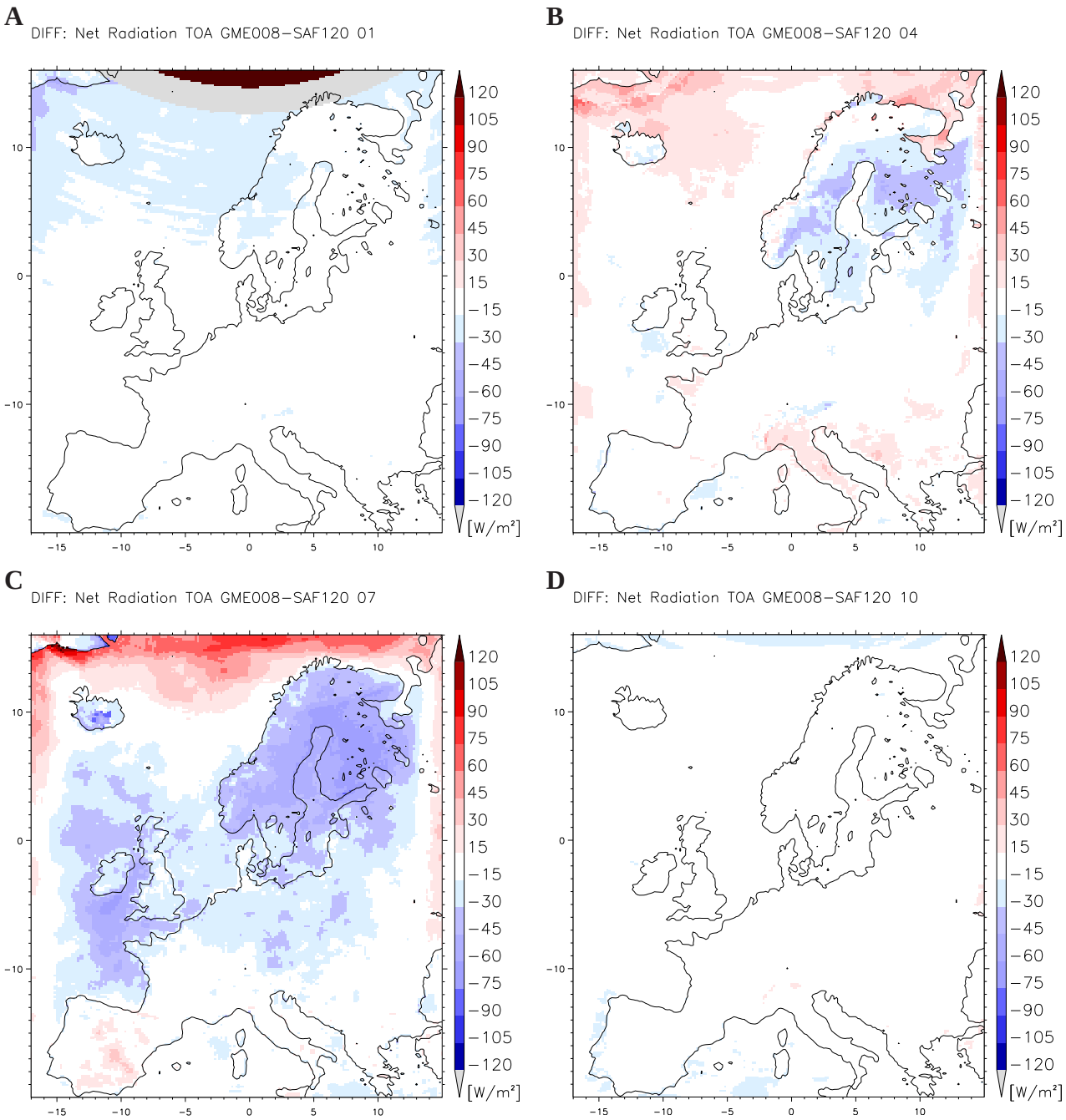

Figure 21 **ToA net radiation:** monthly means of the differences GME008-SAF120 for January (A), April (B), July (C) and October (D) of the time period 2005-2006.

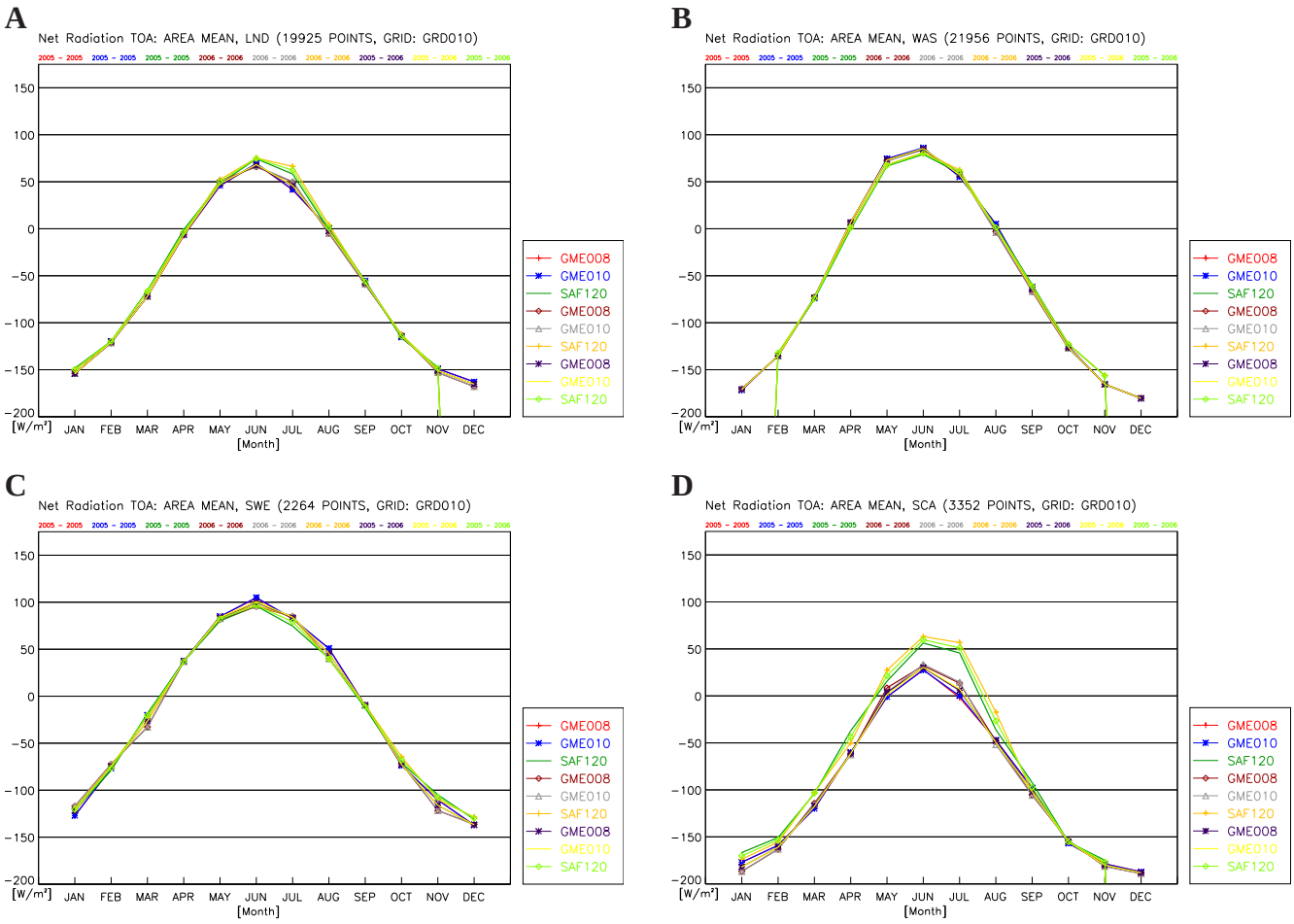

Figure 22 **ToA net radiation:** annual cycle of the monthly means of GME008, GME010 and SAF120 for LND (A), WAS (B), SWE (C) and SCA (D) for the years 2005, 2006 and 2005-2006.

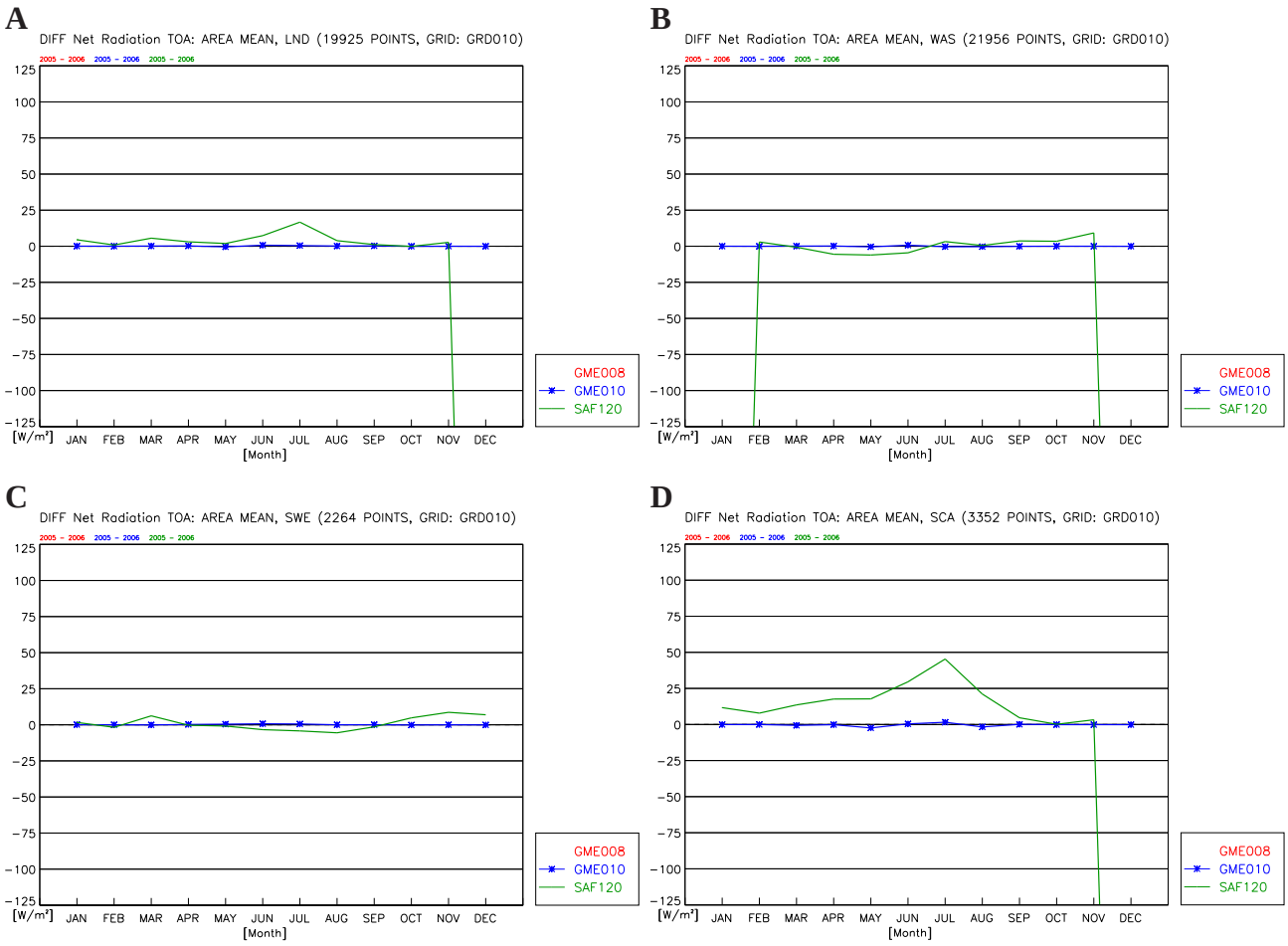

Figure 23 **ToA net radiation:** annual cycle of the monthly mean differences Data-GME008 for LND (A), WAS (B), SWE (C) and SCA (D) for the time period 2005-2006.

6 Cloud Properties and Water Vapour

The CMSAF data provide several parameters characterising the optical properties of the clouds also available from the GME0XX simulations. However, a direct comparison of the cloud properties are not straight forward due to limited detectability of clouds by satellite instruments resulting in a general underestimation of clouds in observations. Furthermore, different model outputs are based on different criteria for clouds. Most of the comparison studies apply corrections to model data. The criteria of these corrections are adjusted in such a way, that the mean deviations between model and satellite are minimised. This makes a comparison of the results of different studies impossible. [*Karlsson et al.*(2008)] describe the known observation restrictions and the correction procedure applied to RCA3 results. Stapelberg (2008) give results for cloud top pressure of the COSMO-DE in dependence on different criteria. In this study no correction of the model output has been applied and not all model variables have been used for the comparison. In this sense the results presented are first and preliminary results.

[*Karlsson et al.*(2008)] stated that the parameters total cloud cover (CLCT), vertical distribution of clouds (low, medium and high) and the cloud optical thickness (COT) are decisive for the radiative properties of the clouds. However, they are not sufficient for the analysis of model and data deficiencies.
In the following CLCT, convective cloud top height (HTOP_CON) and the vertically integrated water vapour (TQV) are investigated. The results for other model (and CMSAF) parameters will presented later.

6.1 Total Cloud Cover, 2006

The satellite derived total cloud cover is denoted by CFC (cloud fractional cover). The corresponding CCLM quantity is $CLCT$ (cloud cover total).

The accuracy of the CMSAF variable CFC is given to be $\Delta_{LND}CFC = 0.1CFC \simeq \pm 0.06$ over land and $\Delta_{WAS}CFC = 0.15CFC \simeq \pm 0.12$ over oceans for monthly means. The internal CCLM variability $\Delta CLCT$ can be derived from Fig.27. It is up to 0.03 for nearly all monthly means of different regions considered. In SCA the internal variability reaches 0.07 in summer months.

Figure 20 A to C shows the annual mean 2006 of the GME008 simulation (A), of SAF150 (B) and their difference GME008-SAF150 (C). The differences GME008-SAF150 are smaller than the accuracy of $\Delta_{12}(CLCT - CFC) = 0.03(0.04WAS)$ over most parts of Europe. We find

- strongly significant positive values over SCA ($(CLCT - CFC) = 0.16$),
- strongly significant negative differences over MED ($(CLCT - CFC) = -0.20$) and over all water surfaces WAS.($(CLCT - CFC) = -0.13$),
- a strong land-sea contrast in the CFC data due to significantly higher CFC over WAS (0.75) in comparison to CLCT over WAS (0.59),

- a strongly significant negative peak bias at the boundaries of up to $(CLCT - CFC) = -0.35$ with influence on the differences within the model domain and
- significant differences between the CMSAF data $(CFC_{SAF210} - CFC_{SAF150}) = 0.07$ over WAS and LND.

The different CMSAF products are inconsistent with respect to the absolute accuracy of the data given assuming a stochastic nature of the inaccuracy. A more careful separation of the stochastic and systematic component (error and bias) is missing.

Figures 25 A to D show the monthly mean differences at all grid points for January (A), April (B), July (C) and October (D) 2006. Additionally Fig. 26 exhibits the annual cycle of the means and 27 the differences between the data sets and GME008 results for all months for the selected regions LND (A), WAS (B), SWE (C) and SCA (D). This allows to relate the model internal variability, the differences between the data sets and between model and data.
On the monthly time scale

- the summer positive difference pattern of $(CLCT_{GME008} - CFC_{SAF150}) = 0.25$ over SCA and $(CLCT_{GME008} - CFC_{SAF150}) = 0.13$ over central Europe (MEU and EEU) and
- the January negative differences over water of $(CLCT_{GME008} - CFC_{SAF210}) = -0.32$ and land $(CLCT_{GME008} - CFC_{SAF210}) = -0.2$

dominate the results. The exceptional deviation of SAF210 in January seems to originate in the satellite data.

The comparison of the absolute values over SCA exhibits that the model also fails to simulate the observed decrease of the total cloud cover in spring to summer. The same behaviour is found in the RCA3 model simulation ([*Karlsson et al.*(2008)] even if the annual mean values are consistent with the satellite data.

The results for January and October clearly show, that the negative boundary difference is independent on the negative bias over WAS.

The attribution of the differences found within the model domain to model deficiencies and/or CMSAF data problems is not possible without longer CMSAF time serieses and additional sensitivity studies. Suggestions are made in the summary of the report.

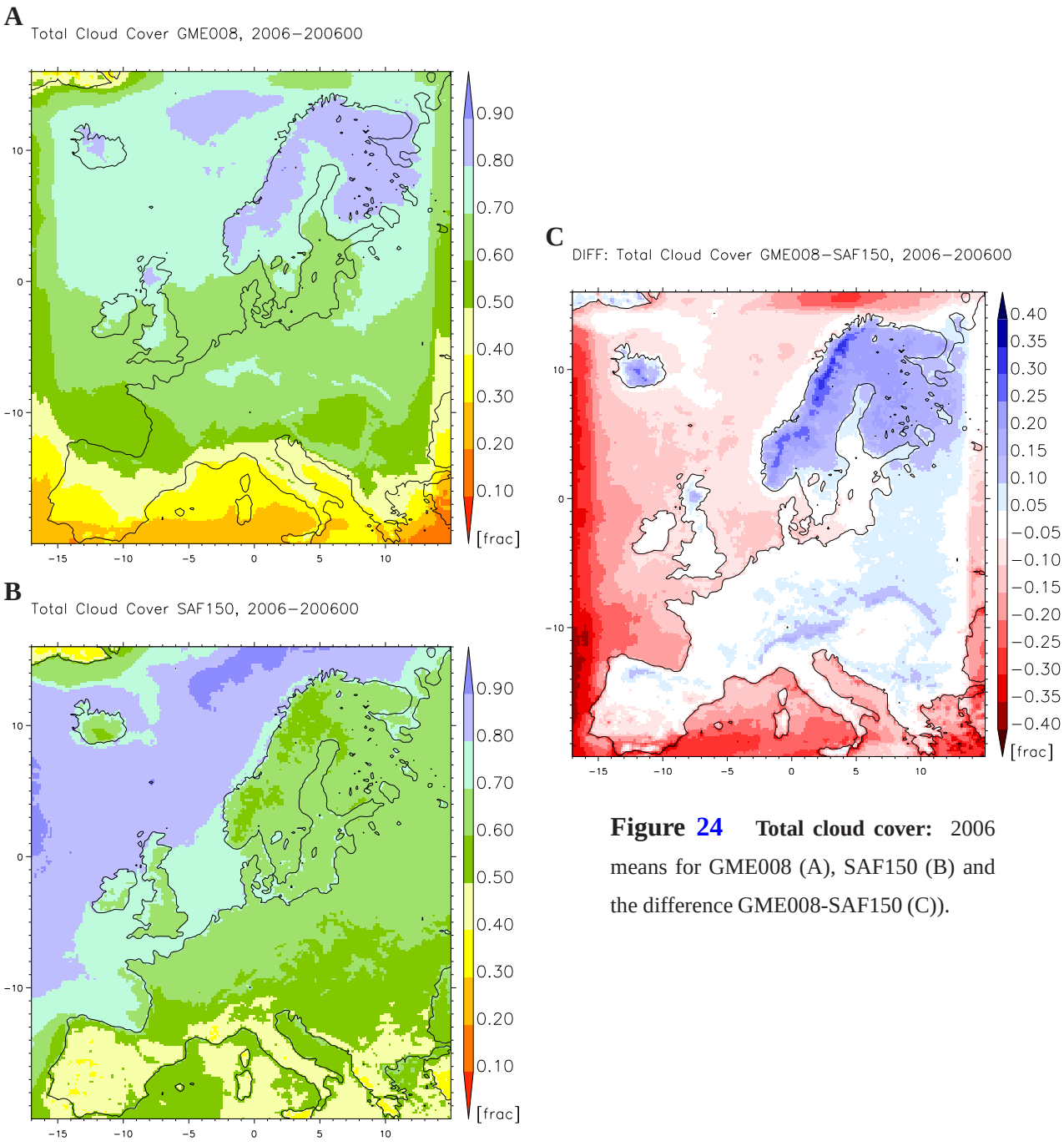

Figure 24 **Total cloud cover:** 2006 means for GME008 (A), SAF150 (B) and the difference GME008-SAF150 (C)).

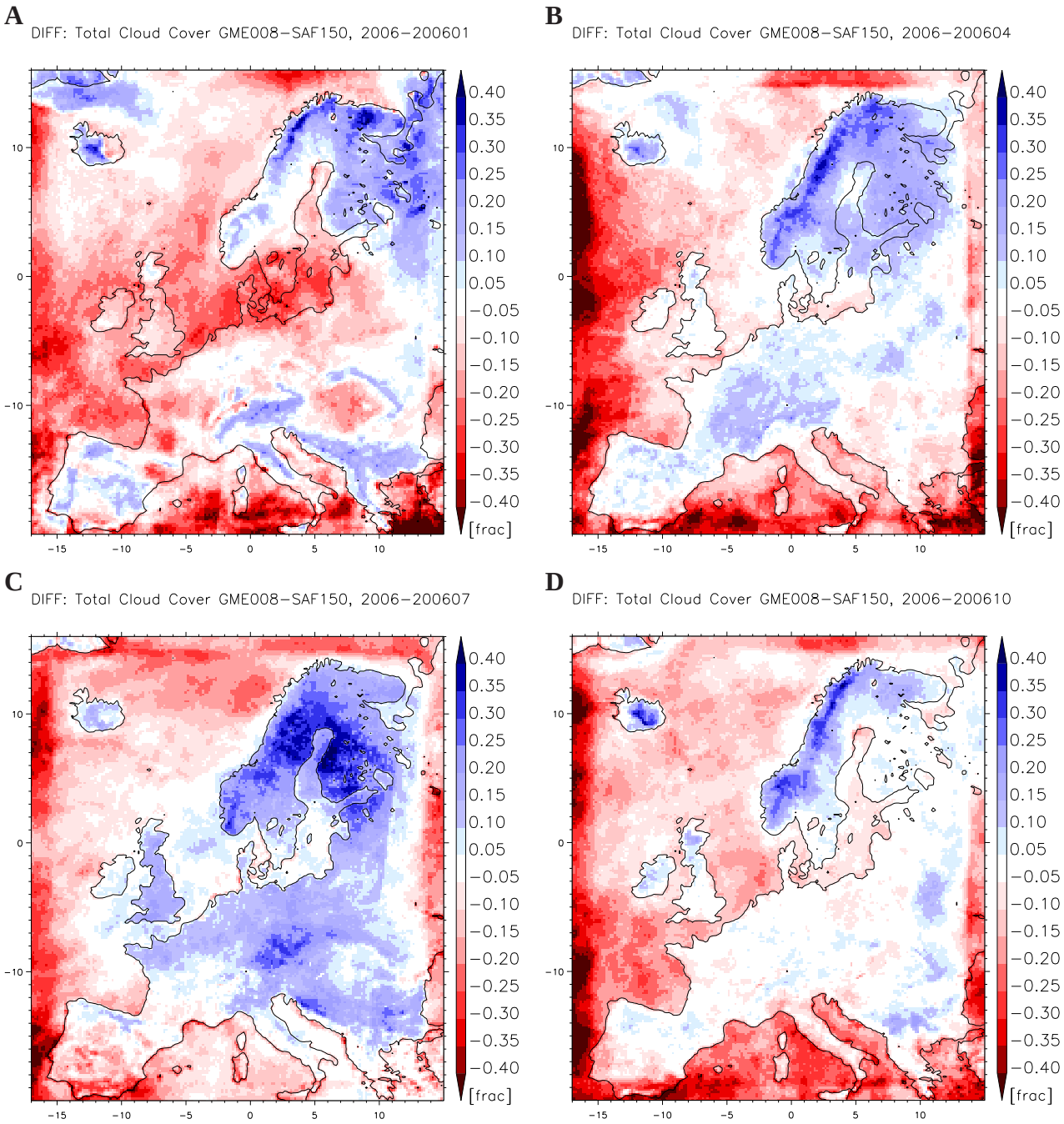

Figure 25 **Total cloud cover:** monthly means of the differences GME008-SAF150 for January (A), April (B), July (C) and October (D) of the year 2006.

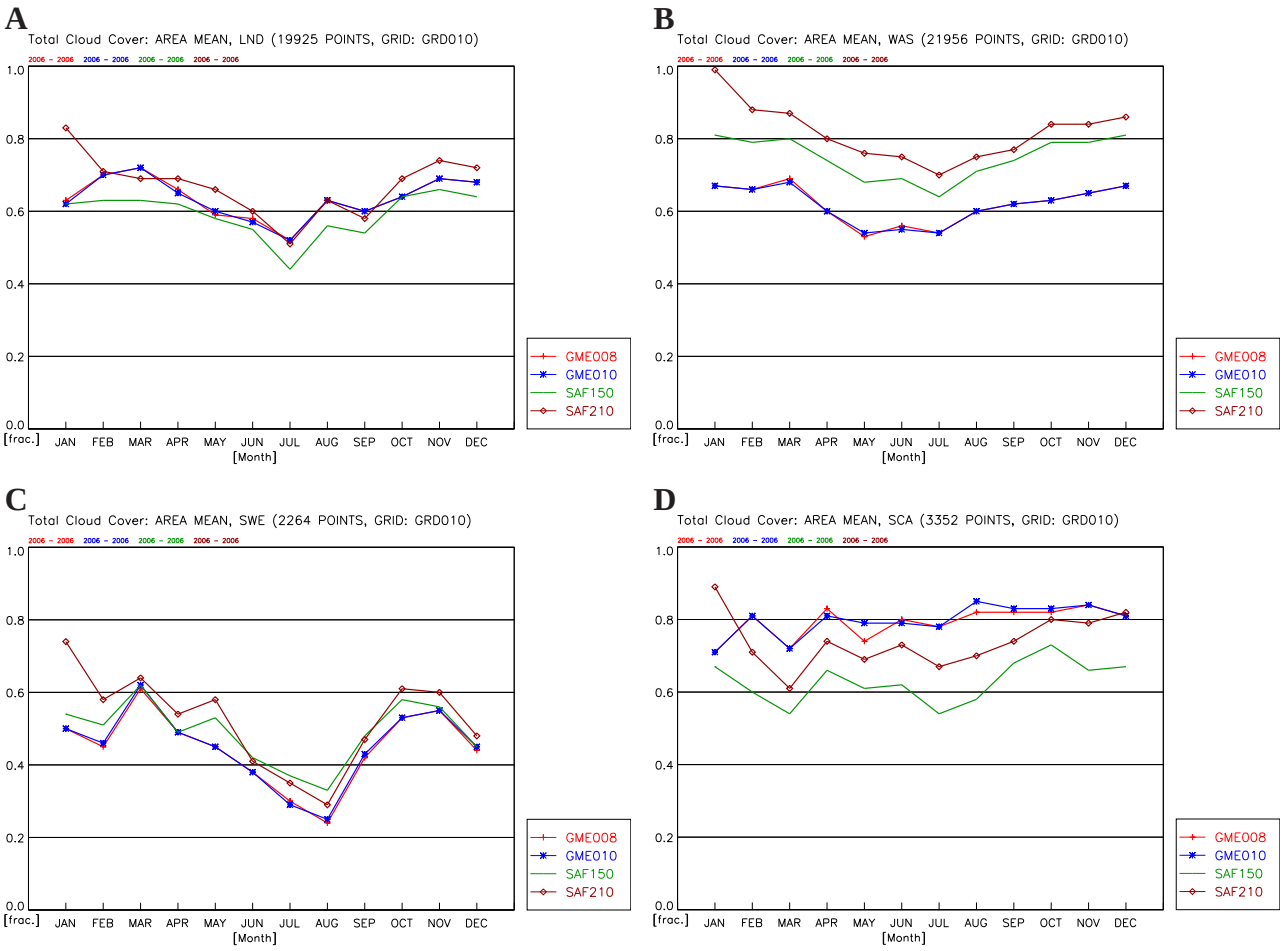

Figure 26 **Total cloud cover:** annual cycle of the monthly means GME008, GME010, SAF150 and SAF210, for LND (A), WAS (B), SWE (C) and SCA (D) for the year 2006.

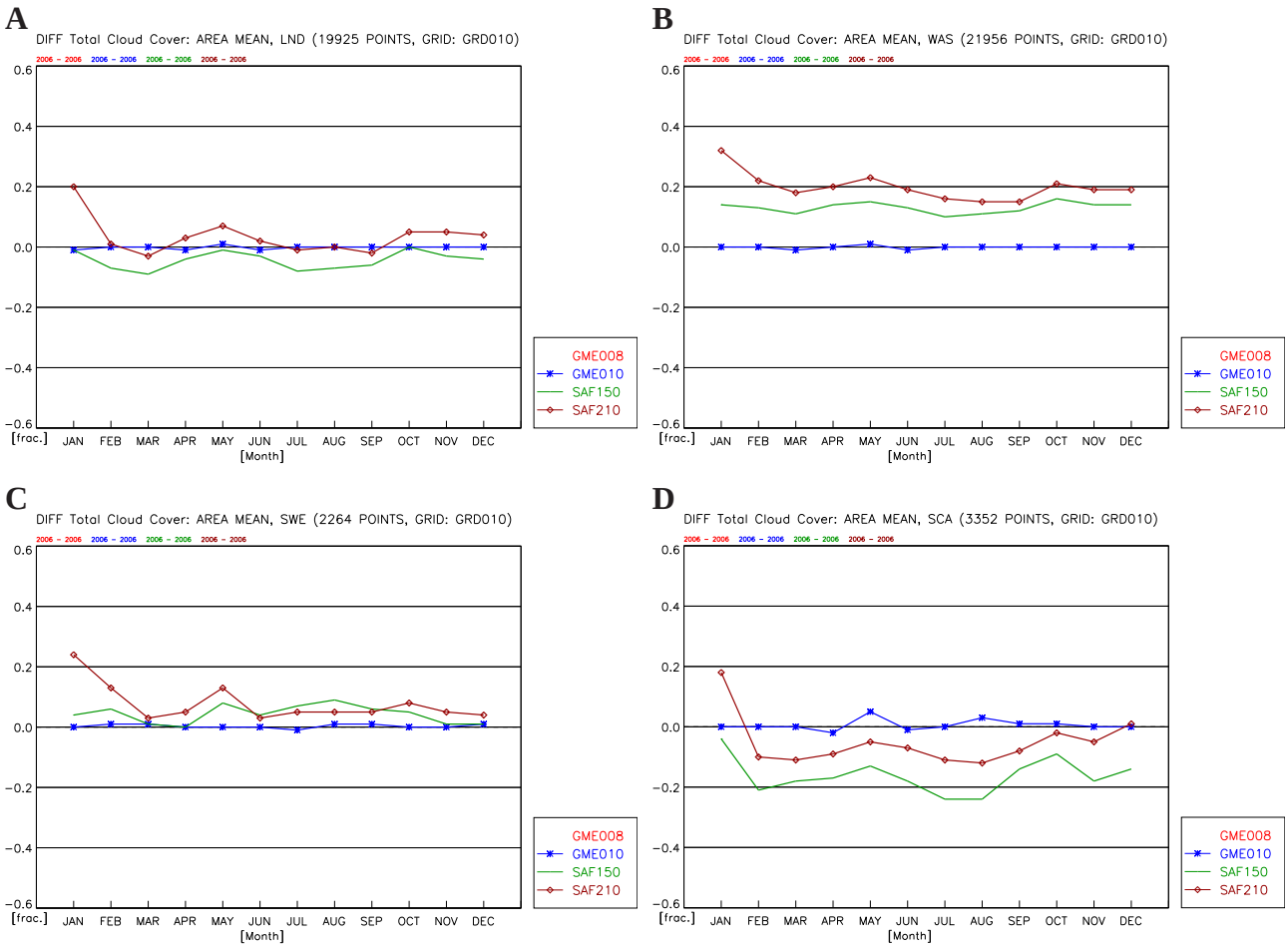

Figure 27 **Total cloud cover:** annual cycle of the monthly mean differences Data-GME008 for LND (A), WAS (B), SWE (C) and SCA (D) for the year 2006.

6.2 Convective Cloud Top Height, 2006

The satellite derived cloud top height is denoted by CTH (Cloud Top Height). The CCLM quantity used for the comparison is $HTOP\_CON$ (Convective Cloud Top Height), which is the convective cloud top height. A detailed investigation of the criteria used in the model for definition of cloud top height and of the accuracy of the instruments (see [*Karlsson et al.*(2008)]) for details) is needed before detailed interpretation of the cloud top height in the model and in CTH. The $HTOP\_CON$ values are expected to be smaller than the CTH values or equal for regions and time periods in which all clouds originate in model convection. This might be the case in summer in the Mediterranean region.

As presented by Stapelberg (2008) different criteria for cloud top height in the model provide substantial differences. This rises the question of model independent definition of CTH and remains for future work.

The accuracy of the CMSAF variable CTH is given to be $\Delta CTH = \pm 1000m$ for monthly means and $\Delta_{12} CTH = \pm 300m$ for annual means. The internal CCLM variability $\Delta HTOP\_CON$ can be derived from Fig.30. It is up to $100m$ for all monthly means of the different regions considered.

Even if the detailed quantitative interpretation of the results remains for future work general conclusions can be drawn from this comparison. Figure 28 A to C shows the annual mean 2006 of the GME008 simulation (A), of SAF150 (B) and their difference GME008-SAF150 (C). The differences GME008-SAF150 are substantial over most parts of northern Europe, as expected. We found

- negative values over NEL, NEW ($HTOP\_CON - CTH = -1500$) and
- significant differences between the CMSAF data SAF150 and SAF210 for most of the regions of $CTH_{SAF210} - CTH_{SAF150} \geq 1000m$.
- a significant increase of the difference from South to Nord. This indicates a much stronger convective activity in the Mediterranean, as expected.

Figures 29 A to D show the monthly mean differences at all grid points for January (A), April (B), July (C) and October (D) 2006. Additionally Fig. 30 exhibits the spatial averages of the monthly means and Fig.31 the differences between the data sets and GME008 results for the selected regions LND (A), NEW (B), SWE (C) and SCA (D) for the time period 2006.
Fig.29 shows that the $HTOP\_CON$ values in winter months and in the North are substantially smaller than the CTH values. This confirms the general expectation. However $HTOP\_CON_{GME008} - CTH_{SAF150} \simeq 1000$ in the summer in the Mediterranean region, which indicates an overestimation of convection in the model or an underestimation of cloud top height in SAF150. Fig.30 and 31 show additionally the results for the CTH taken from SAF210. The results are strongly affected by the features of this particular year. However, CTH taken from SAF210 is more than 2000m higher in SWE than that from SAF150 in the region of South-West Europe (SWE) and $HTOP\_CON$ increases by roughly 2000m in June and July, which seems to be unrealistic.

Due to the inconsistency of the SAF-products with respect to the accuracy specifications, a too short

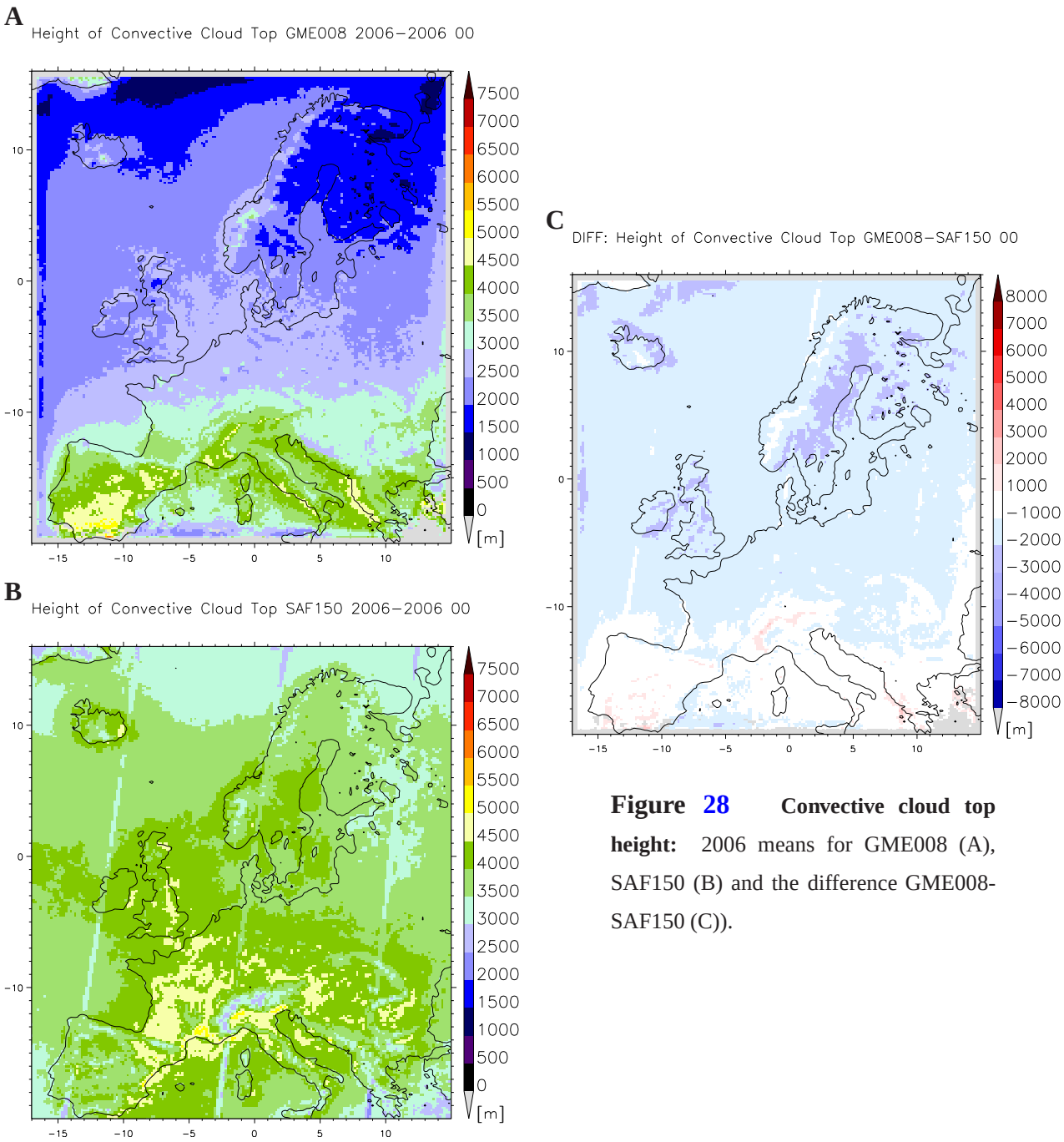

Figure 28 **Convective cloud top height:** 2006 means for GME008 (A), SAF150 (B) and the difference GME008-SAF150 (C)).

time series of the SAF data and inadequate model variable it is not possible to draw conclusions. The comparison shows the high potential of further investigation of the cloud properties.

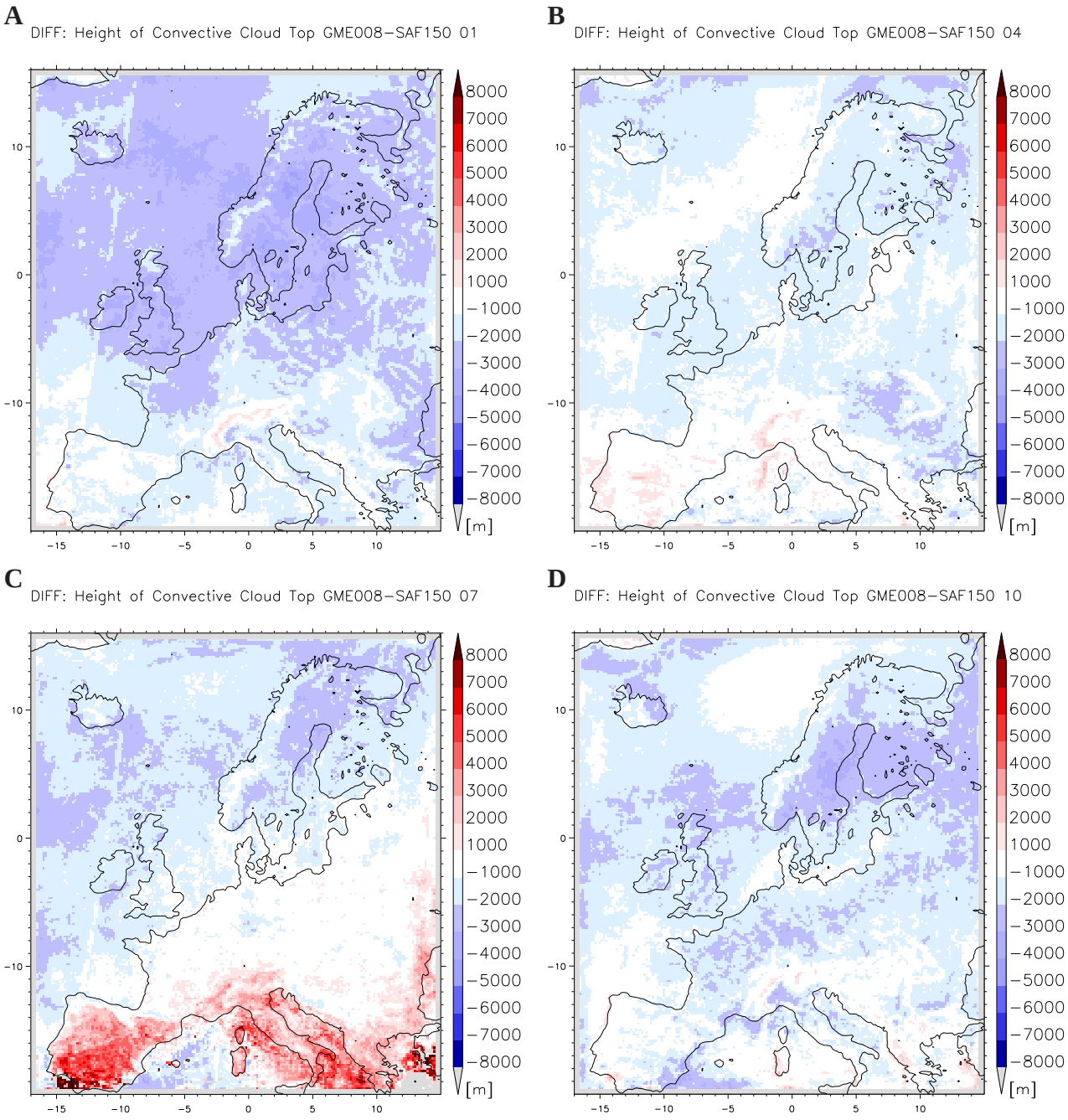

Figure 29 **Convective cloud top height:** monthly means of the differences GME008-SAF150 for January (A), April (B), July (C) and October (D) of the year 2006.

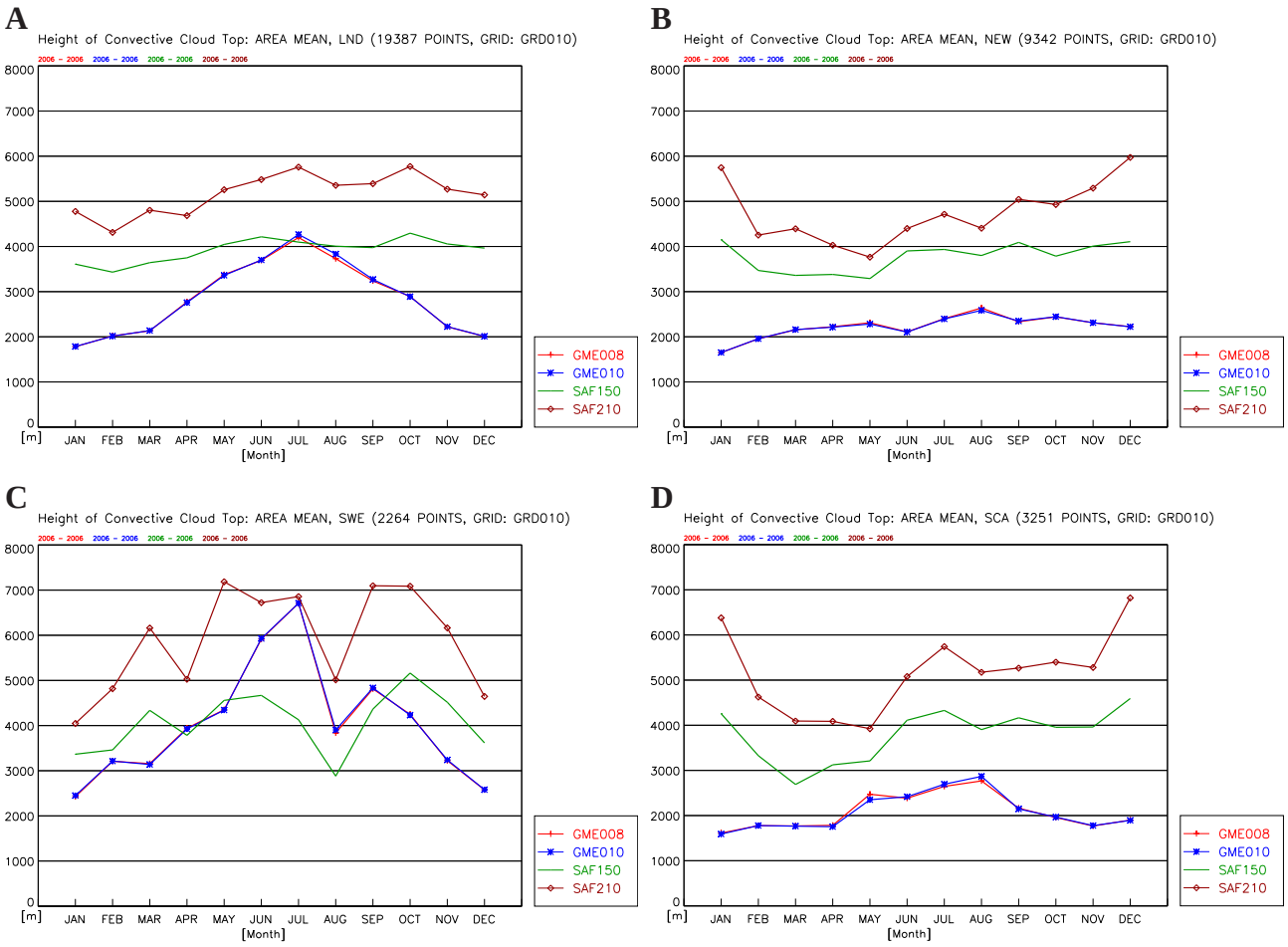

Figure 30 **Convective cloud top height:** annual cycle of the monthly means GME008, GME010, SAF150 and SAF210 for LND (A), NEW (B), SWE (C) and SCA (D) for the year 2006.

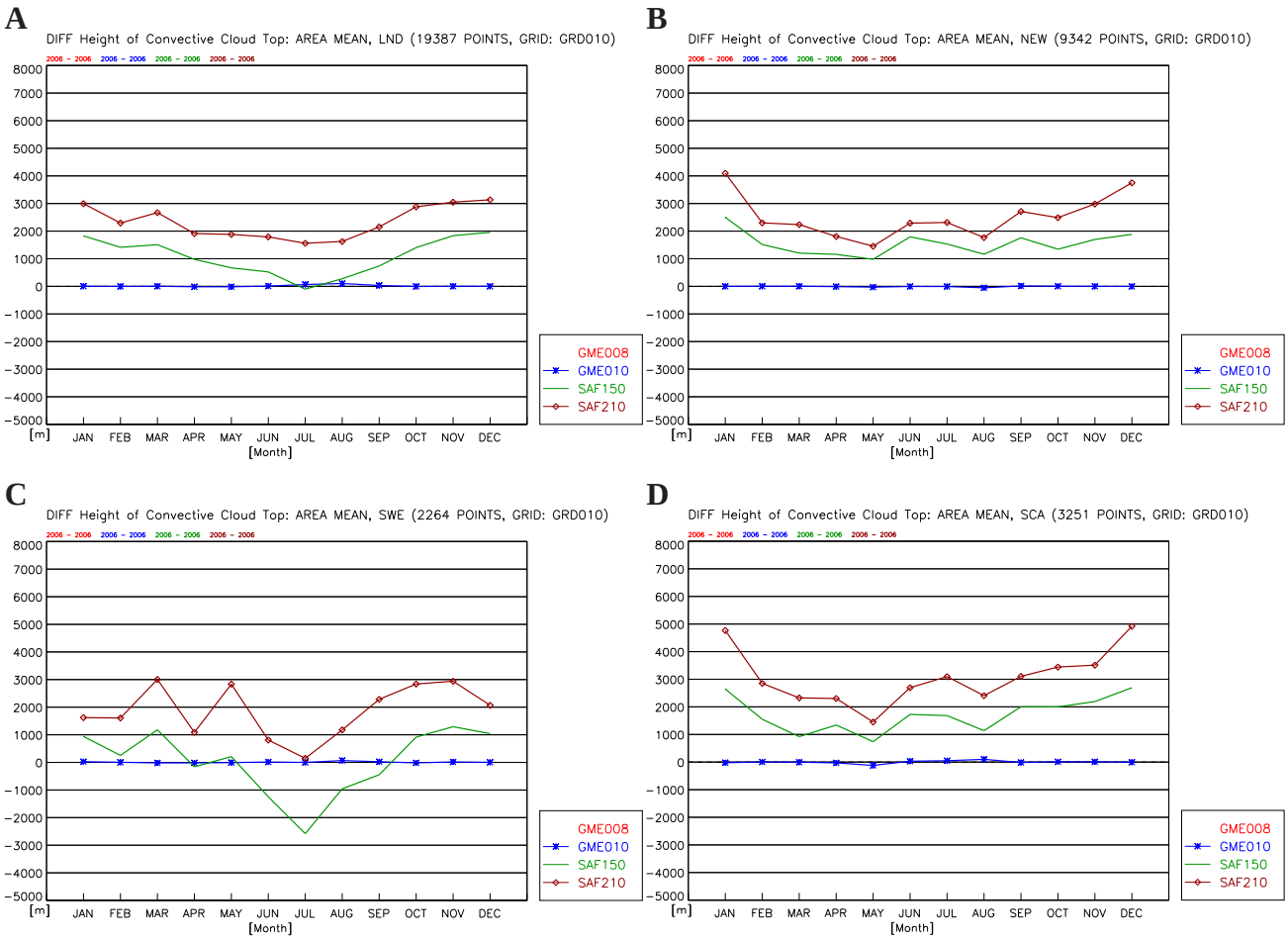

Figure 31 **Convective cloud top height:** annual cycle of the monthly mean differences Data-GME008 for LND (A), NEW (B), SWE (C) and SCA (D) for the year 2006.

6.3 Vertically Integrated Water Vapour, 2006

The satellite derived vertically integrated water vapour is denoted by HTW_TPW. The corresponding CCLM quantity is TQV (total QV, QV: water vapour).

The accuracy of the CMSAF variable HTW_TPW is given to be $\Delta HTW\_TPW = \pm 1mm$ for monthly means. The internal CCLM variability ΔTQV can be derived from Fig.35. It is up to $\pm 0.5mm$ for monthly means of different regions considered.

Figure 32 A to C shows the annual mean 2006 of TQV of GME008 simulation (A), of HTW_TPW of SAFH30 data (B) and their difference $TQV - HTW\_TPW$ (C). We found the following significant differences with respect to the accuracy $\Delta_{12}(TQV - HTW\_TPW) = 0.04mm$:

- negative differences over most parts of central and southern Europe.
- positive differences ($TQV - HTW\_TPW = 0.93$) in the Poe valley and weakly significant positive differences on the North side of the Alps. They might result from different spatial resolutions of the data and different orographies.

These differences come together with

- a stronger decrease of TQV in the model over land with 20.65 mm over MED and 16.42 mm over SUE in comparison with 20.92 mm over MED and 18.42 mm over SUE for HTW_TPW.

A more careful analysis of the vertically integrated water vapour over land and over sea in the Mediterranean region is needed in order to attribute the differences between model and satellite data to the model results and/or to the satellite products.

Figures 33 A to D show the monthly mean differences at all grid points for January (A), April (B), July (C) and October (D) 2006. Additionally Fig.34 exhibits the annual cycle of the spatial averages of the monthly means for the selected regions LND (A), WAS (B), SWE (C) and SCA (D) for 2006. Furthermore, Fig.35 shows the differences between the data sets GME010 and SAFH30 and the GME008 results shown in Fig.34.
On the monthly time scale we found:

- winter negative difference pattern with $(TQV_{GME008} - HTW\_TPW_{SAFH30}) = -1.23$ over WAS and $(TQV_{GME008} - HTW\_TPW_{SAFH30}) = -2.34$ over SCA,
- summer negative difference pattern $(TQV_{GME008} - HTW\_TPW_{SAFH30}) = -2.84$ over southern Europe and
- summer positive difference pattern $(TQV_{GME008} - HTW\_TPW_{SAFH30}) = 2.64$ over the POE valley.

The results for the annual means, the January and October clearly show, that the negative difference at the coasts of Italy and the Balkan region is independent on the negative difference over WAS. Furthermore, Fig.73 exhibits, that the precipitation is not overestimated over these land sites.

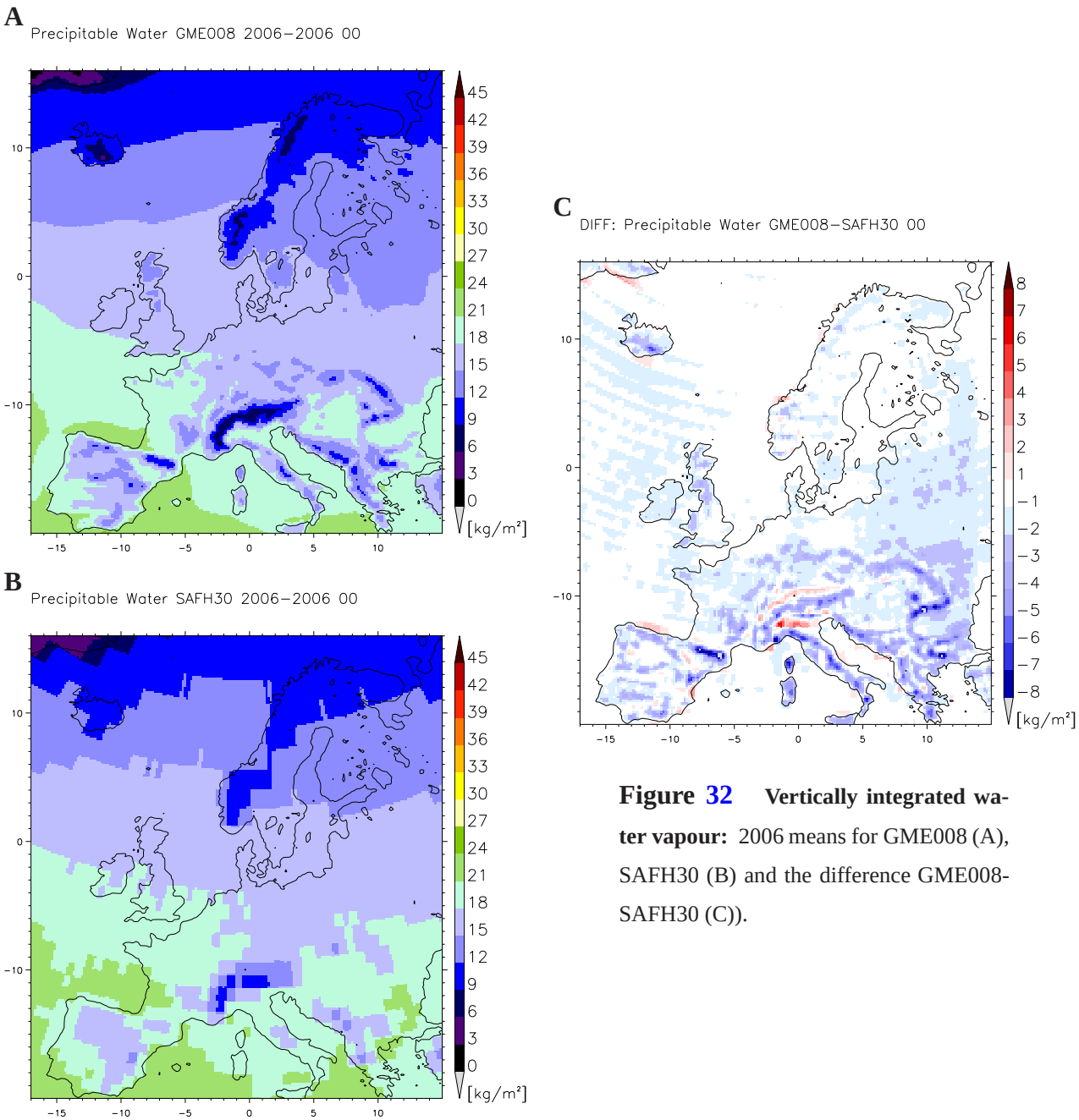

Figure 32 **Vertically integrated water vapour:** 2006 means for GME008 (A), SAFH30 (B) and the difference GME008-SAFH30 (C)).

The attribution of the origin of the differences requires a longer time series of SAF data and an additional comparison on the grid of SAFH30 data.

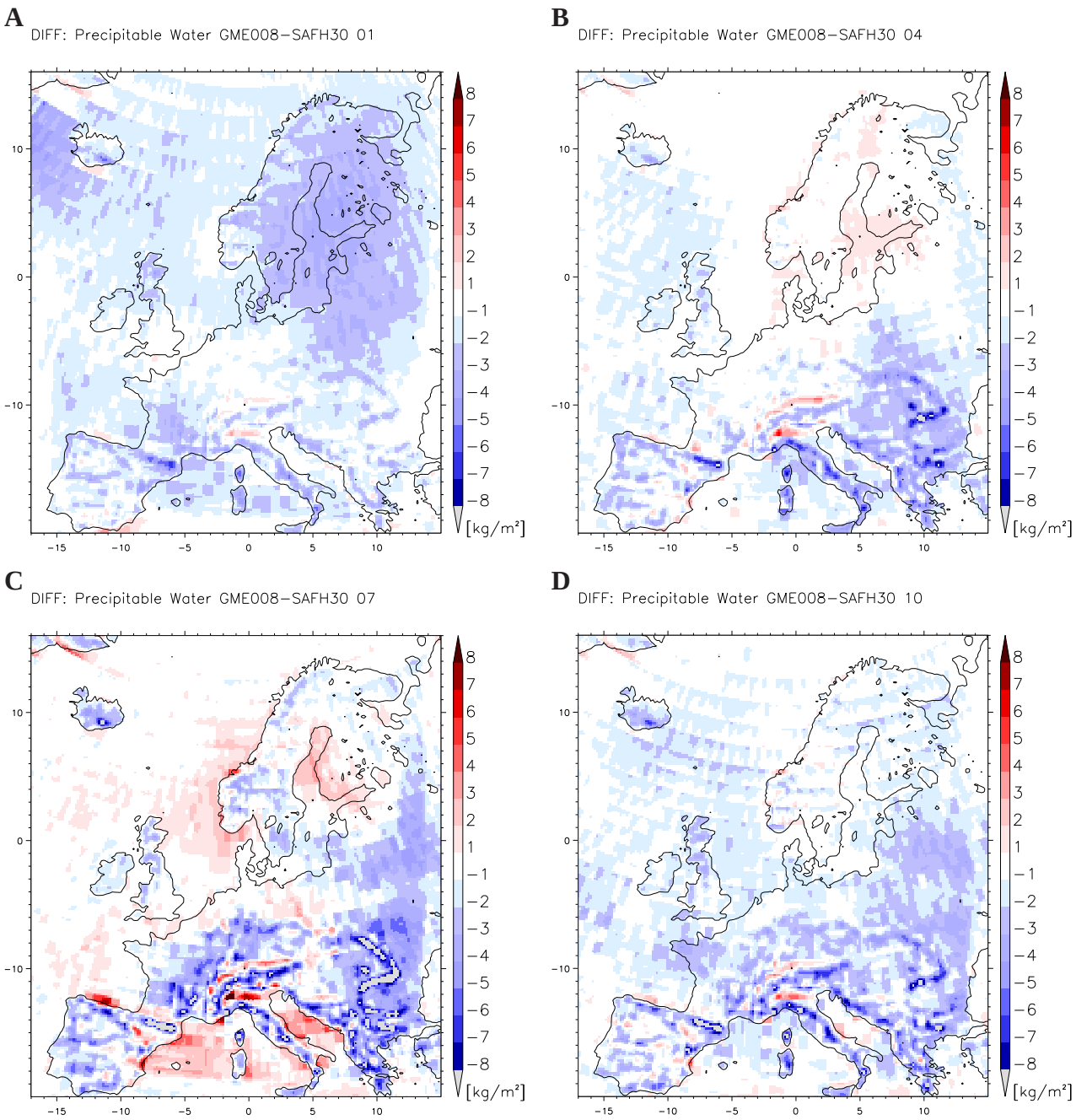

Figure 33 **Vertically integrated water vapour:** monthly means of the differences GME008-SAFH30 for January (A), April (B), July (C) and October (D) of the year 2006.

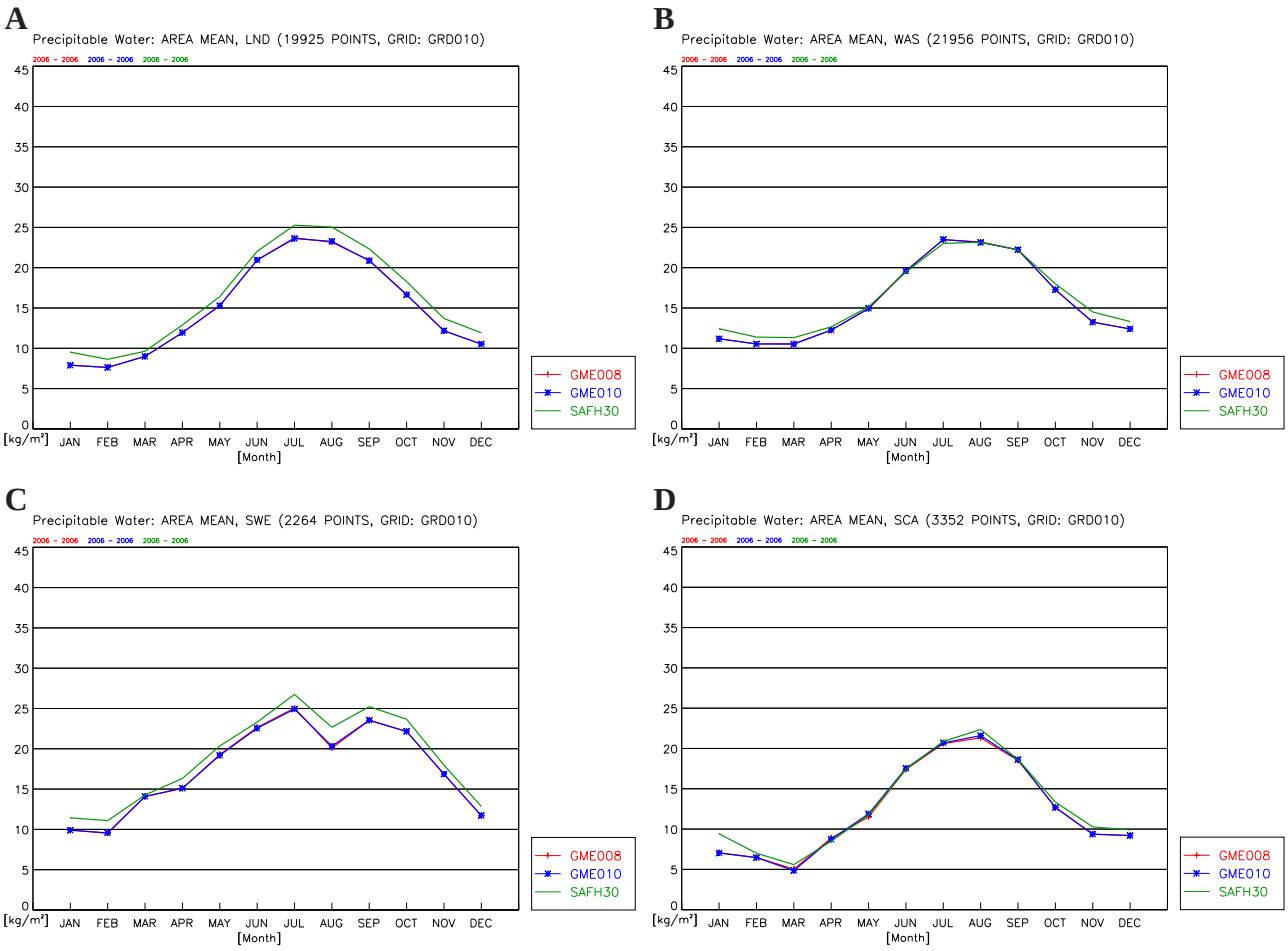

Figure 34 **Vertically integrated water vapour:** annual cycle of the monthly means GME008, GME010 and SAFH30 for LND (A), WAS (B), SWE (C) and SCA (D) for the year 2006.

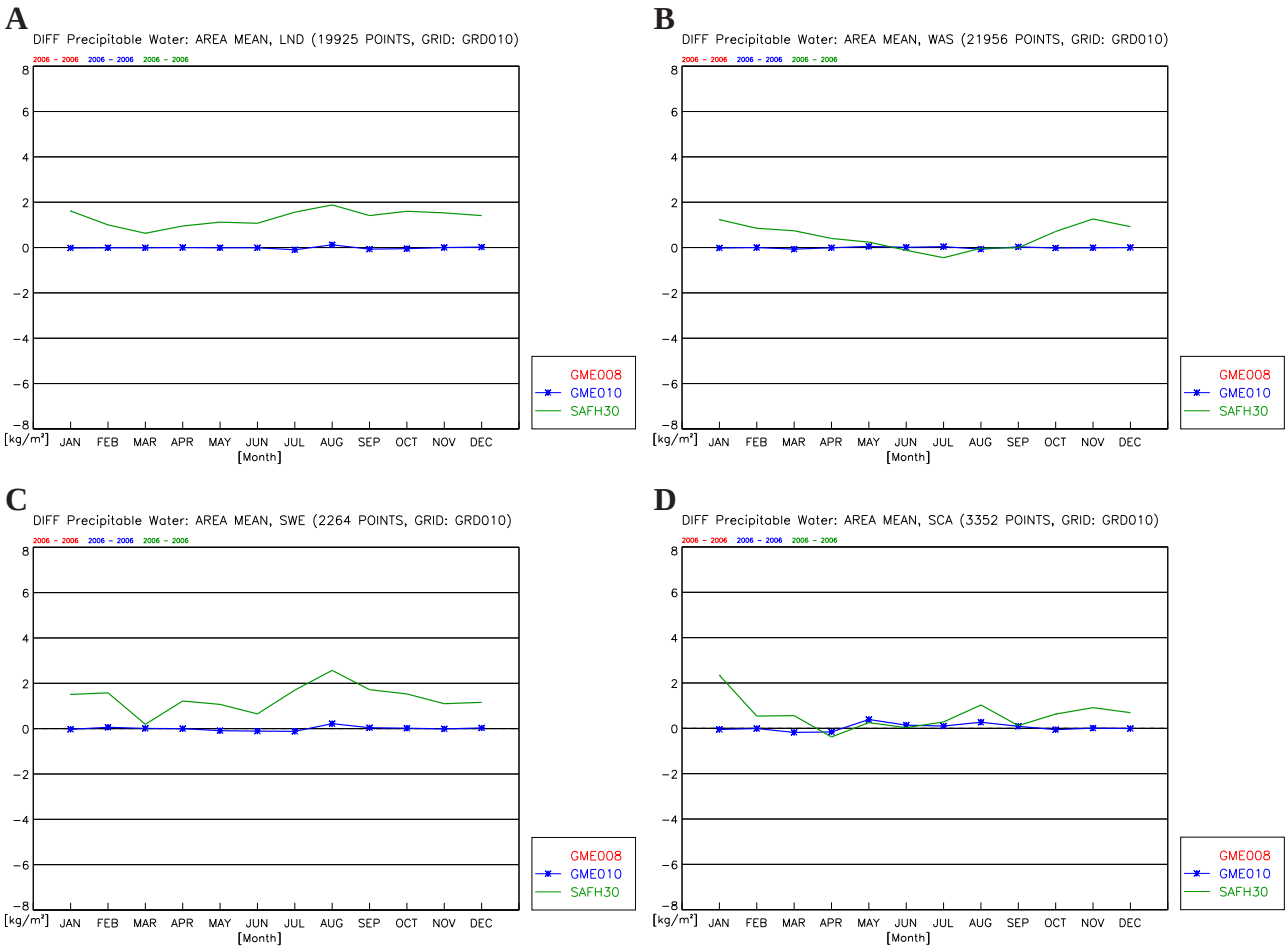

Figure 35 **Vertically integrated water vapour:** annual cycle of the monthly mean differences Data-GME008 for LND (A), WAS (B), SWE (C) and SCA (D) for the year 2006.

7 Surface

7.1 Surface down SW, 2006

The satellite derived surface down solar radiation is denoted by SIS (surface incoming solar). The corresponding CCLM quantity $ASWG\_S$ (short wave global down at the surface) is a sum of two components: the direct $ASWDIR\_S$ and the diffusive down $ASWDIFD\_S$ short-wave radiation at the surface.

The accuracy of SIS is given as $\Delta SIS = 10\,W/m^2$ for monthly means. The internal CCLM variability $\Delta ASWG\_S$ can be derived from Fig.39. It is up to $5\,W/m^2$ for summer to winter months and up to $\Delta ASWG\_S = 15\,W/m^2$ in spring with peak values in SCA. The resulting accuracy for the difference is $\Delta(ASWG\_S - SIS) = 12(17)\,W/m^2$.

Figure 36 A to C shows the annual mean 2006 of the GME008 simulation (A), of SAF210 (B) and their difference GME008-SAF210 (C). The differences GME008-SAF210 exceed the accuracy $\Delta_{12}(ASWG\_S - SIS) = 4(7)W/m^2$ over most parts of Europe. We found:

- Significant negative differences $(ASWG\_S - SIS) = 12\,W/m^2$ over the model domain except for the northern, western and eastern boundary parts of Italy and the Balkan region.
- Significant positive differences $(ASWG\_S - SIS) = 10\,W/m^2$ over the northern, western and eastern boundary.

Figures 37 A to D show the monthly mean differences at all grid points for January (A), April (B), July (C) and October (D) 2006. Additionally Fig.38 and Fig.39 exhibit the mean deviations for all months for the selected regions LND (A), WAS (B), SWE (C) and SCA (D) in a more quantitative manner. On the monthly time scale the deviations GME008-SAF210 exhibit additional spatial and temporal structures with significant deviations of $(ASWG\_S - SIS) \geq 12\,W/m^2$:

- negative differences over the central model domain in the period May to September with peak values in July of $(ASWG\_S - SIS) = -50\,W/m^2$ and $(ASWG\_S - SIS) = -96.1\,W/m^2$ over SSK,
- no significant positive differences over the northern, western and eastern boundary in winter, as for the total cloud cover.
- significant positive differences of $(ASWG\_S - SIS) = 6\,W/m^2$ in SUE in Spring with peak values in ALP of $23.1W/m^2$.
- weakly significant positive differences of $(ASWG\_S - SIS) = 12.1\,W/m^2$ in northern Scandinavia (NSK) in April.

All significant patterns of deviation are hypothesised to have different reasons.

- The positive deviation in SUE in April (Italy, Balkan and Greece) may be an exception of the April 2006 caused by models internal variability.

- The positive deviations in ALP and SCA with peak values in April are correlated with the deviations of the albedo and are probably caused by overestimation of the snow albedo and increased incoming diffusive short wave radiation.
- The positive deviation in the boundary zone may be caused by inappropriate boundary conditions for humidity quantities causing an underestimation of the cloud cover.
- The strong negative deviation over the model domain in the summer with peak values in May to September over Scandinavia comes along with too high cloud cover (see Fig. 25) and too high relative humidity near the ground (not shown here) and no significant differences in water vapour content indicating an overestimation of convection and/or an underestimation of entrainment/detrainment between the boundary layer and the free atmosphere in the model run.
- A not significant north-south gradient of roughly $10\,W/m^2$ per 2000km occurs in the January difference of Figure 37, which is nearly free of the effects discussed above. This may be caused by inappropriate adjustment of the satellite measurements.

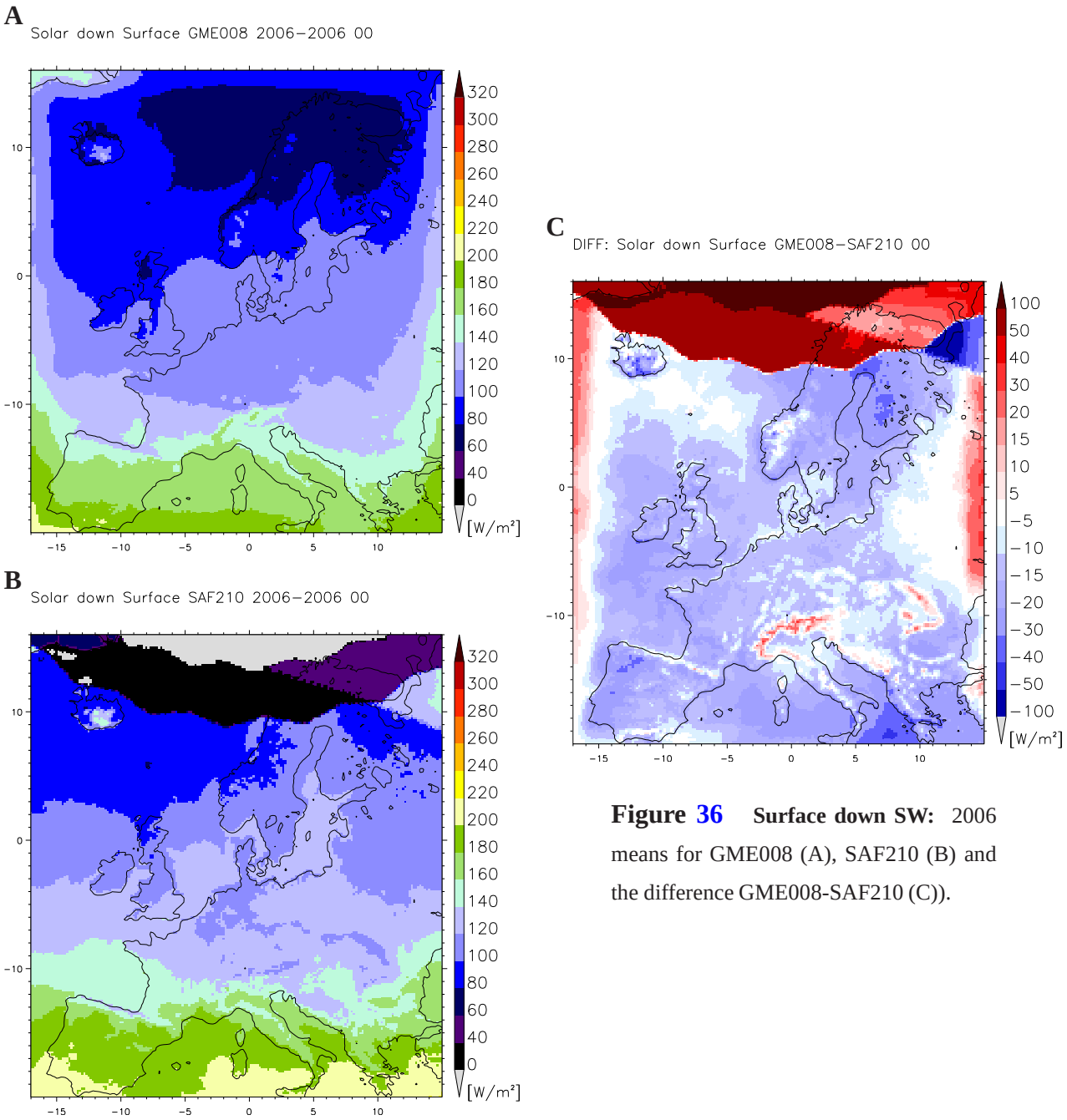

Figure 36 **Surface down SW:** 2006 means for GME008 (A), SAF210 (B) and the difference GME008-SAF210 (C)).

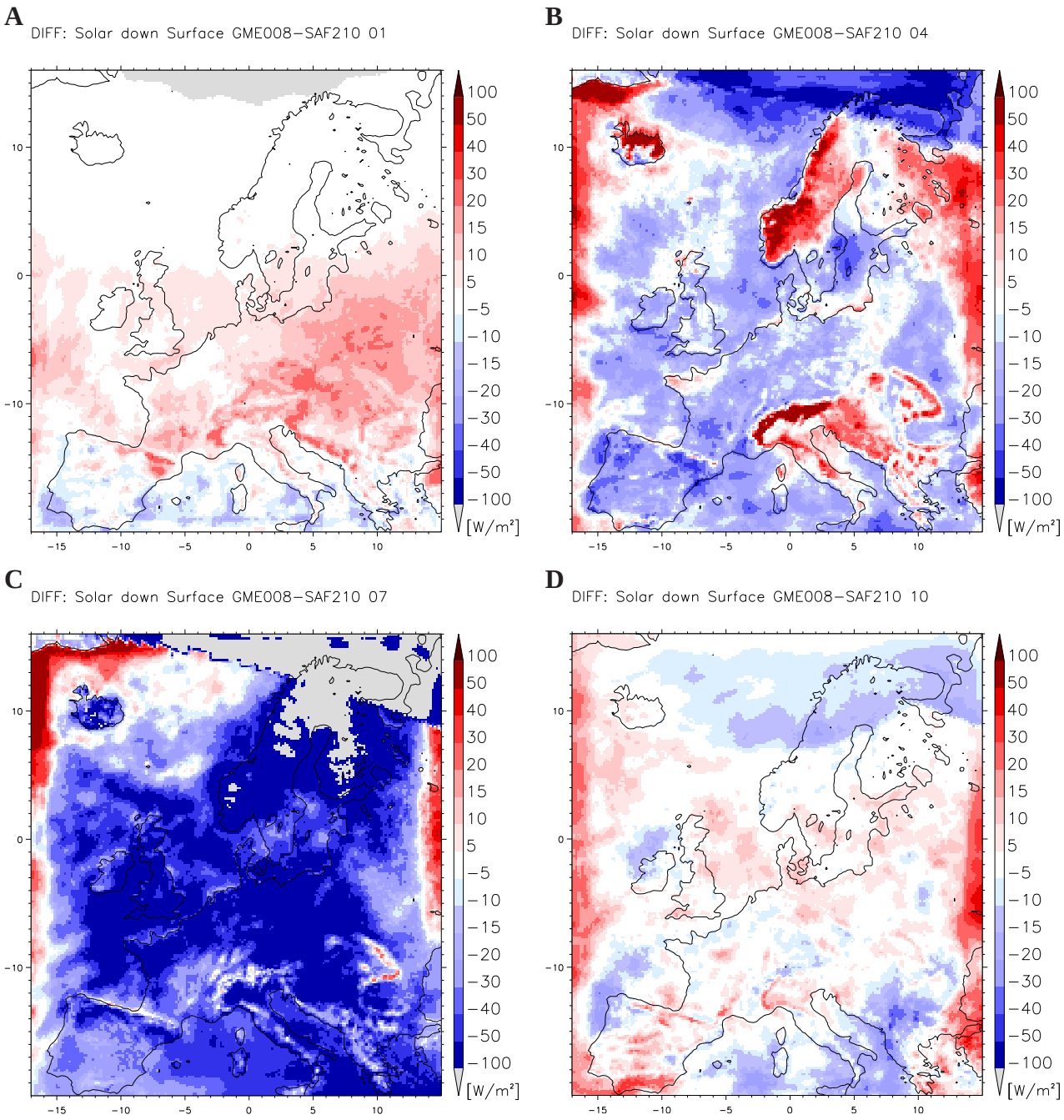

Figure 37 **Surface down SW:** monthly means of the differences GME008-SAF210 for January (A), April (B), July (C) and October (D) of the year 2006.

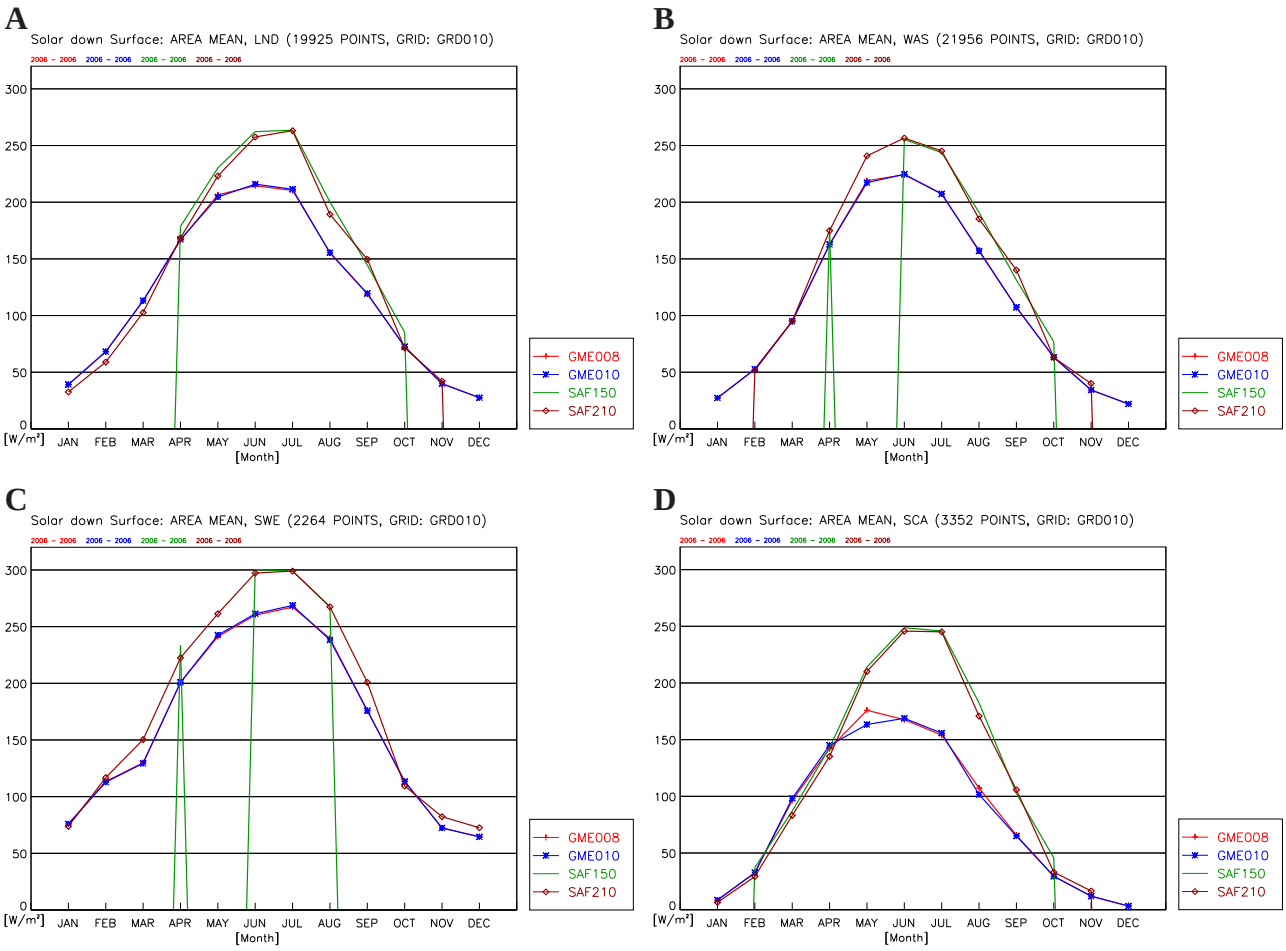

Figure 38 **Surface down SW:** annual cycle of the monthly means GME008, GME010, SAF150 and SAF210 for LND (A), WAS (B), SWE (C) and SCA (D) for the year 2006.

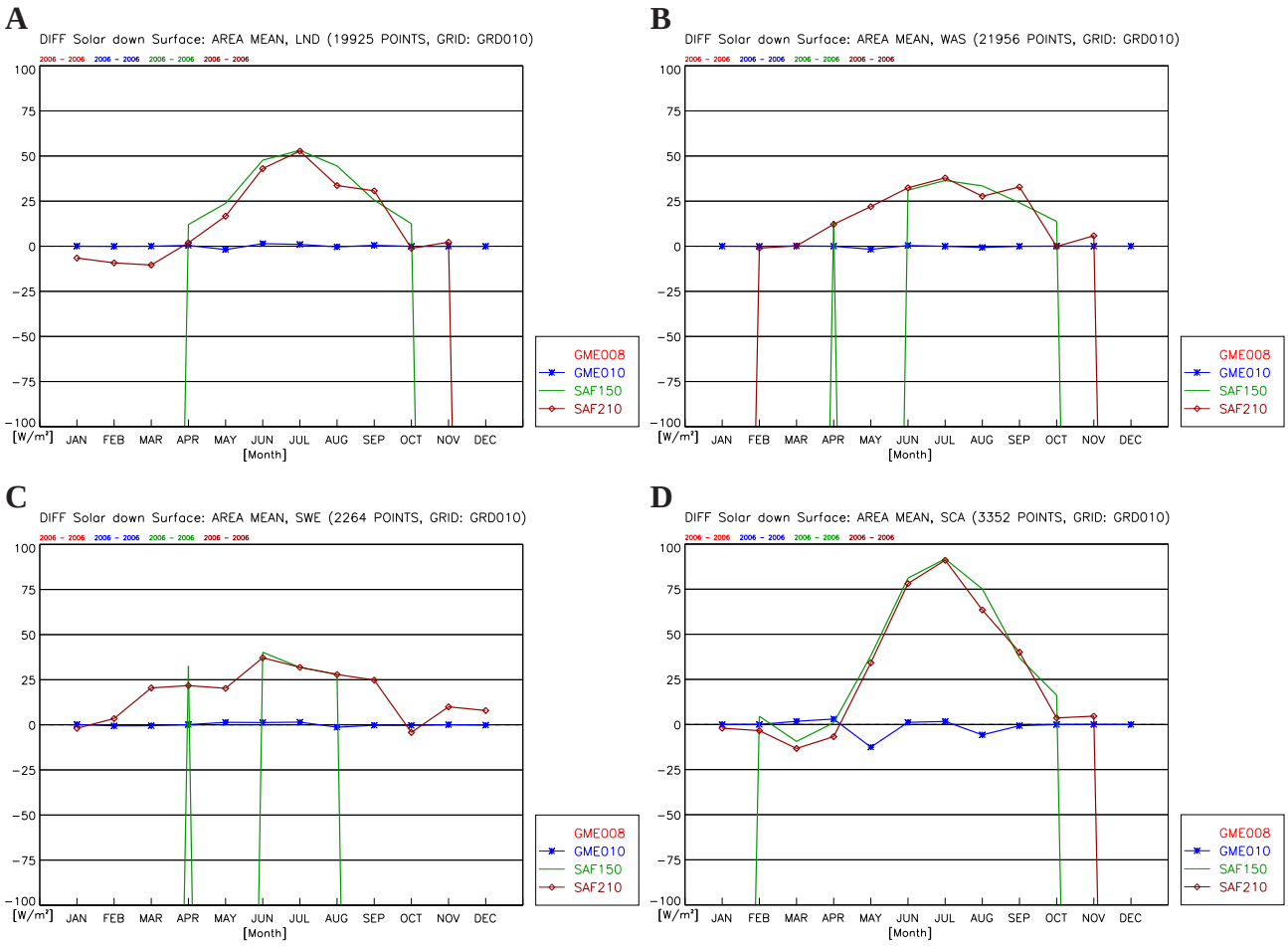

Figure 39 **Surface down SW:** annual cycle of the monthly mean differences Data-GME008 for LND (A), WAS (B), SWE (C) and SCA (D) for the year 2006.

7.2 Surface Albedo, 2006

The satellite derived surface albedo is denoted by SAL (surface albedo). The corresponding CCLM quantity is denoted by ALB_RAD (albedo of the radiation at the surface).

The accuracy of SAL is given as $\Delta SAL = 25\% SAL \simeq 0.05$ for monthly means. It has to be mentioned, that the surface albedo is derived from observations at day light conditions only. The internal CCLM variability of ΔALB_RAD resulting from different soil humidities can be derived from Fig.43. It is up to 0.05. The resulting accuracy of the differences is $\Delta(ALB\_RAD - SAL) = 0.07$

Figure 40 A to C shows the annual mean 2006 of the GME008 simulation (A), of SAF150 (B) and their difference GME008-SAF150 (C). The Satellite data provide annual data for the southern part of Europe over land areas only. We found

- No significant differences higher than of $(ALB\_RAD - SAL) = \pm 0.02$ over all parts of southern Europe except for the alpine region ALP and
- significant positive differences over the region ALP ($(ALB\_RAD - SAL) = 0.05$ and weakly significant differences over other mountains in south-east Europe.
- The satellite data exhibit much more regional variability than the model albedo reflecting deficiencies in external parameters on the regional scale.

Figures 41 A to D show the monthly mean differences GME008-SAF150 at all grid points for January (A), April (B), July (C) and October (D) 2006 covering all land areas in March to September. The SAF210 data have a significantly smaller data coverage in the North. Additionally Fig.42 shows the means and Fig.43 the mean deviations for 2006 and all months for the selected regions LND (A), ALP (B), SWE (C) and SCA (D) in a more quantitative manner. On the monthly time scale the deviations GME008-SAF150 exhibit the following additional spatial and temporal structures with significant deviations of $(ALB\_RAD - SAL) \geq 0.07$:

- Highly significant positive differences in winter over South-East Europe with peak values over the region ALP $(ALB\_RAD - SAL) = 0.16$ in January.
- Highly significant positive differences in Spring over SCA $(ALB\_RAD - SAL) = 0.23$. Differences for October to February are not available.

The significant difference patterns indicate that

- the snow albedo is overestimated in the model. It can be expected, that a substantial part of this deviation can be reduced by introduction of a fractional snow albedo in evergreen forest.
- the regional variability of the land surface is missing in the model.

The direct comparison of the difference in the surface albedo with the snow height in the model remains for future work.

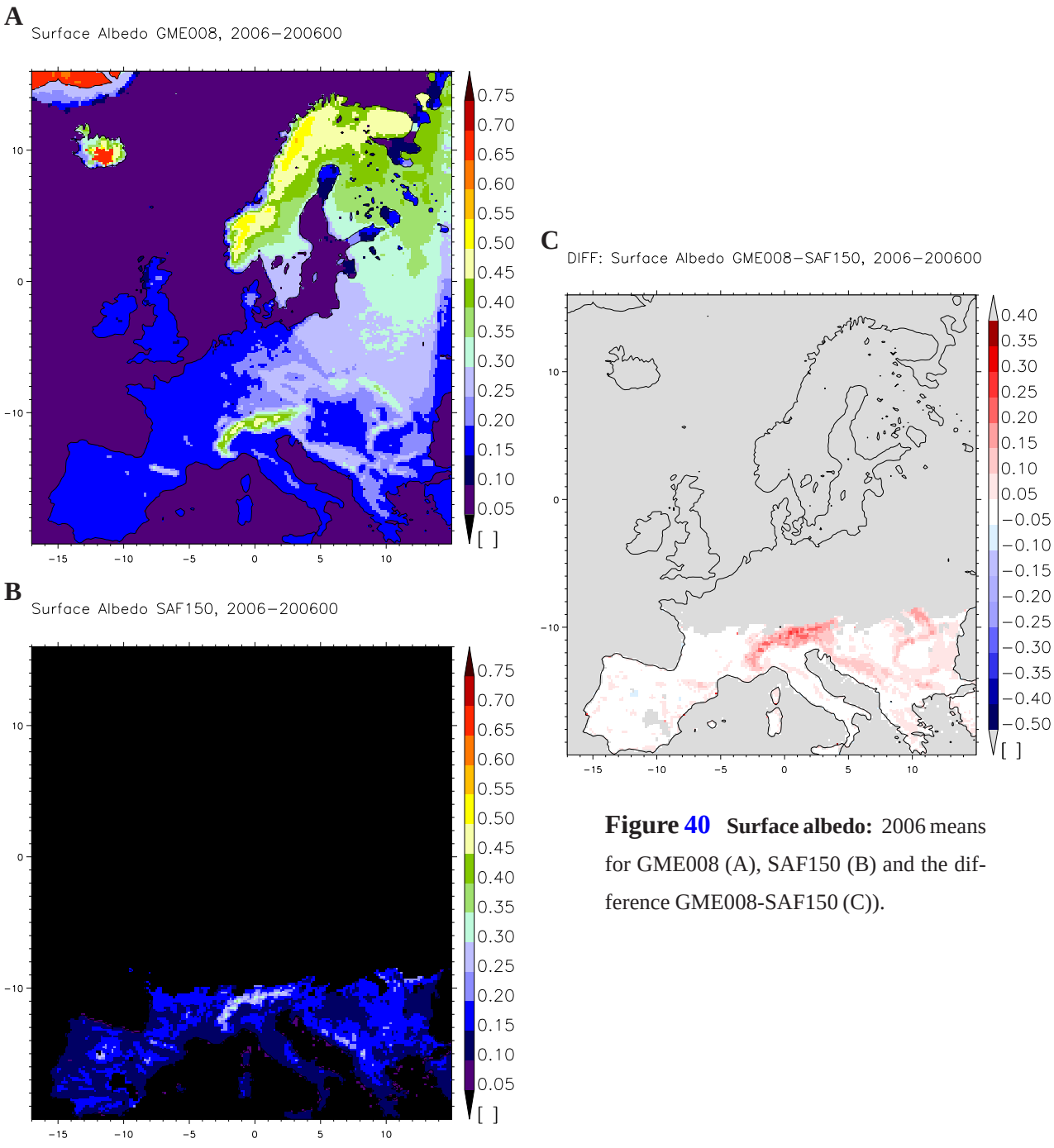

Figure 40 **Surface albedo:** 2006 means for GME008 (A), SAF150 (B) and the difference GME008-SAF150 (C)).

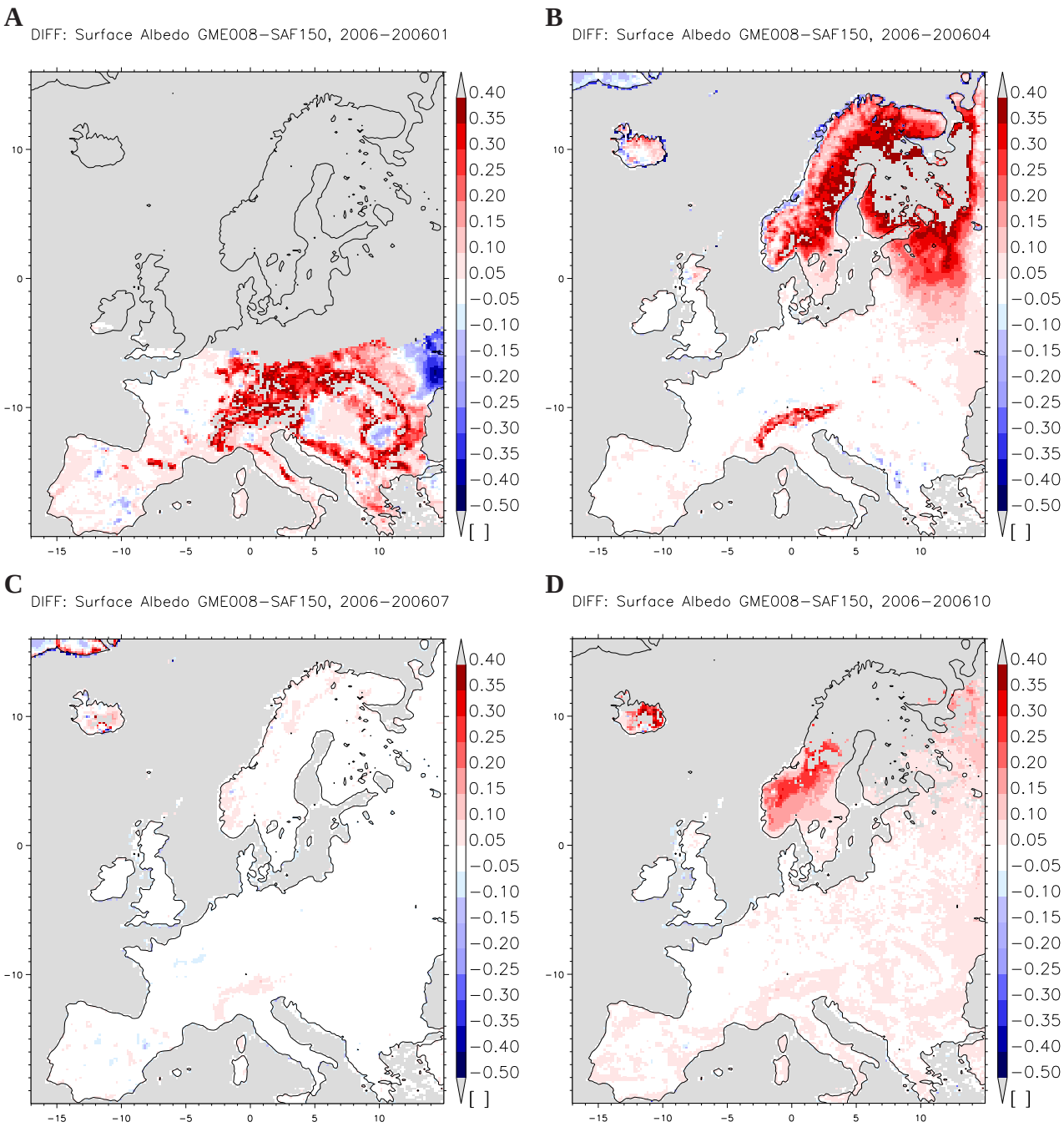

Figure 41 **Surface albedo:** monthly means of the differences GME008-SAF150 for January (A), April (B), July (C) and October (D) of the year 2006.

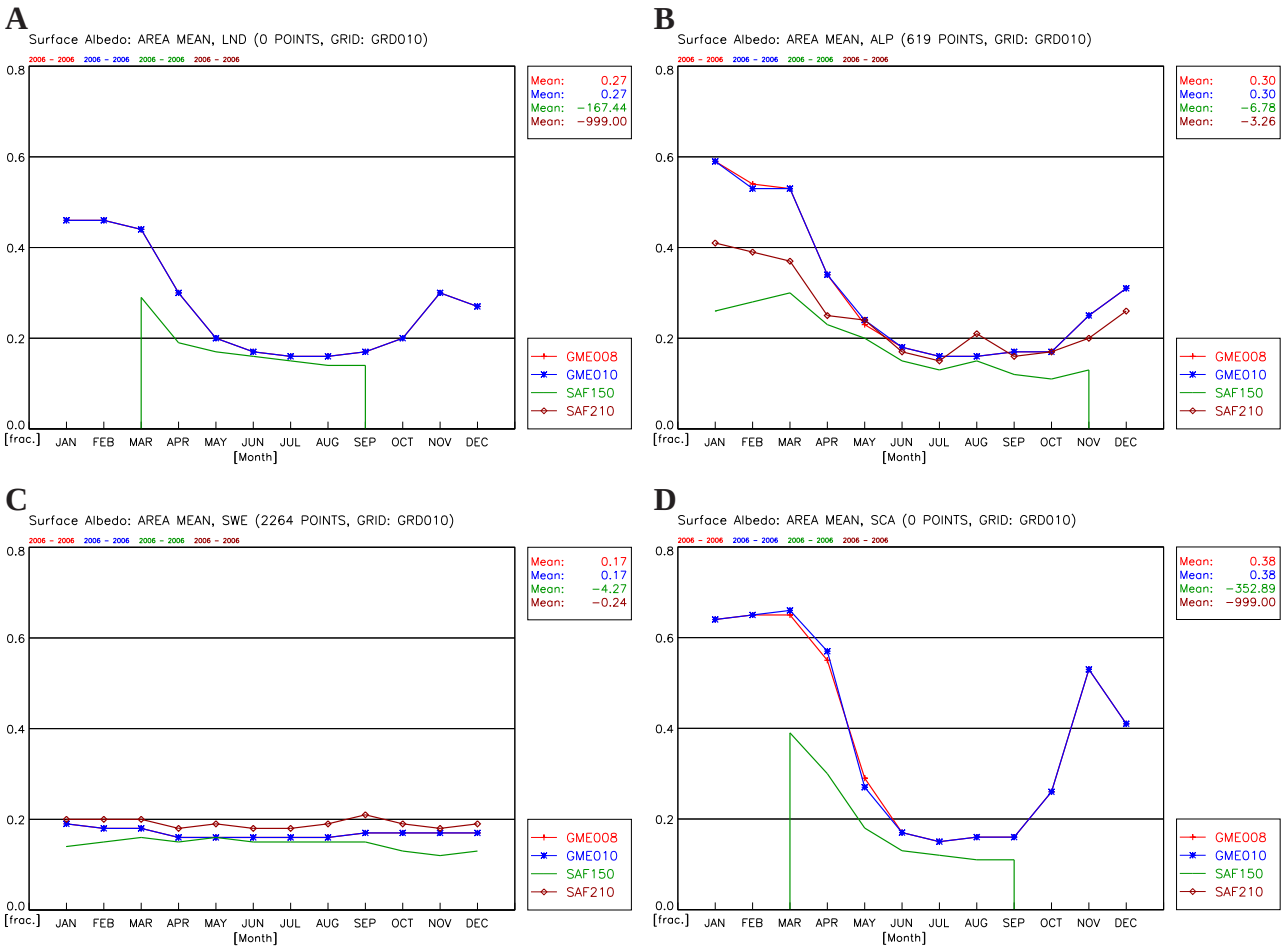

Figure 42 **Surface albedo:** annual cycle of the monthly means GME008, GME010, SAF150 and SAF210 for LND (A), ALP (B), SWE (C) and SCA (D) for the year 2006.

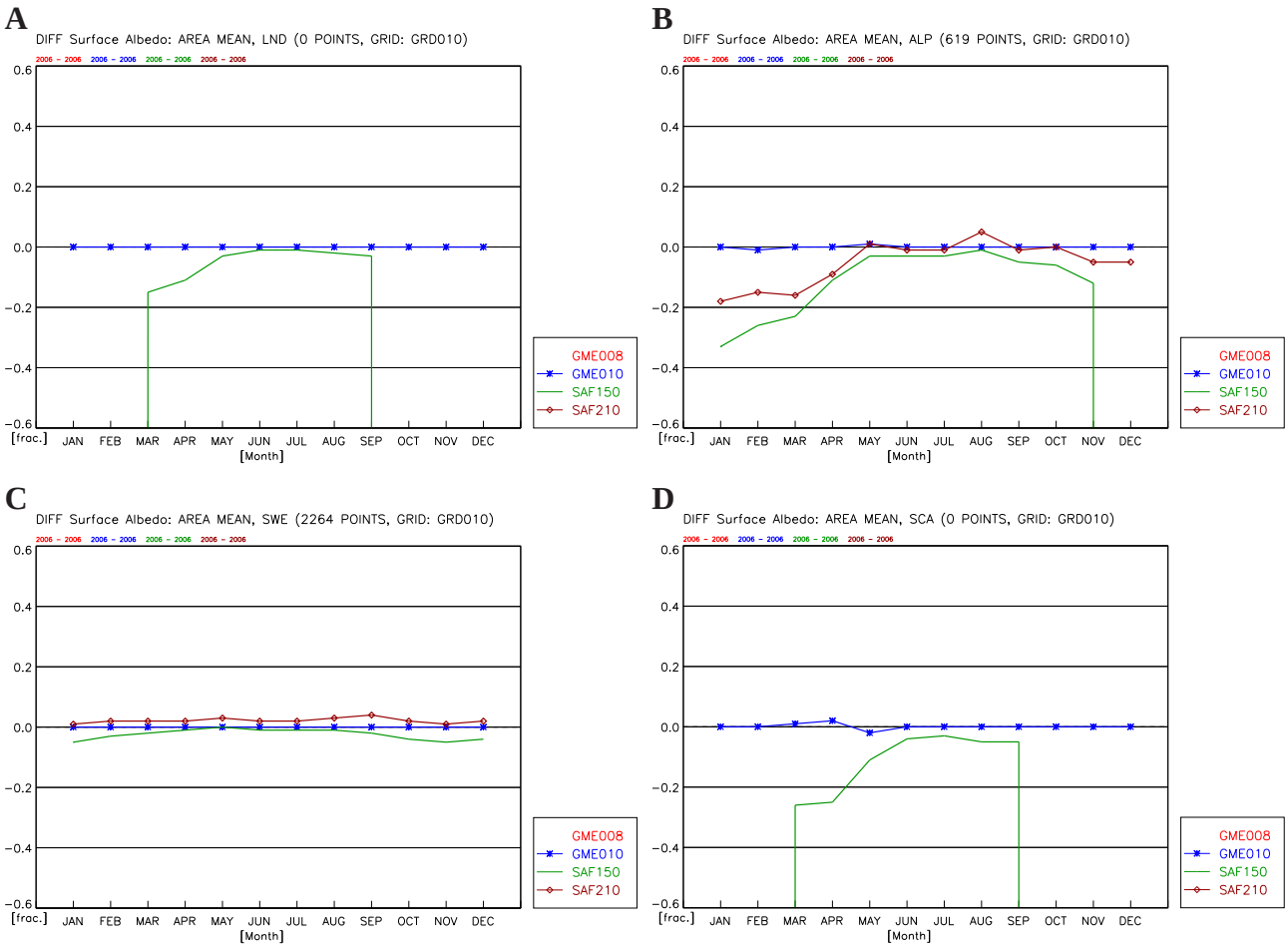

Figure 43 **Surface albedo:** annual cycle of the monthly mean differences Data-GME008 for LND (A), ALP (B), SWE (C) and SCA (D) for the year 2006.

7.3 Surface up SW, 2006

The surface up solar radiation is calculated as $SIS - SNS$ and is denoted by SRS (surface reflected solar). The corresponding CCLM quantity is the diffusive upward short wave radiation at the surface ($ASWDIFU\_S$).

The accuracy of SRS is derived from the components to be $\Delta SRS = 18\,W/m^2$ for monthly means. The internal CCLM variability $\Delta ASWDIFU\_S$ can be derived from Fig.47. It is up to $5\,W/m^2$ for all regions except for SCA, where it reaches $\Delta ASWDIFU\_S = 10\,W/m^2$ in spring. The resulting accuracy for monthly mean differences is $\Delta(ASWDIFU\_U - SRS) = 19(21)\,W/m^2$ assuming statistical independence of the single contributions to the accuracy.

Figure 44 A to C shows the annual mean 2006 of the GME008 simulation (A), of SAF210 (B) and their difference GME008-SAF210 (C). The differences GME008-SAF210 exceed the accuracy $\Delta_{12}(ASWDIFU\_S - SRS) = 7W/m^2$ in the following way:

- Significant negative differences over western Europe land areas with peak values in NWE ($(ASWDIFU\_S - SRS) = -7.26\,W/m^2$).
- Significant positive differences $(ASWDIFU\_S - SRS) = 9\,W/m^2$ over SCA and ALP.
- significant regional structures in most parts of Europe.

Figures 45 A to D show the monthly mean differences at all grid points for January (A), April (B), July (C) and October (D) 2006. Additionally Fig.46 shows the area averages of the means and Fig.47 of the mean differences for all months in 2006 for the selected regions LND (A), WAS (B), SWE (C) and SCA (D). On the monthly time scale the deviations GME008-SAF210 exhibit additional spatial and temporal structures with significant deviations of $(ASWDIFU\_S - SRS) \geq 20\,W/m^2$:

- Weakly significant negative differences over all European land areas except for SSK in the period May to September with peak values in August for DTL $(ASWDIFU\_S - SRS) = -17.4\,W/m^2$.
- Significant positive differences in late winter in east Europe (EEU) with $(ASWDIFU\_S - SRS) = 36.6\,W/m^2$.
- Strongly significant positive differences in Spring of $(ASWDIFU\_S - SRS) = 57.2\,W/m^2$ in April in SCA and $(ASWDIFU\_S - SRS) = 37.9\,W/m^2$ in march in ALP.
- significant regional structures, especially within SWE, in spring to summer months.

All significant patterns of deviation are hypothesised to have different reasons.

- The negative deviation all over Europe land areas are consistent with the underestimation of down solar radiation over the model domain in summer and small albedo values over WAS.

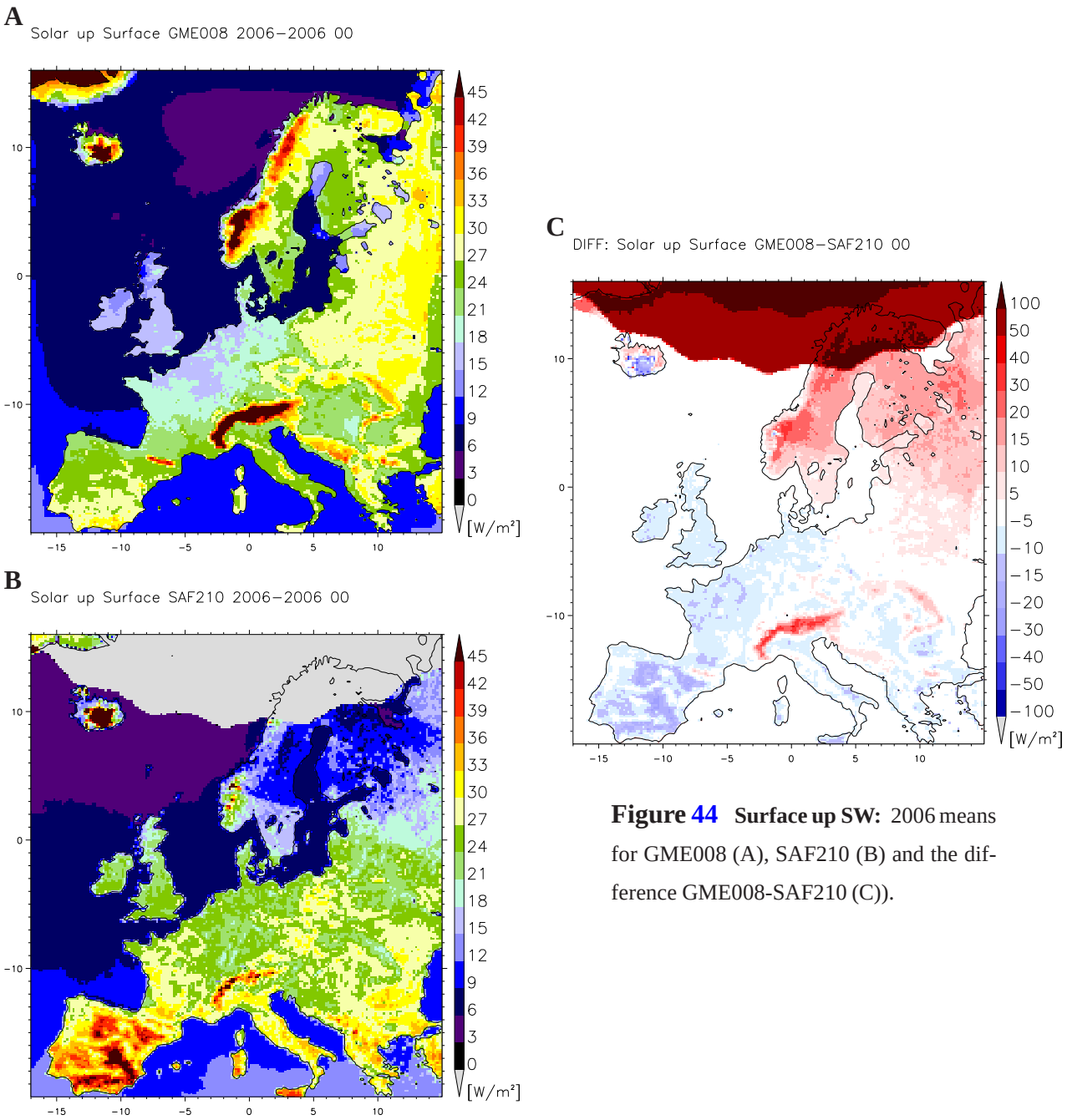

Figure 44 **Surface up SW:** 2006 means for GME008 (A), SAF210 (B) and the difference GME008-SAF210 (C)).

- The positive deviations in late winter over east Europe and in march / April in SCA and ALP, are consistent with higher albedo values, probably due to overestimation of snow albedo (see Fig. 41).

- the regional structure of the differences originates in the regional structure of the SAF data, not visible in the model results. This originates in the low resolution of the soil and vegetation parameters used.

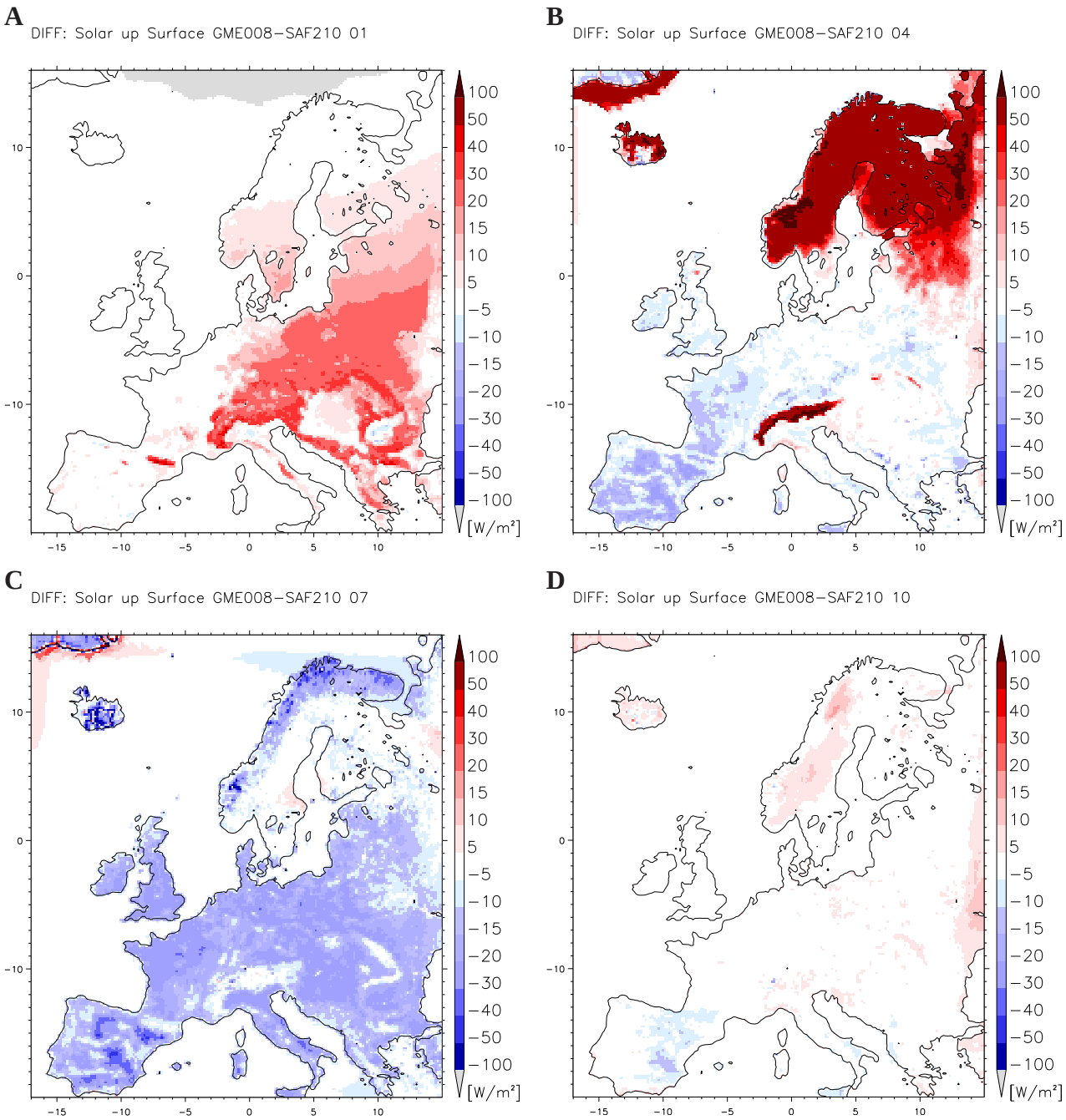

Figure 45 **Surface up SW:** monthly means of the differences GME008-SAF210 for January (A), April (B), July (C) and October (D) of the year 2006.

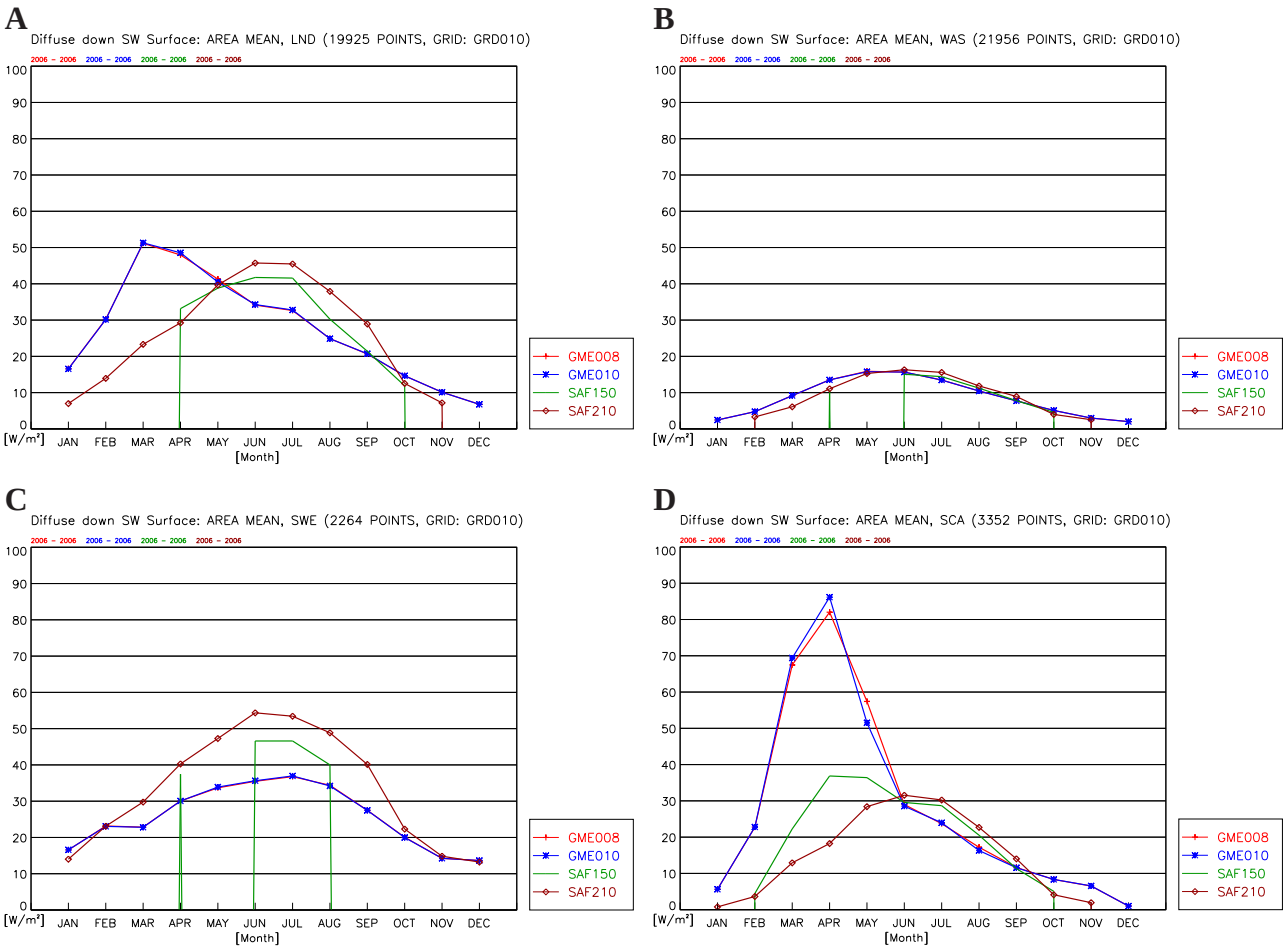

Figure 46 **Surface up SW:** annual cycle of the monthly means GME008, GME010, SAF150 and SAF210 for LND (A), WAS (B), SWE (C) and SCA (D) for the year 2006.

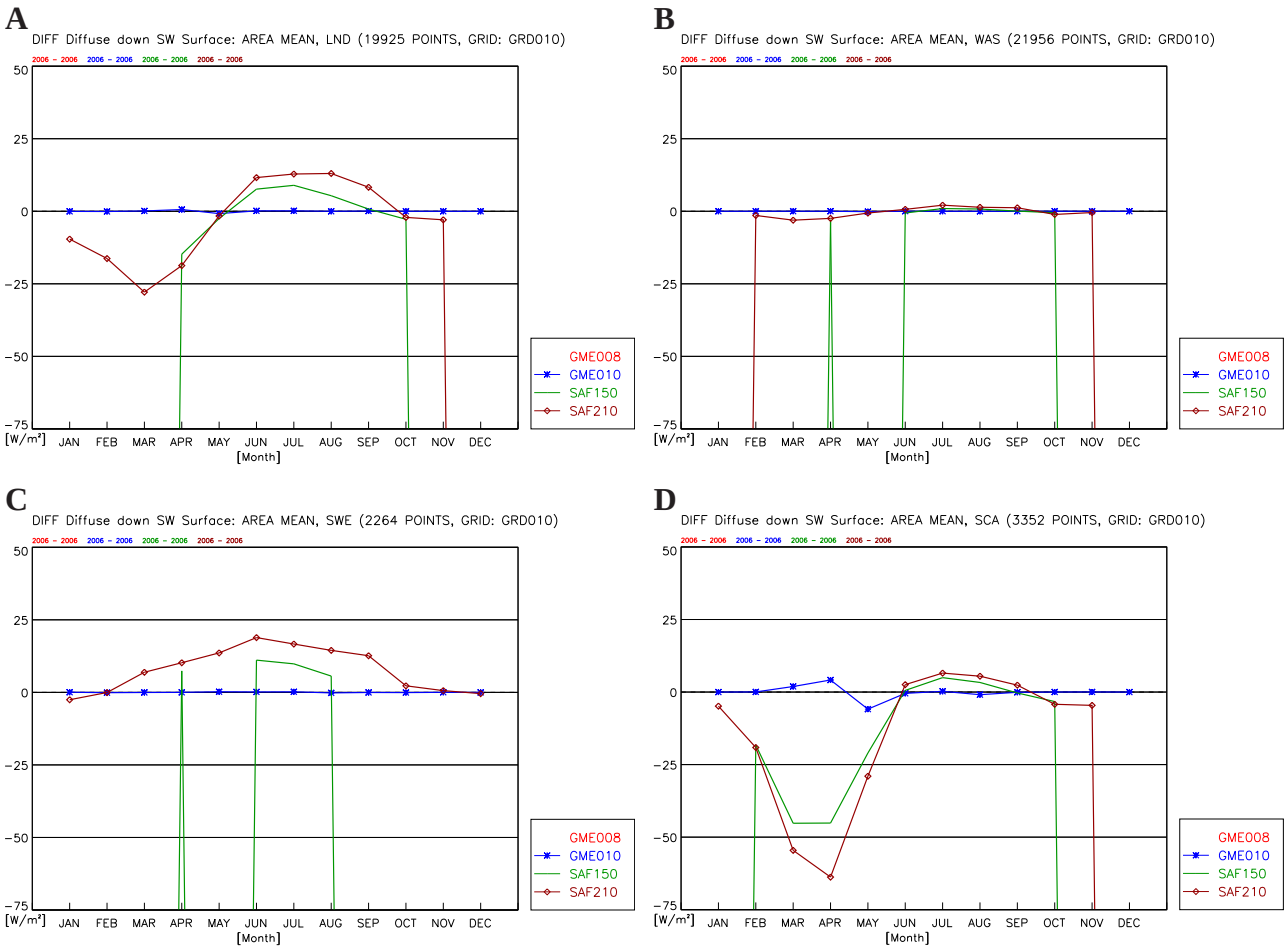

Figure 47 **Surface up SW:** annual cycle of the monthly mean differences Data-GME008 for LND (A), WAS (B), SWE (C) and SCA (D) for the year 2006.

7.4 Surface net SW, 2006

The surface net solar radiation derived from satellite observations and GME model results is named SNS in the CMSAF data base. The corresponding CCLM quantity is the solar budget radiation at the surface ($ASOB\_S$).

The accuracy of SNS is given as $\Delta SNS = 15\,W/m^2$ for monthly means. The internal CCLM variability $\Delta ASOB\_S$ can be derived from Fig.51. It is up to $5\,W/m^2$ for all regions except for SCA, where it reaches $\Delta ASOB\_S = 10\,W/m^2$ in spring and summer. The resulting accuracy for monthly means is $\Delta(ASOB\_S - SNS) = 16(18)\,W/m^2$.

Figure 48 A to C shows the annual mean 2006 of the GME008 simulation (A), of SAF210 (B) and their difference GME008-SAF210 (C). The differences GME008-SAF210 exceed the accuracy $\Delta_{12}(ASOB\_S - SNS) = 7W/m^2$ in the following way:

- Significant negative differences over water areas with peak values in MED ($(ASOB\_S - SNS) = -18.4\,W/m^2$).
- Significant negative differences over Scandinavia of($(ASOB\_S - SNS) = -37.6\,W/m^2$).

Figures 49 A to D show the monthly mean differences at all grid points for January (A), April (B), July (C) and October (D) 2006. Additionally Fig.50 shows the area average of the 2006 monthly means and Fig.51 its differences for all months for the selected regions LND (A), WAS (B), SWE (C) and SCA (D). On the monthly time scale additional spatial and temporal structures of deviations GME008-SAF210 occur with significant values $(ASOB\_S - SNS) \geq 16\,W/m^2$:

- Strongly significant negative differences in summer over water areas with peak values in BIS ($(ASOB\_S - SNS) = -47.8\,W/m^2$) and in MED ($(ASOB\_S - SNS) = -39.4\,W/m^2$) in July.
- Strongly significant negative differences over Scandinavia in March to September with peak values in July of $(ASOB\_S - SNS) = -84.5\,W/m^2$.
- Significant negative differences over DTL in July of $(ASOB\_S - SNS) = -39.7\,W/m^2$.
- Weakly significant positive differences in south-east Europe in April and May with peak values in the POE area $(ASOB\_S - SNS) = 17.8\,W/m^2$.

The significant patterns of deviation are hypothesised to have the following reasons:

- The negative summer deviations with peak values over BIS, MED, SCA and DTL originate in the differences in down solar radiation.
- The positive deviations in April and May over south-east Europe originate in the differences in down solar radiation too.

The differences in the albedo and the reflected down solar radiation have a minor influence on the solar radiation budget at the surface.

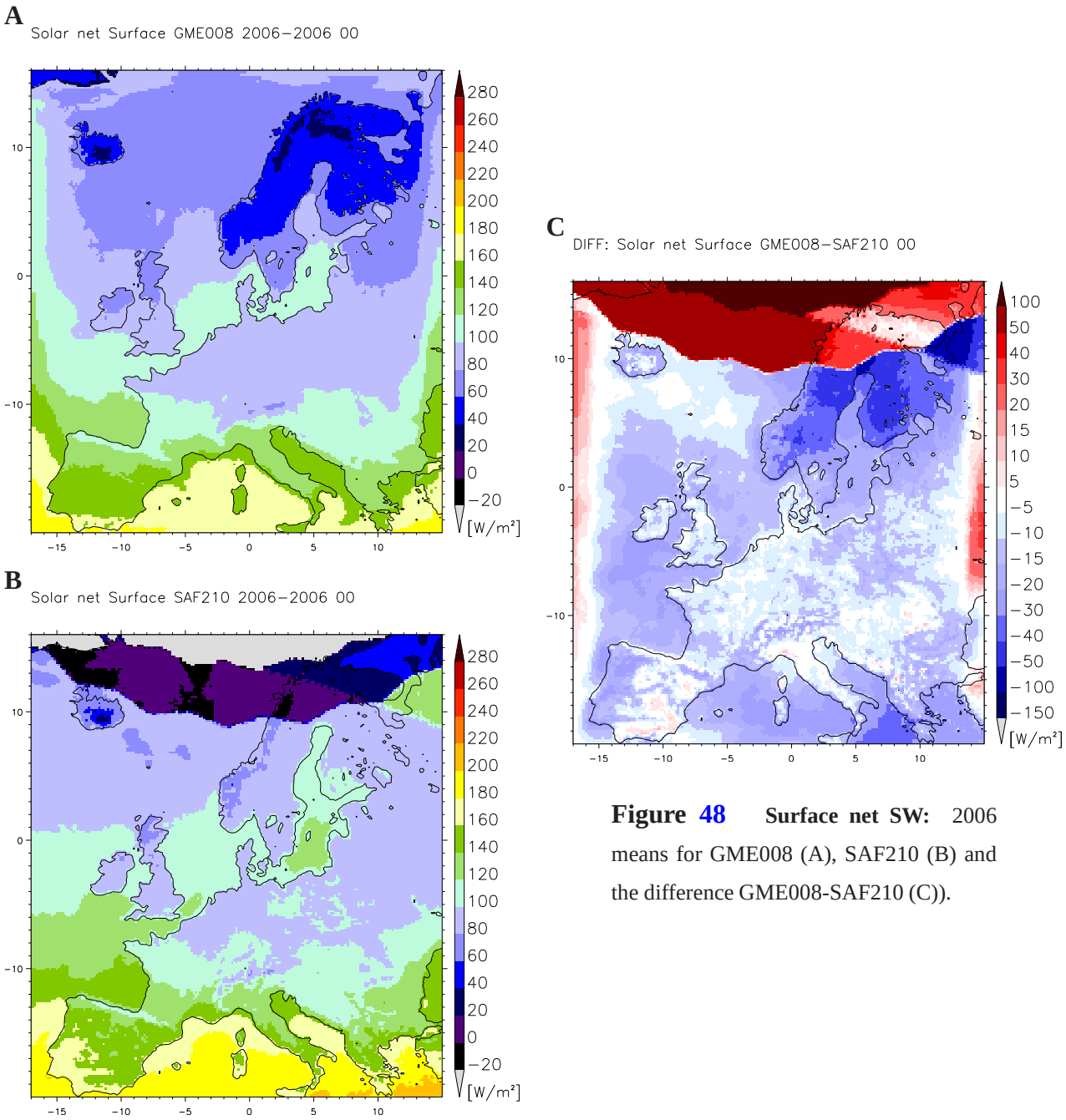

Figure 48 **Surface net SW:** 2006 means for GME008 (A), SAF210 (B) and the difference GME008-SAF210 (C)).

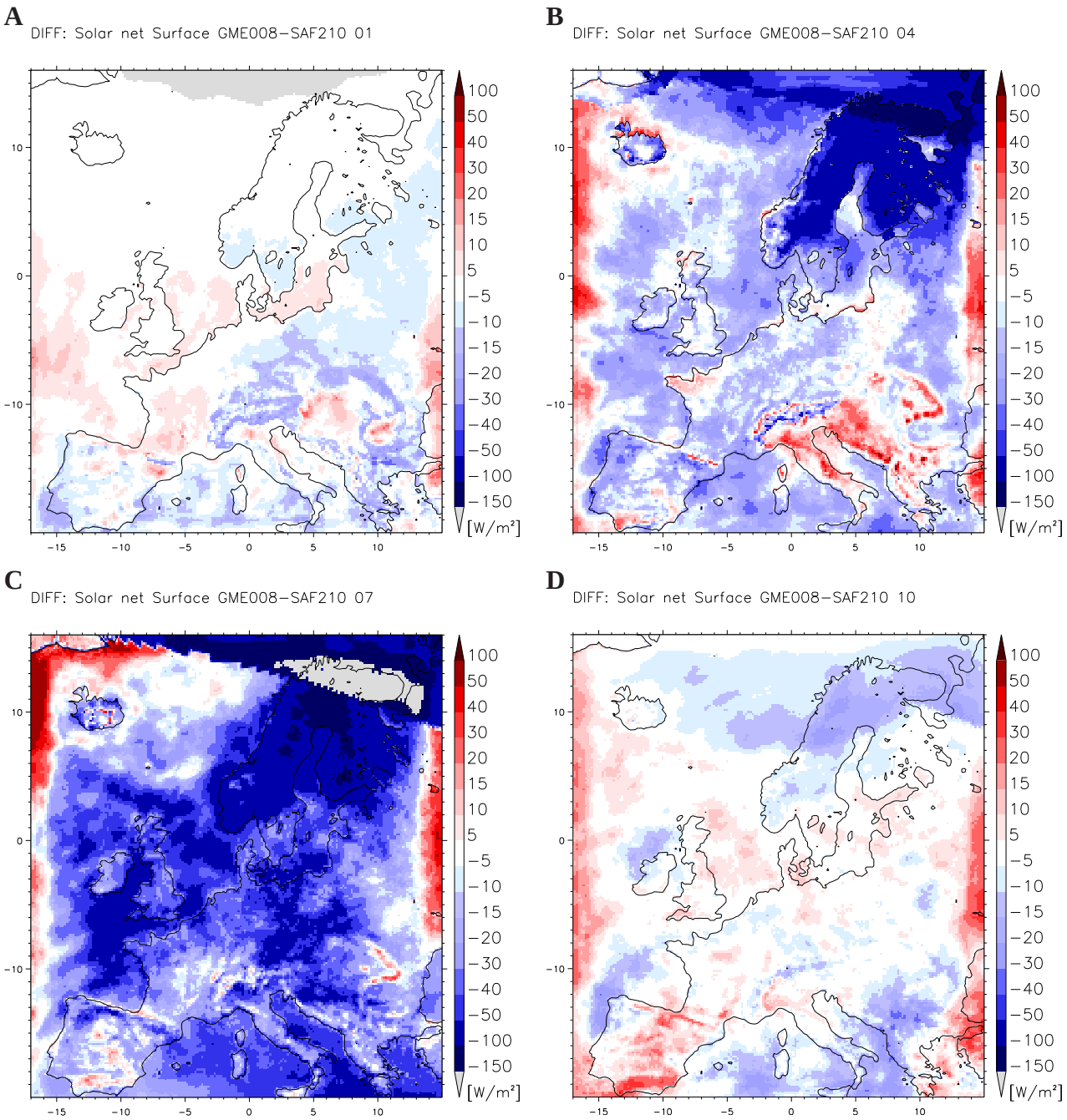

Figure 49 **Surface net SW:** monthly means of the differences GME008-SAF210 for January (A), April (B), July (C) and October (D) of the year 2006.

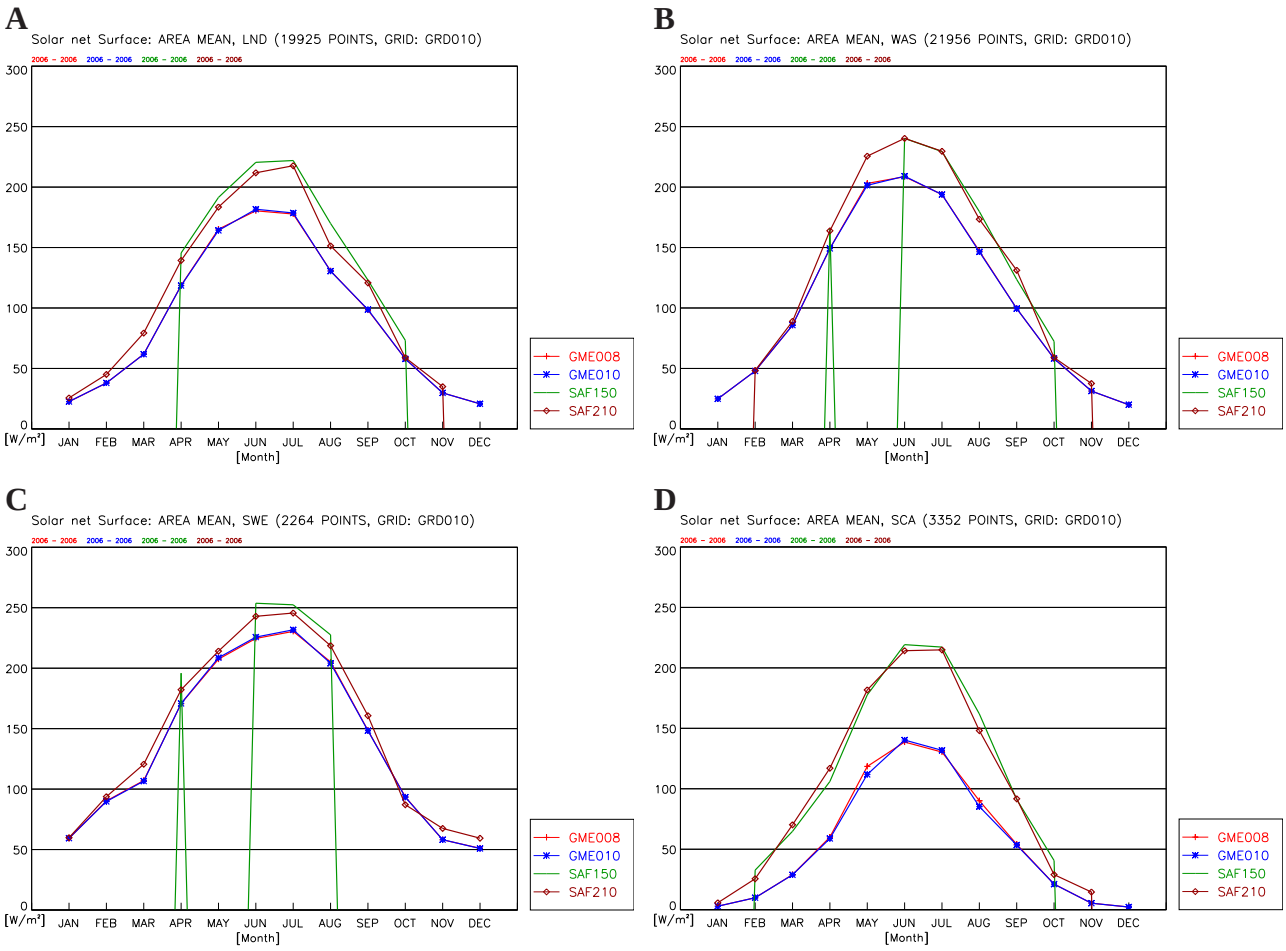

Figure 50 **Surface net SW:** annual cycle of the monthly means GME008, GME010, SAF150 and SAF210 for LND (A), WAS (B), SWE (C) and SCA (D) for the year 2006.

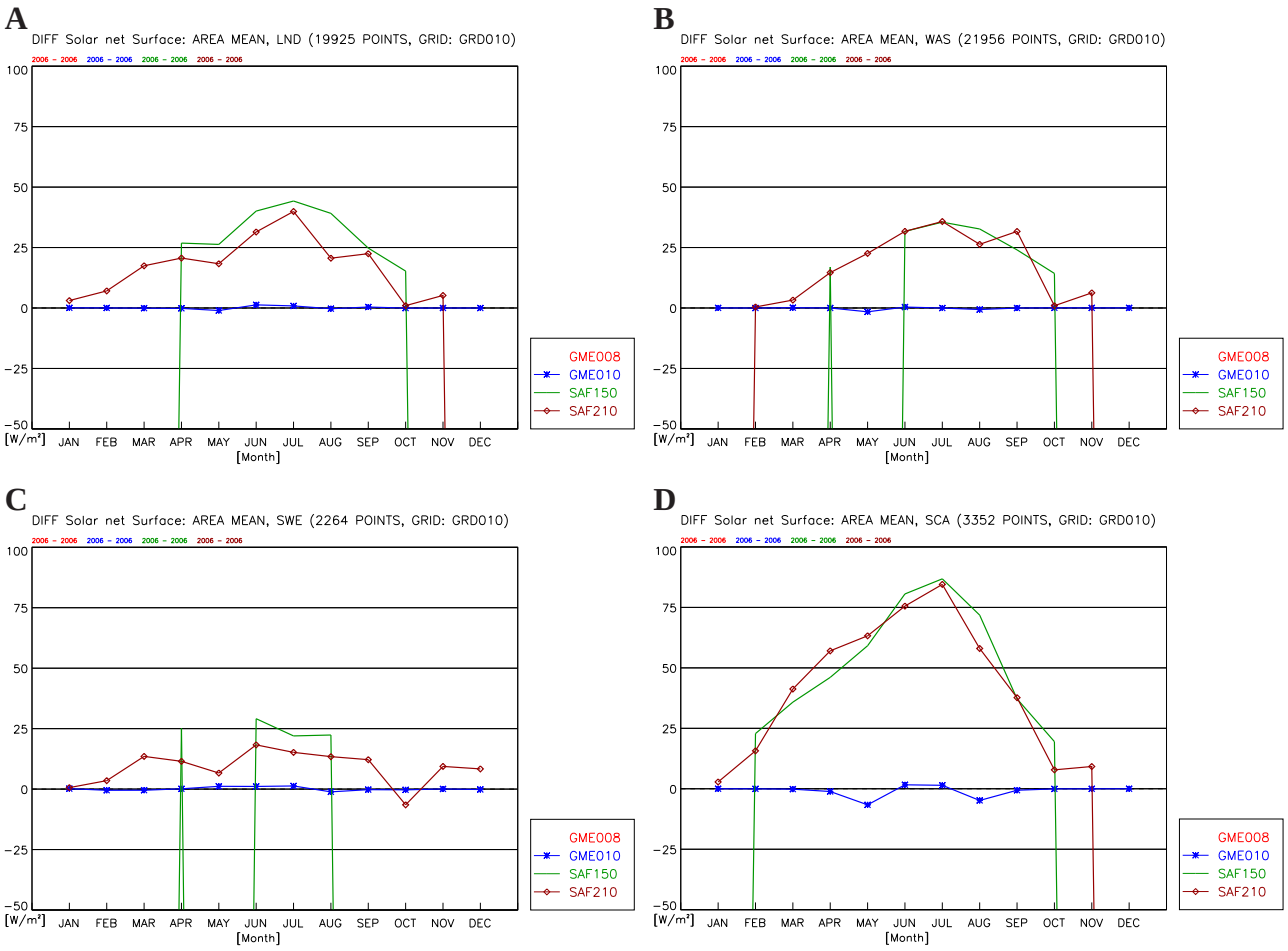

Figure 51 **Surface net SW:** annual cycle of the monthly mean differences Data-GME008 for LND (A), WAS (B), SWE (C) and SCA (D) for the year 2006.

7.5 Surface down LW, 2006

The satellite and GME derived surface down long-wave radiation is denoted by SDL (surface down long-wave radiation). The corresponding CCLM quantity is $ALWD\_S$ (accumulated long-wave down radiation at the surface).

The accuracy of SDL is given as $\Delta SDL = 10\,W/m^2$ for monthly means. The internal CCLM variability $\Delta ALWD\_S$ can be derived from Fig.55. It is up to $6\,W/m^2$ for all regions and months. The resulting accuracy is $\Delta(ALWD\_S - SDL) = 12\,W/m^2$.

Figure 52 A to C shows the annual mean 2006 of the GME008 simulation (A), of SAF210 (B) and their difference GME008-SAF210 (C). The differences GME008-SAF150 exceed the accuracy $\Delta_{12}(ALWD\_S - SDL) = 5W/m^2$ over several parts of Europe. We found the following patterns:

- Significant positive differences $(ALWD\_S - SDL) = 10.7\,W/m^2$ over SCA.
- Significant negative differences of $(ALWD\_S - SDL) = -11.2\,W/m^2$ over MED and $-8\,W/m^2$ over WAS with peak values at the western and northern boundary of the model domain.

Figures 53 A to D show the monthly mean differences GME008-SAF210 at all grid points for January (A), April (B), July (C) and October (D) 2006. Additionally Fig.54 shows the area average of the 2006 monthly means and Fig.55 its differences for all months for the selected regions LND (A), WAS (B), SWE (C) and SCA (D). On the monthly time scale the deviations GME008-SAF150 exhibit additional spatial and temporal structures with significant deviations of $(ALWD\_T - SDL) \geq 12\,W/m^2$:

- Peak positive differences $(ALWD\_S - SDL) = 22.9\,W/m^2$ over SCA in December.
- significant negative differences $(ALWD\_S - SDL) \simeq -13\,W/m^2$ over MED in October to June and over WAS in April and May of $(ALWD\_S - SDL) = -11\,W/m^2$.

The significant patterns of deviation are hypothesised to have the following reasons:

- The strong correlation over WAS between $(ALWD\_S - SDL)$ and $(CLCT - CFC)$ reflects the main contribution of clouds to LW down radiation at the surface.
- The correlation over LND is much weaker, especially in summer due to additional influence of temperature differences at the surface, which are responsible for LW up radiation at the surface, the most important source for LW down. In summer the negative T_2m deviation in central Europe causes negative $ALWU\_S$ values and compensates the positive differences in total cloud cover.

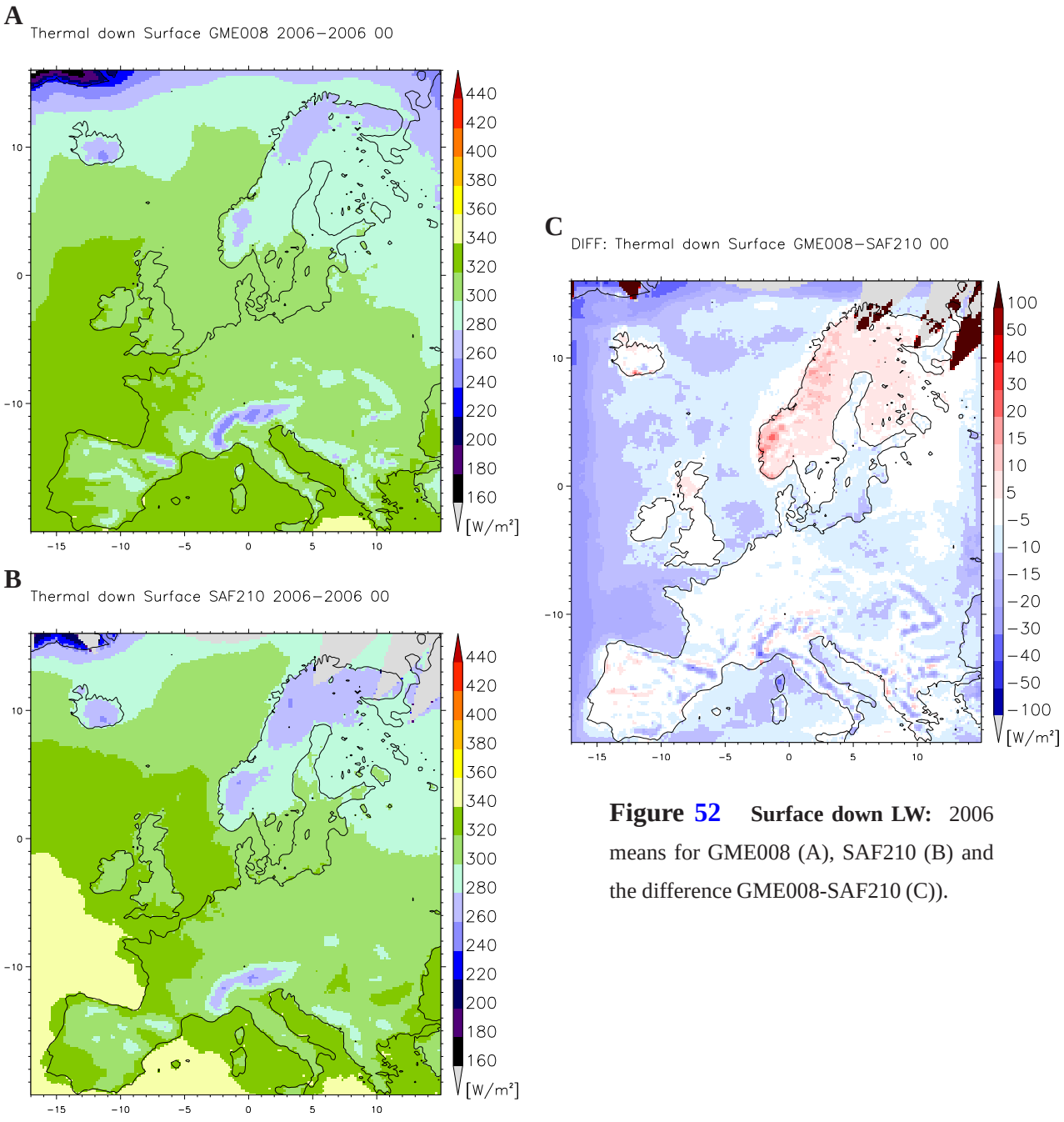

Figure 52 **Surface down LW:** 2006 means for GME008 (A), SAF210 (B) and the difference GME008-SAF210 (C)).

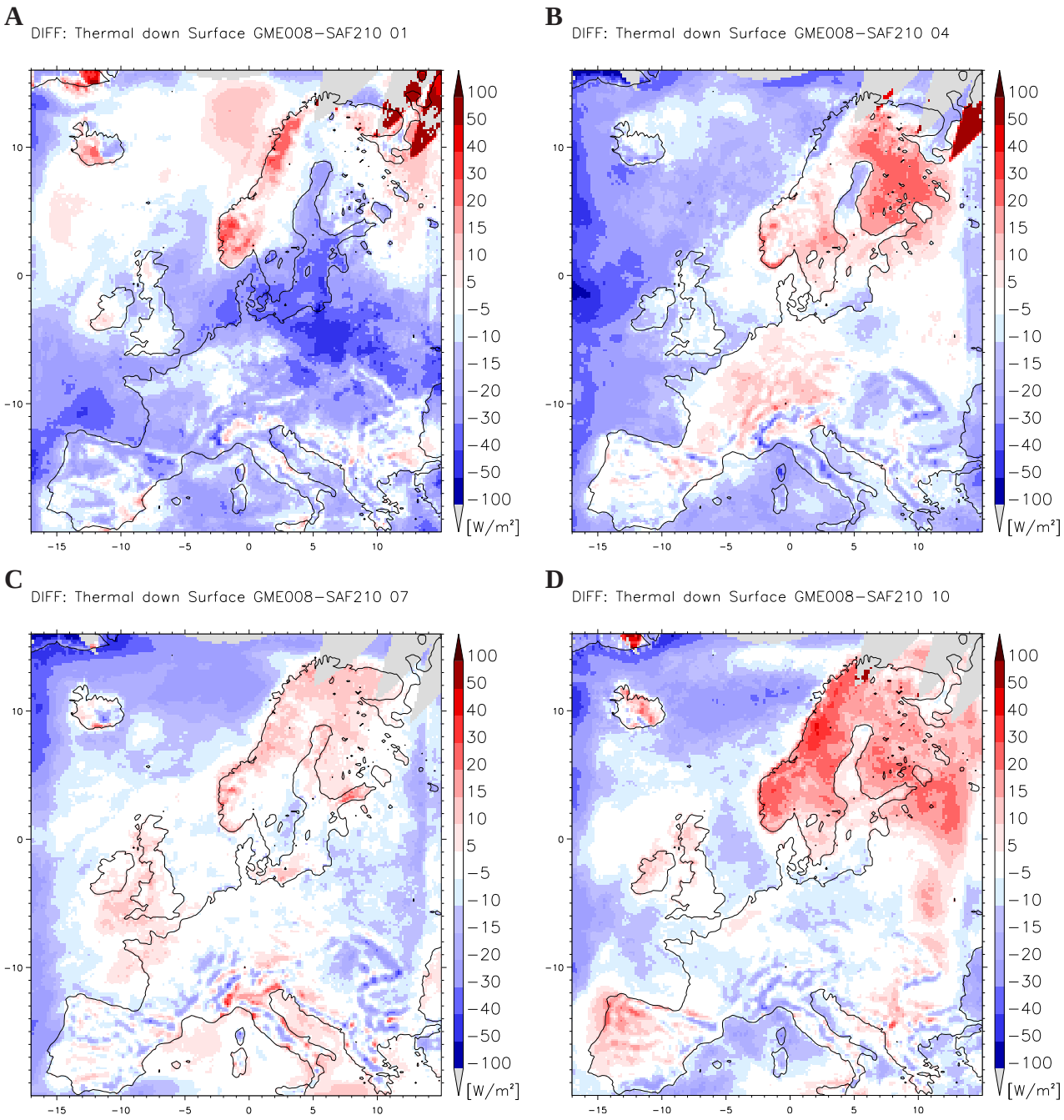

Figure 53 **Surface down LW:** monthly means of the differences GME008-SAF210 for January (A), April (B), July (C) and October (D) of the year 2006.

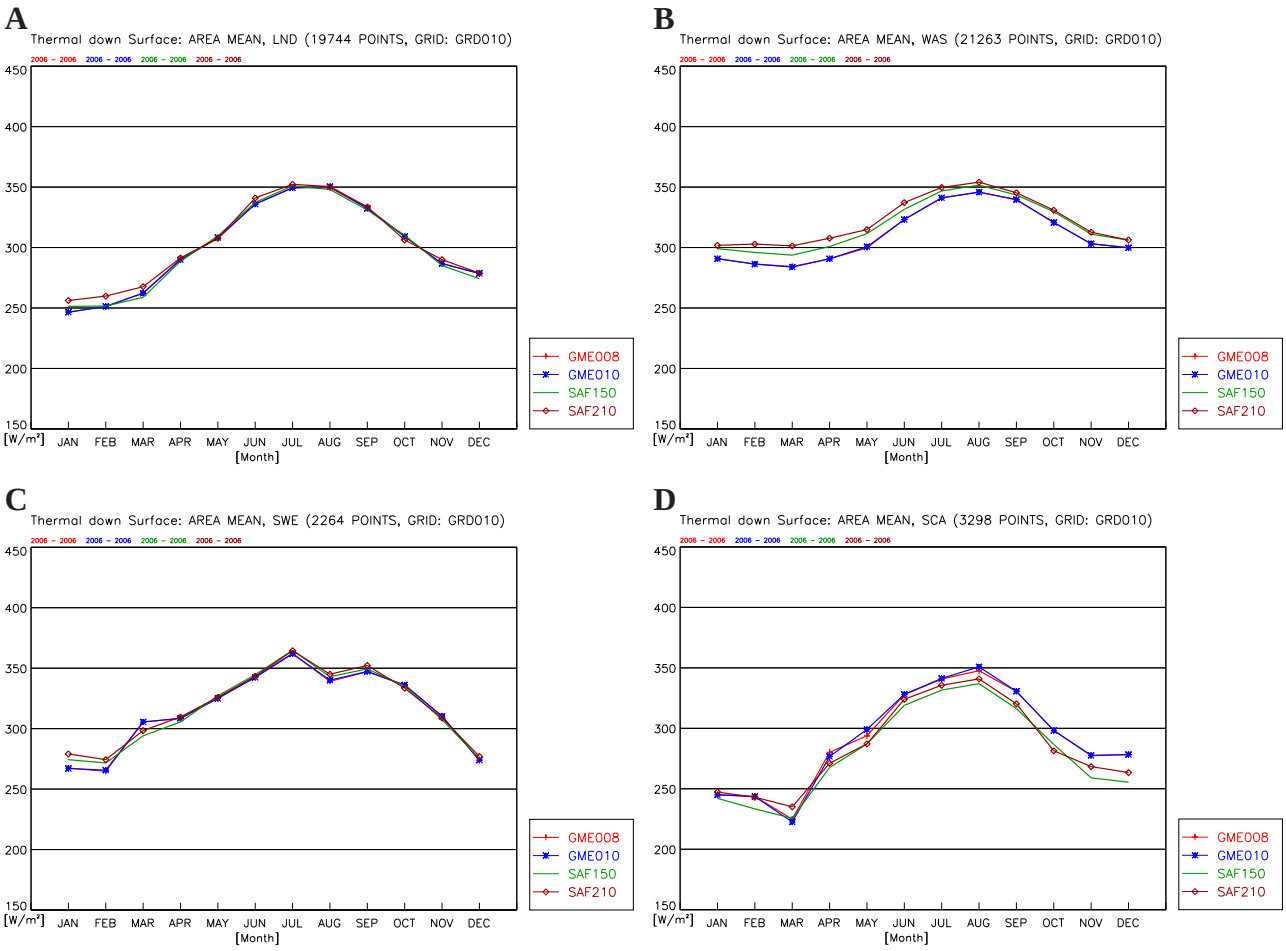

Figure 54 **Surface down LW:** annual cycle of the monthly means GME008, GME010, SAF150 and SAF210 for LND (A), WAS (B), SWE (C) and SCA (D) for the year 2006.

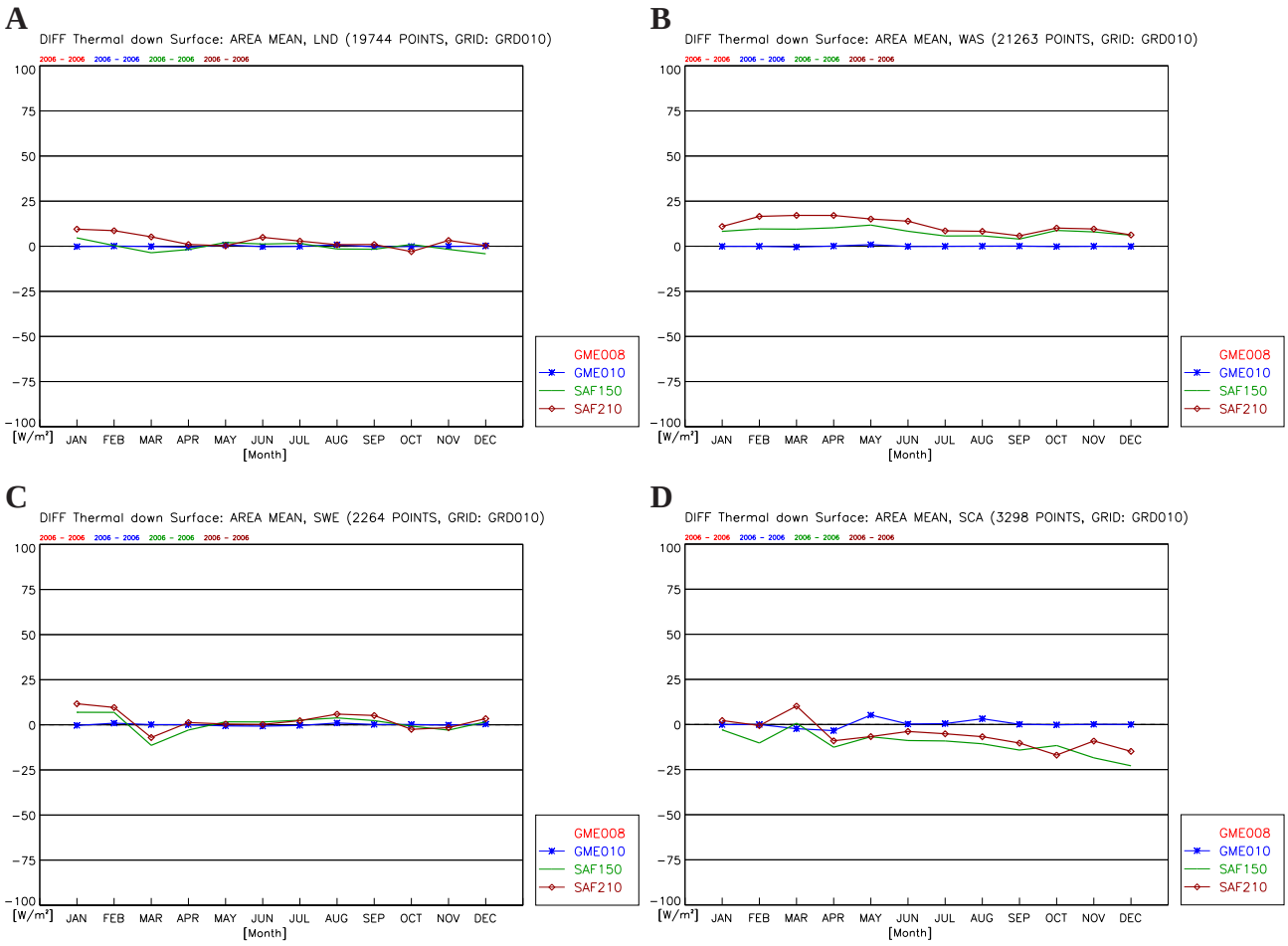

Figure 55 **Surface down LW:** annual cycle of the monthly mean differences Data-GME008 for LND (A), WAS (B), SWE (C) and SCA (D) for the year 2006.

7.6 Surface up LW, 2006

The surface up long-wave radiation is denoted by SOL (surface outgoing long-wave radiation). It is derived from GME analyses. The corresponding CCLM quantity is $ALWU\_S$ (accumulated long-wave up radiation at the surface). Therefore this comparison exhibits differences between the analysed data of GME used as initial and boundary conditions and the regional climate model configuration COSMO-CLM.

The accuracy of SOL is given as $\Delta SOL = 10\,W/m^2$ for monthly means. The internal CCLM variability $\Delta ALWU\_S$ can be derived from Fig.59. It is up to $2\,W/m^2$ for all regions and months. The resulting accuracy is $\Delta(ALWU\_S - SOL) = 10\,W/m^2$.

Figure 56 A to C shows the annual mean 2006 of the GME008 simulation (A), of SAF210 (B) and their difference GME008-SAF210 (C). The differences GME008-SAF210 exceed the accuracy $\Delta_{12}(ALWU\_S - SOL) = 4W/m^2$ over several parts of Europe. We found the following patterns:

- Significant positive differences in southern Europe with peak values in the POE valley of $(ALWU\_S - SOL) = 9.8\,W/m^2$.
- Significant negative differences in central Europe of $(ALWU\_S - SOL) = -5\,W/m^2$ over MEU with peak values over DTL of $(ALWU\_S - SOL) = -5.6\,W/m^2$.

Figures 57 A to D show the monthly mean differences GME008-SAF210 at all grid points for January (A), April (B), July (C) and October (D) 2006. Additionally Fig.58 shows the area average of the 2006 monthly means and Fig.59 its differences for all months for the selected regions LND (A), WAS (B), SWE (C) and SCA (D). On the monthly time scale the deviations GME008-SAF210 exhibit additional spatial and temporal structures with significant deviations of $(ALWU\_T - TOL) \geq 10\,W/m^2$:

- Peak positive differences in the POE area of $(ALWU\_S - SOL) = 20\,W/m^2$ in April and weakly significant values in Spring in SUE and UNG.
- Peak positive differences over SCA in December of $(ALWU\_S - SOL) = 22.9\,W/m^2$.
- Peak positive differences over ALP in February and December of $(ALWU\_S - SOL) = 12\,W/m^2$.
- Negative differences over central (MEU) and northern (SCA) Europe in summer with peak values in July: $(ALWU\_S - SOL) = -18\,W/m^2$ in MEU, $(ALWU\_S - SOL) = -17\,W/m^2$ in SCA. The differences are strongly correlated with the differences in the 2m temperature and also with the total cloud cover $(CLCT - CFC)$.

The significant patterns of deviation are hypothesised to have the following reasons:

- The 2m temperature differences shown in 68 to 70 are highly correlated with the summer negative differences.
- The positive differences over SCA are correlated with the total cloud cover.

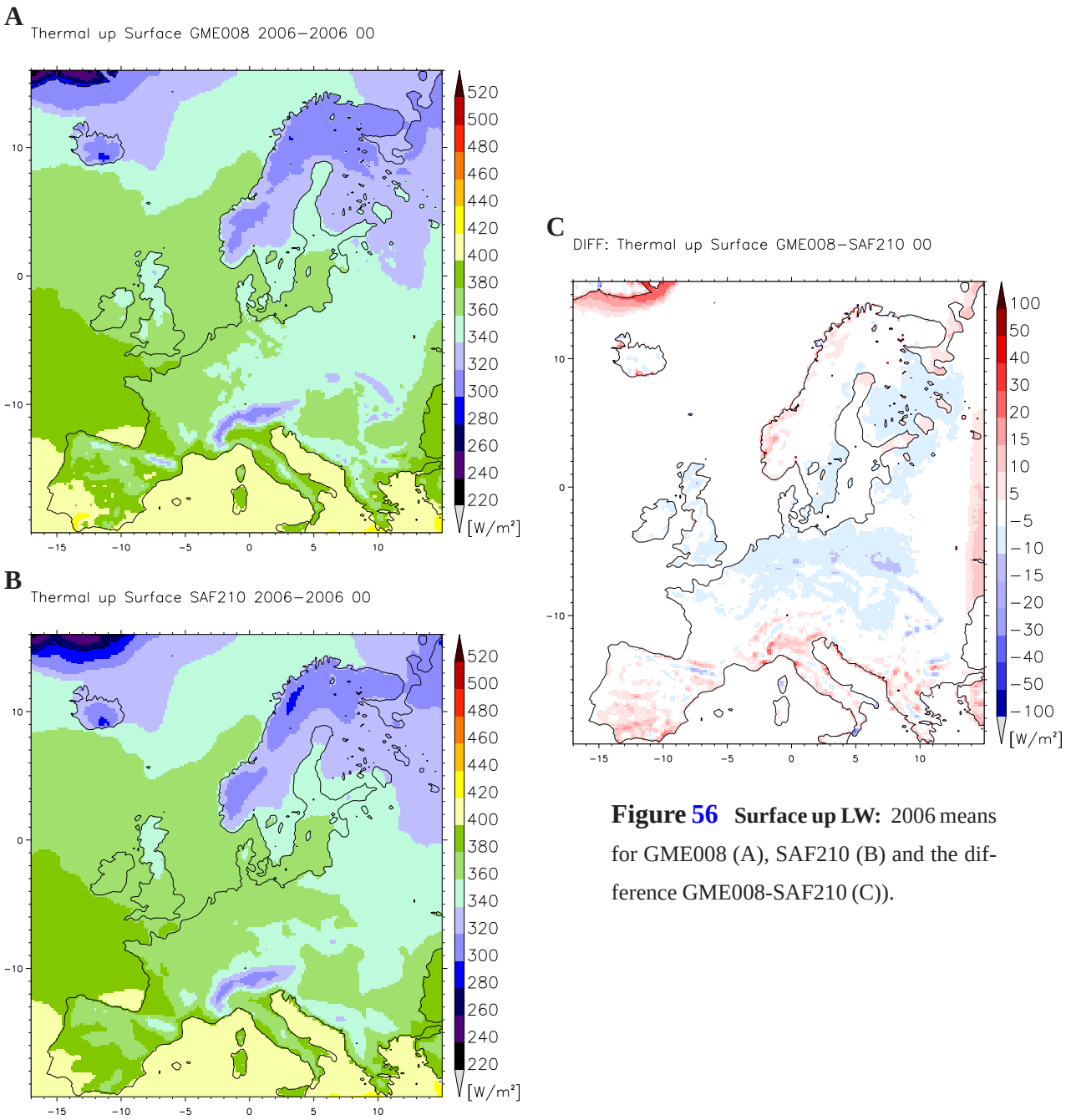

Figure 56 **Surface up LW:** 2006 means for GME008 (A), SAF210 (B) and the difference GME008-SAF210 (C)).

- The positive deviations in spring to autumn in the Poe valley and in southern Europe in spring and autumn come together with the underestimation of the 2m temperature all over the year in comparison with ECAD01 (also known as E-OBS data [*Haylock et al.*(2008)]). This indicates, that cosmo-clm has the tendency to repair the GME cold bias with the exception of the cosmo-clm summer cold bias in the GME008 configuration.

- The differences over ALP seem to be features of the specific year not captured by the regional climate model.

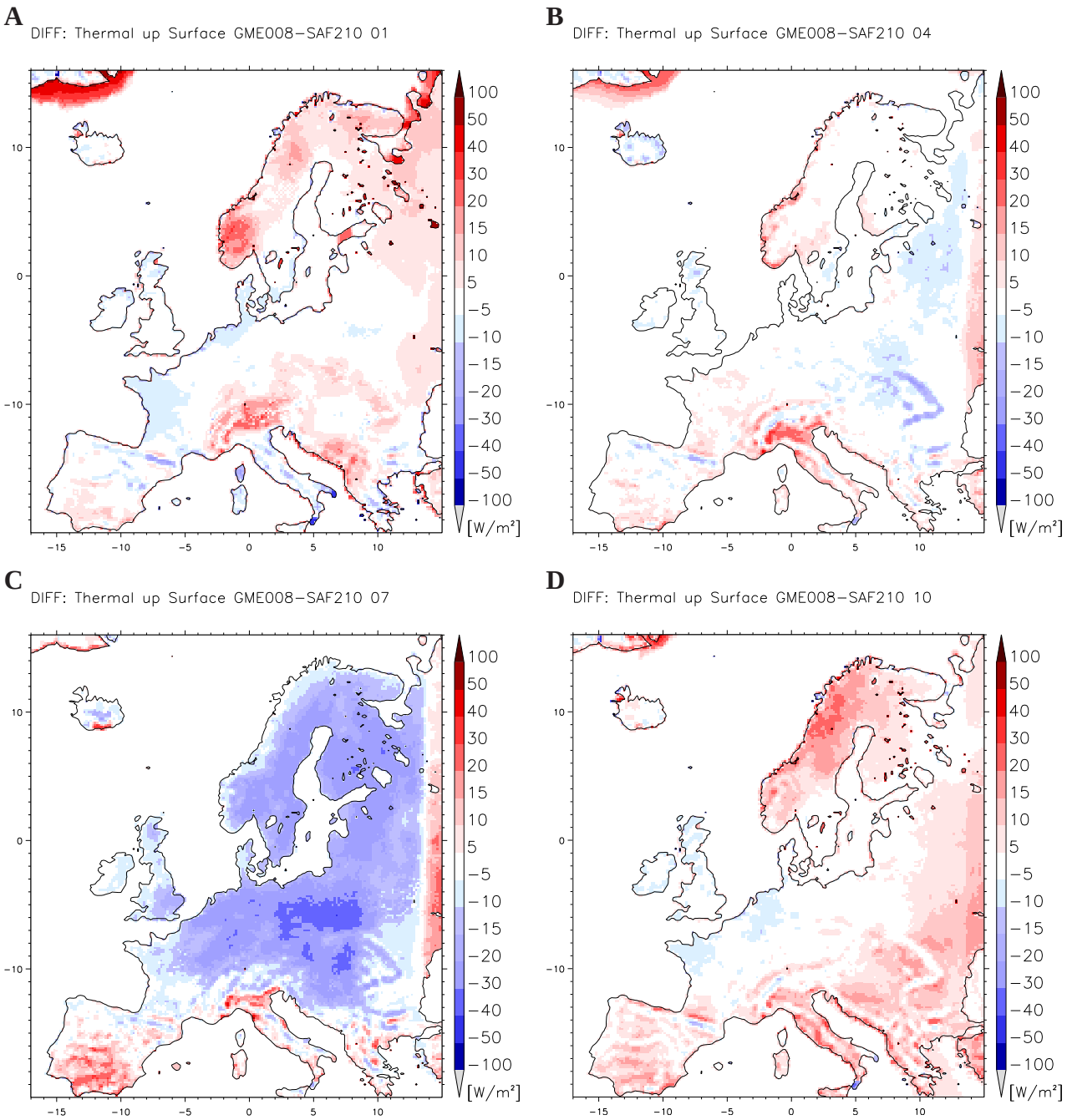

Figure 57 **Surface up LW:** monthly means of the differences GME008-SAF210 for January (A), April (B), July (C) and October (D) of the year 2006.

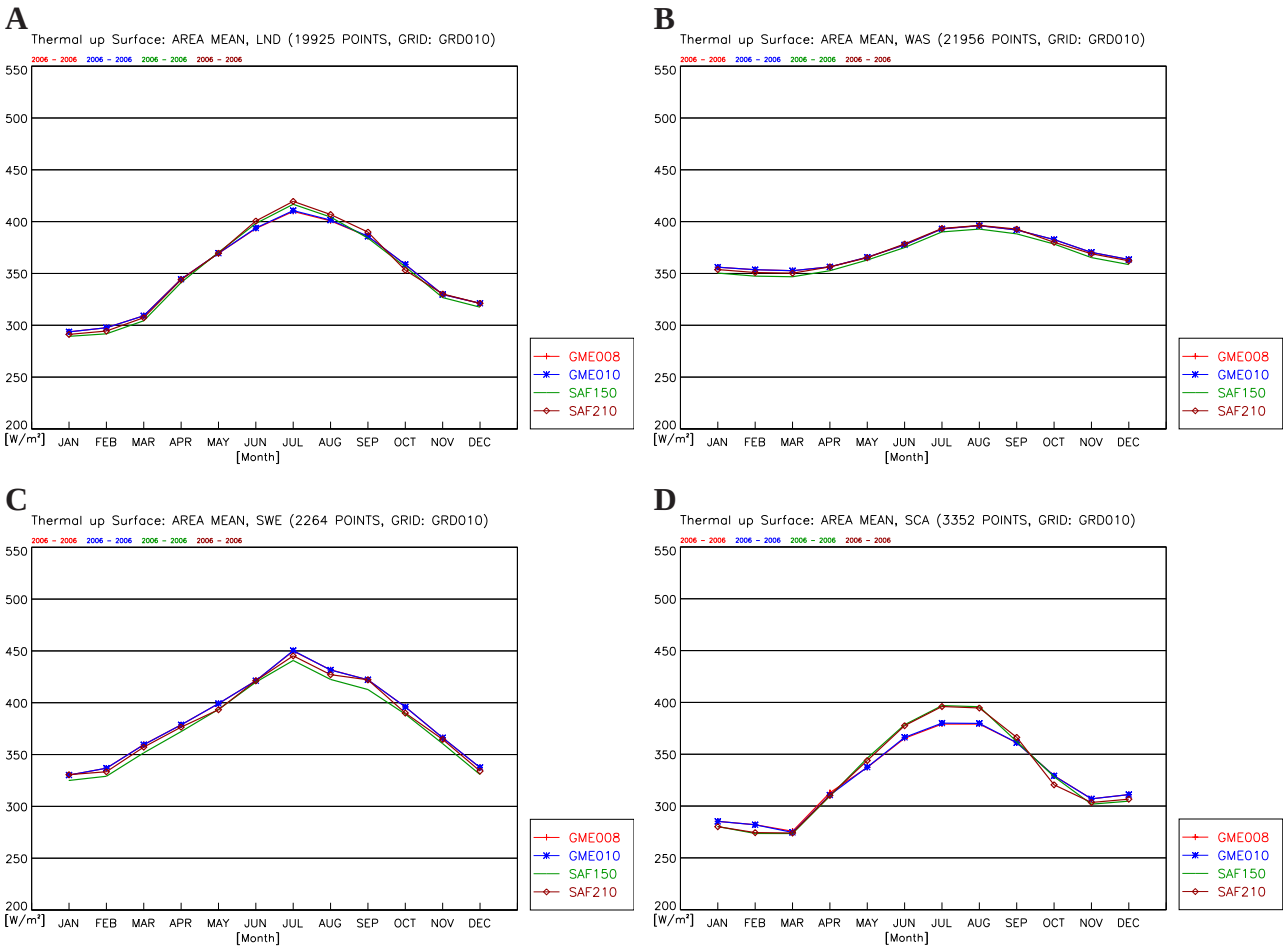

Figure 58 **Surface up LW:** annual cycle of the monthly means GME008, GME010, SAF150 and SAF210 for LND (A), WAS (B), SWE (C) and SCA (D) for the year 2006.

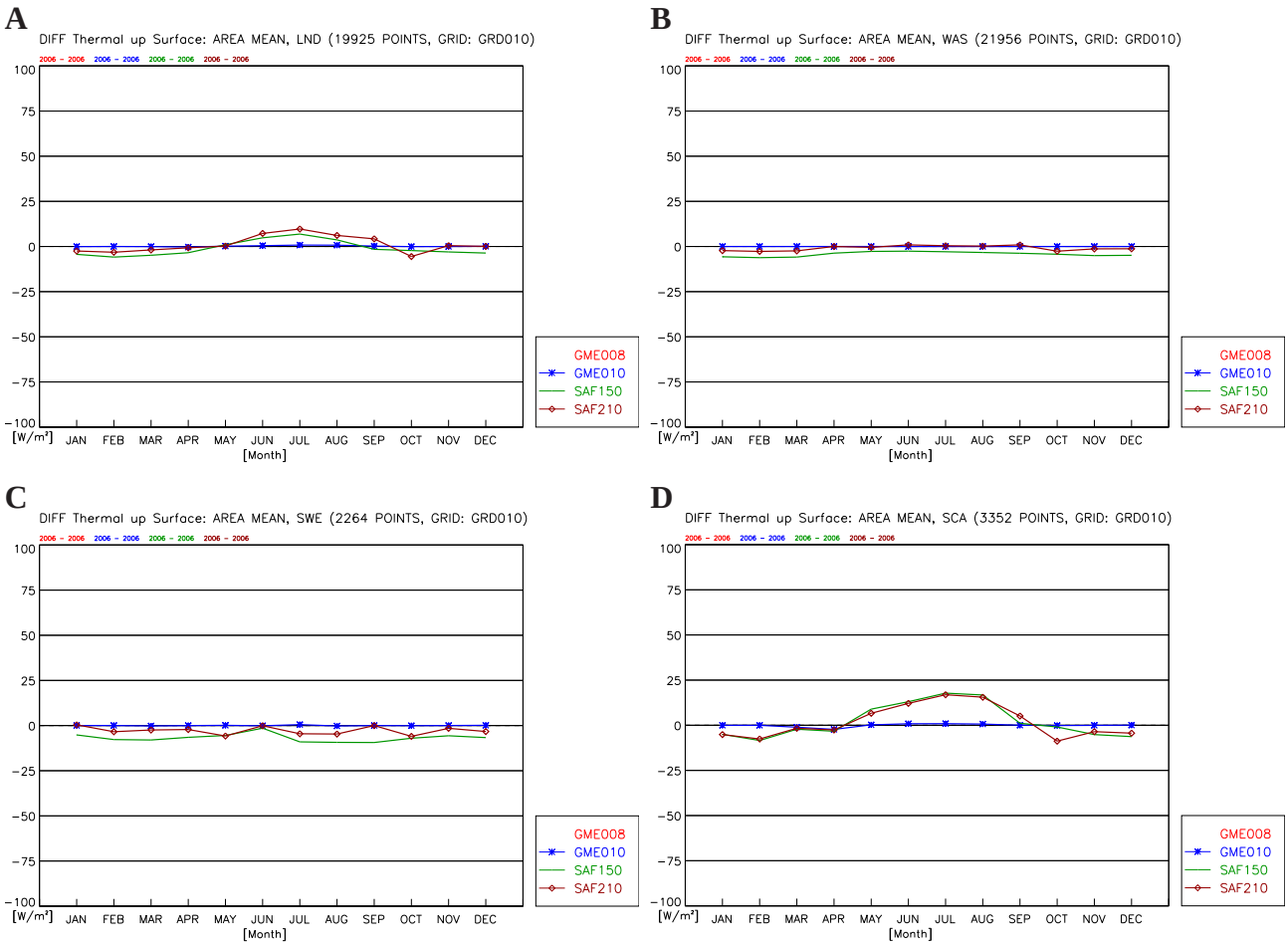

Figure 59 **Surface up LW:** annual cycle of the monthly mean differences Data-GME008 for LND (A), WAS (B), SWE (C) and SCA (D) for the year 2006.

7.7 Surface net LW, 2006

The satellite and GME derived surface net long-wave radiation is denoted by SNL (surface net long-wave radiation). The corresponding CCLM quantity is $ATHB\_S$ (accumulated thermal budget at the surface).

The accuracy of SNL is given as $\Delta SNL = 15\,W/m^2$ for monthly means. The internal CCLM variability $\Delta ATHB\_S$ can be derived from Fig.55. It is up to $8\,W/m^2$ for all regions and months. The resulting accuracy is $\Delta(ATHB\_S - SNL) = 17\,W/m^2$.

Figure 60 A to C shows the annual mean 2006 of the GME008 simulation (A), of SAF210 (B) and their difference GME008-SAF210 (C). The differences GME008-SAF210 exceed the accuracy $\Delta_{12}(ATHB\_S - SNL) = 5W/m^2$ over several parts of Europe. We found the following patterns:

- Significant positive differences $(ATHB\_S - SNL) = 12.8\,W/m^2$ over SCA originating in differences in $ALWD\_S$.
- Significant negative differences over water surfaces with $(ATHB\_S - SNL) = -15.9\,W/m^2$ over MED and $(ATHB\_S - SNL) = -12.2\,W/m^2$ over WAS with peak values at the western and northern boundary of the model domain originating in differences in ALWD_S.
- Significant negative differences $(ATHB\_S - SNL) = -12.7\,W/m^2$ near the coasts of the Mediterranean Sea with peak values in the POE area dominated by differences in ALWU_S.

Figures 61 A to D show the monthly mean differences GME008-SAF210 at all grid points for January (A), April (B), July (C) and October (D) 2006. Additionally Fig.62 shows the area average of the 2006 monthly means and Fig.63 its differences for all months for the selected regions LND (A), WAS (B), SWE (C) and SCA (D). On the monthly time scale the deviations GME008-SAF210 exhibit additional spatial and temporal structures with significant deviations of $(ATHB\_S - SNL) \geq 17\,W/m^2$:

- Positive differences $(ATHB\_S - SNL) = 16.5\,W/m^2$ over SCA in December originating in ALWD_S and a compensation of the differences up and down in autumn. $(ATHB\_S - SNL) = 16.5\,W/m^2$
- Positive differences over SCA (up to $27.5\,W/m^2$) and central Europe (MEU up to $14.5\,W/m^2$) in summer originating in ALWU_S.
- Negative differences over EEU ($-19.8\,W/m^2$) in February originating in ALWD_S.
- Significant negative differences over MED in October to June of up to $(ATHB\_S - SNL) = -19.8\,W/m^2$ and weakly significant over WAS of up to $(ATHB\_S - SNL) = -15.8\,W/m^2$ originating in differences in ALWD_S.

Both components of the long-wave radiation budget (up and down) are strongly influenced by surface temperature and cloud cover causing higher variability of the resulting net variable. This exemplifies the advantages of the investigation of each component for finding of possible causes of the deviations.

However, the important climatological variable is the energy budget and not necessarily the single components.
The significant patterns of the deviation are hypothesised to have the following reasons:

- The summer cold bias of the model dominates the positive budget differences in summer in SCA and central Europe (MEU).
- Over WAS the negative surface budget all over the year appears together with a significantly higher cloud cover with peak values at the boundaries.
- The negative differences over POE area are connected with the differences over MED originating in negative differences of the cloud cover.

The significant patterns of the deviation are hypothesised to have the following climatological consequences:

- The summer cold bias of the model in summer in SCA and central Europe (MEU) reduces the evaporation and increases the humidity of the soil, which again reduces the temperature, a feedback mechanism.
- Over WAS the negative surface budget all over the year has no feedback on the climate due to prescribed SSTs over WAS.
- The influence of the POE are on the climate is estimated to be small due to relatively small area of the Poe valley.

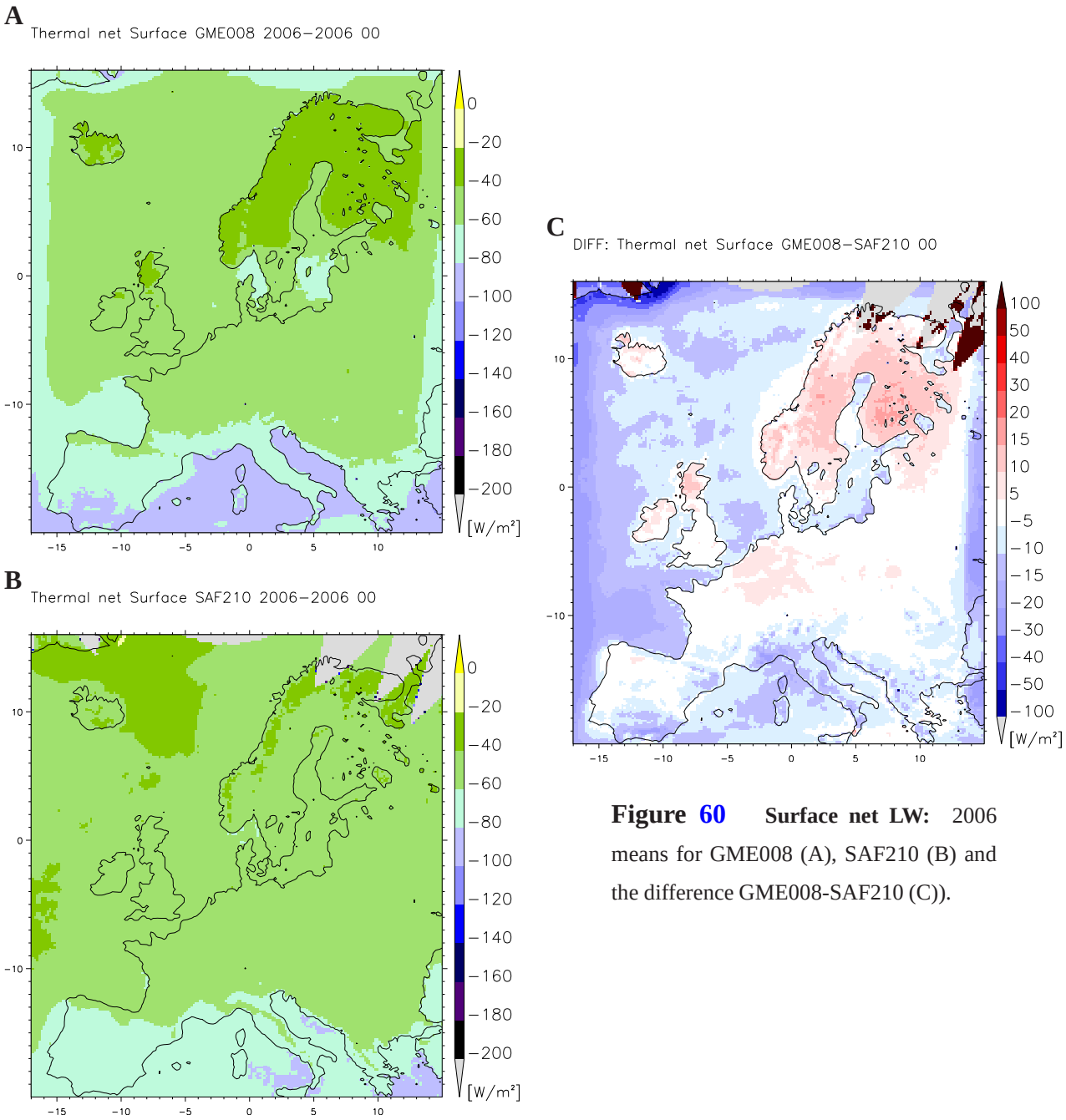

Figure 60 **Surface net LW:** 2006 means for GME008 (A), SAF210 (B) and the difference GME008-SAF210 (C)).

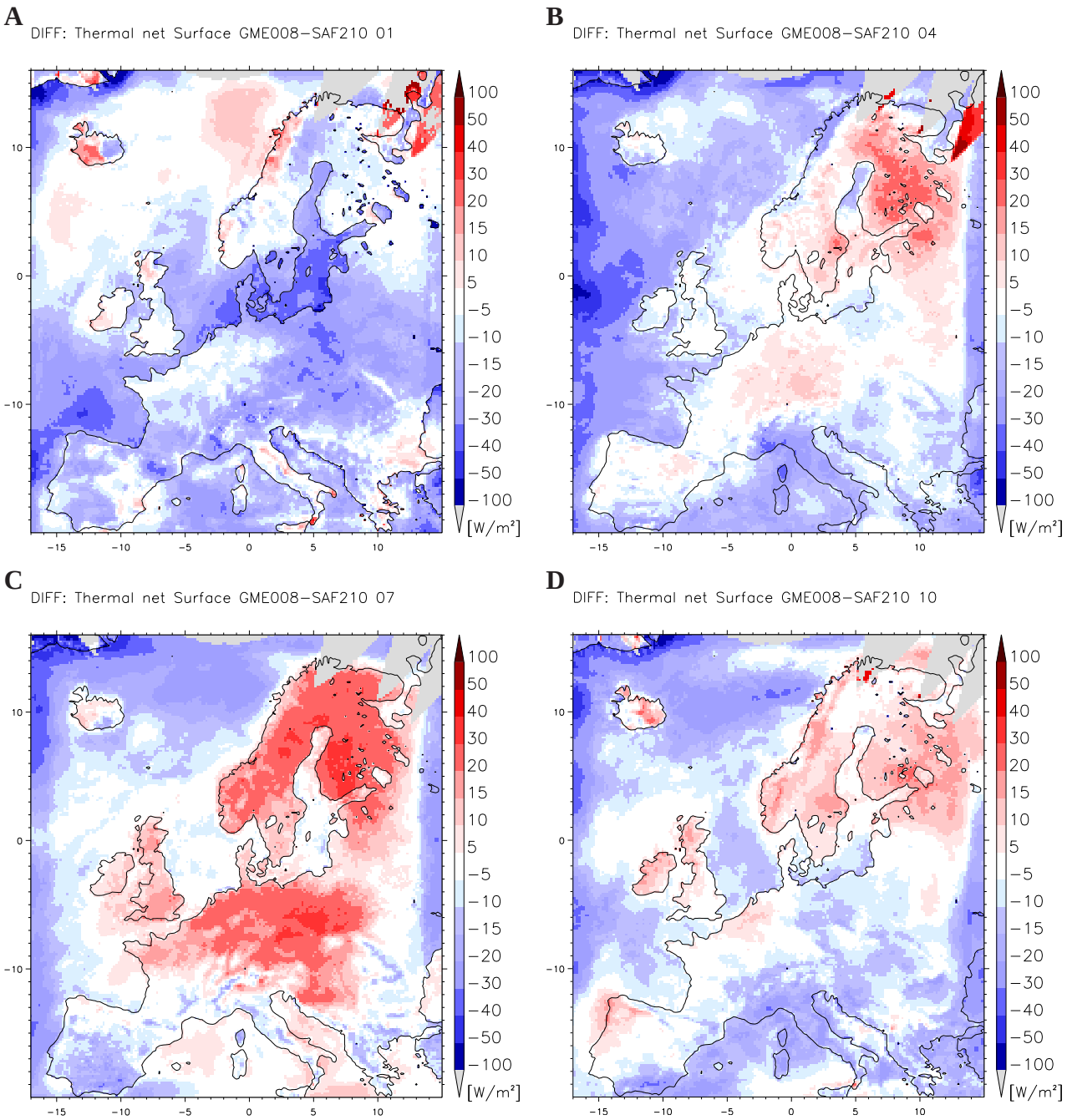

Figure 61 **Surface net LW:** monthly means of the differences GME008-SAF210 for January (A), April (B), July (C) and October (D) of the year 2006.

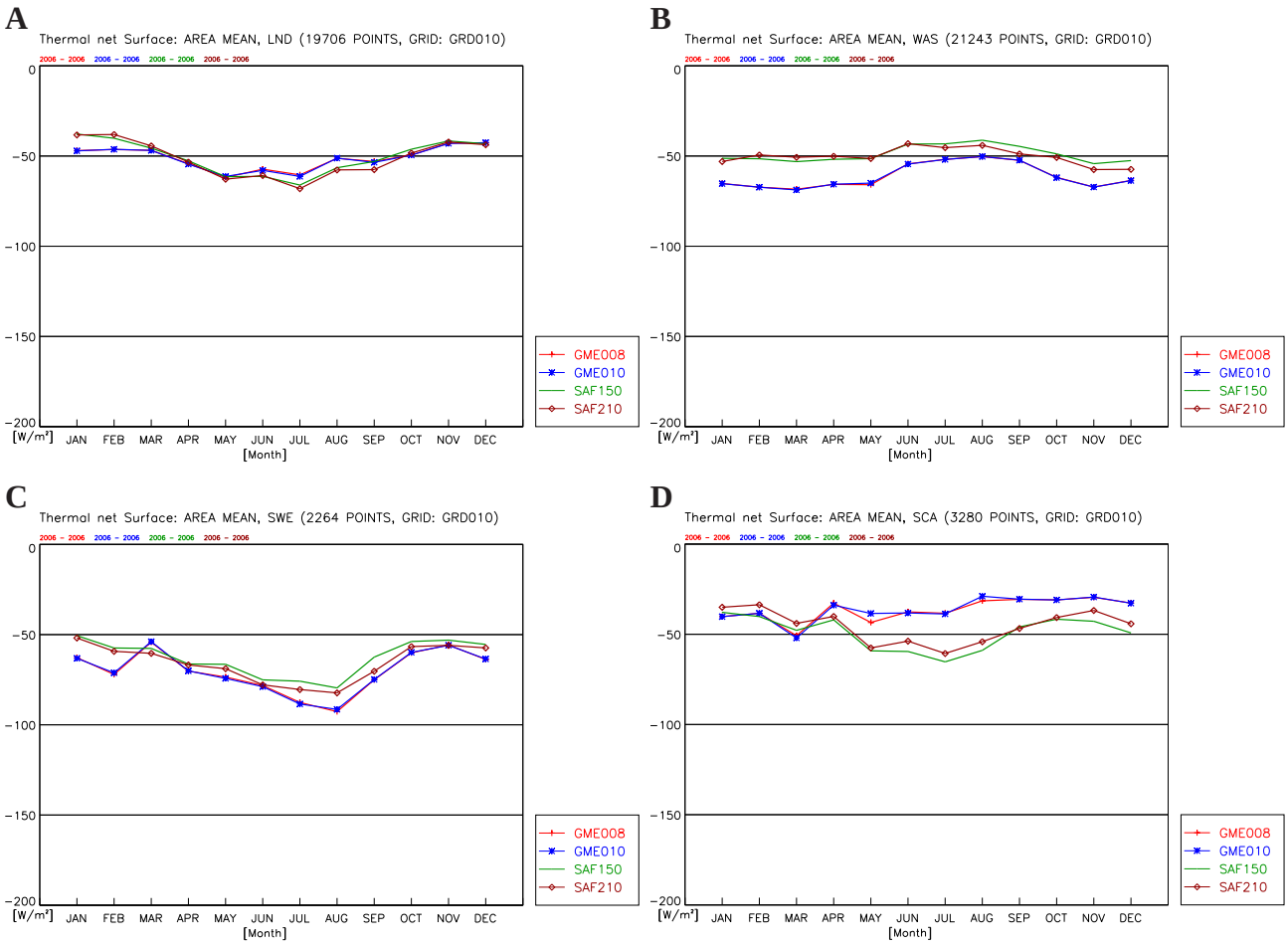

Figure 62 **Surface net LW:** annual cycle of the monthly means GME008, GME010, SAF150 and SAF210 for LND (A), WAS (B), SWE (C) and SCA (D) for the year 2006.

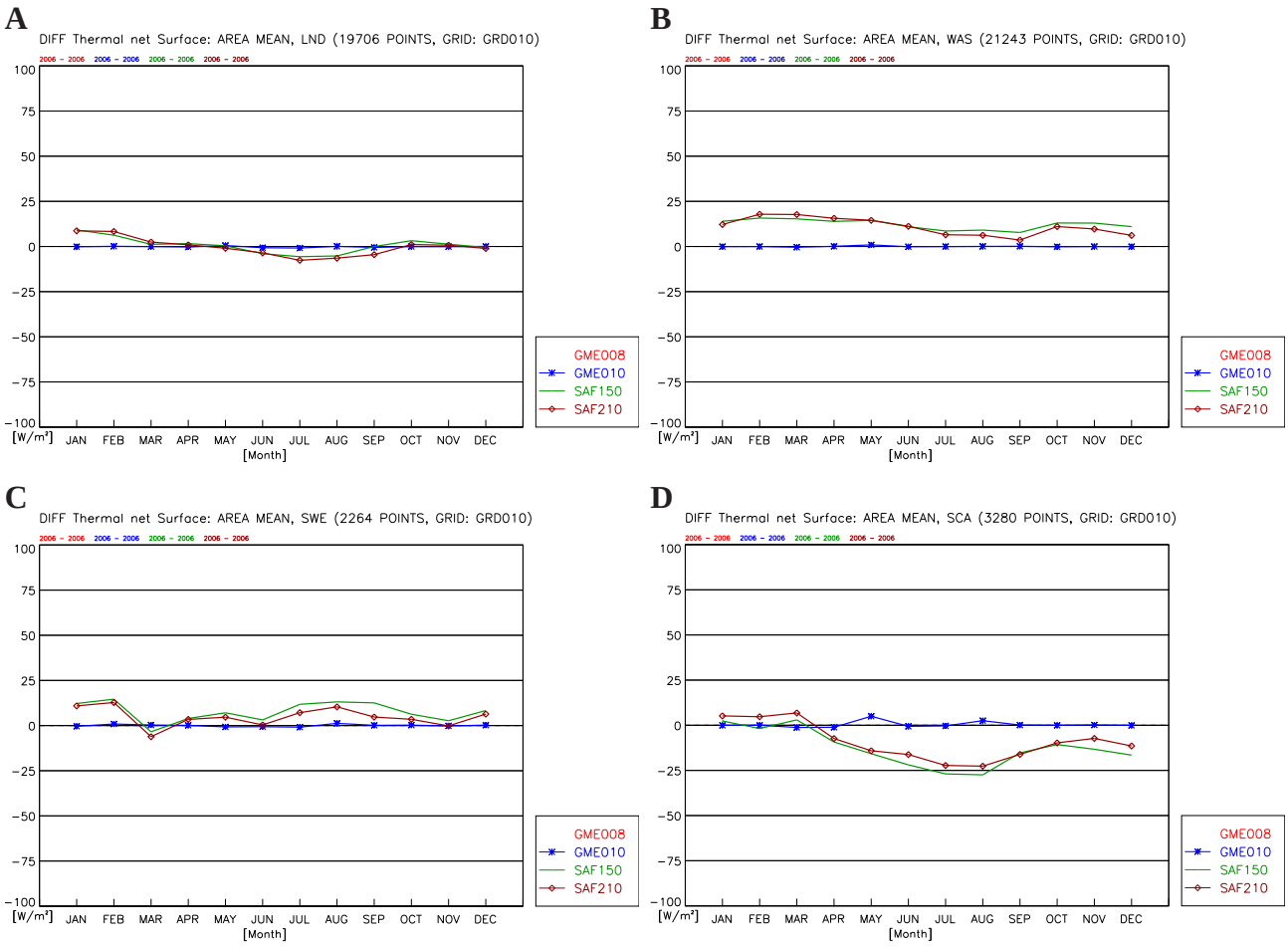

Figure 63 **Surface net LW:** annual cycle of the monthly mean differences Data-GME008 for LND (A), WAS (B), SWE (C) and SCA (D) for the year 2006.

7.8 Surface net radiation, 2006

The satellite and GME derived surface net radiation is denoted by SRB (surface radiation budget). The corresponding CCLM quantity is $ANRB\_S$ (accumulated net radiation budget at the surface).

The accuracy of SRB is given as $\Delta SRB = 21\,W/m^2$ for monthly means. The internal CCLM variability $\Delta ANRB\_S$ can be derived from Fig.67. It is up to $5\,W/m^2$ for all regions and months. The resulting accuracy is $\Delta(ANRB\_S - SRB) = 22\,W/m^2$.

Figure 64 A to C shows the annual mean 2006 of the GME008 simulation (A), of SAF210 (B) and their difference GME008-SAF210 (C). The differences GME008-SAF210 exceed the accuracy $\Delta_{12}(ANRB\_S - SRB) = 7W/m^2$ over several parts of Europe. We found the following for GME008-SAF210 and/or GME008-SAF150:

- Significant negative differences $(ANRB\_S - SRB) = -35\,W/m^2$ over SCA originating in differences in ASOB_S.
- Significant negative differences over water surfaces with $(ANRB\_S - SRB) = -26.2\,W/m^2$ over MED and $(ANRB\_S - SRB) = -25\,W/m^2$ over WAS originating in ASWG_S and ALWD_S.
- Significant negative differences in southern Europe with $(ANRB\_S - SRB) = -15.6\,W/m^2$ in SUE and $(ANRB\_S - SRB) = -13.7\,W/m^2$ in SWE as combined effect of long and short wave radiation budgets.

The reduced incoming radiation over water surfaces has no feedback on the regional climate. This is different for the land surfaces. In SCA and southern Europe a reduced heating of the surface explains parts of the 2m temperature difference, shown in Fig.68.

Figures 65 A to D show the monthly mean differences GME008-SAF210 at all grid points for January (A), April (B), July (C) and October (D) 2006. Additionally Fig.66 shows the area average of the 2006 monthly means and Fig.67 its differences for the selected regions LND (A), WAS (B), SWE (C) and SCA (D) in a more quantitative manner. On the monthly time scale the deviations GME008-SAF150/GME008-SAF210 exhibit additional spatial and temporal structures with significant deviations of $(ANRB\_S - SRB) \geq 22\,W/m^2$:

- Negative differences over SCA in spring to autumn with peak values in summer ($(ANRB\_S - SRB) = -60\,W/m^2$) originating in ASOB_S and reduced by the long-wave budget ATHB_S.
- Negative differences over other land areas, except in winter months, especially over southern Europe with peak values in summer ($(ANRB\_S - SRB)_{SWE} = -23\,W/m^2$, $(ANRB\_S - SRB)_{SUE} = -26\,W/m^2$, $(ANRB\_S - SRB)_{UNG} = -25\,W/m^2$) originating in summer in ASOB_S and in winter in ATHB_S.
- Significant negative differences over water surfaces with peak values in spring to summer with $(ANRB\_S - SRB)_{WAS} = -44\,W/m^2$ and $(ANRB\_S - SRB)_{MED} = -42\,W/m^2$ in July originating in differences in ALWD_S.

The radiation budget and its four components are strongly connected with the surface temperature and the cloud dynamics. This makes the identification of the origins difficult. In the following the relations identified by inspection of the single components are taken into account:

- Negative differences with peak values over WAS in summer are dominated by the negative differences in down SW at the surface.
- Negative differences over central Europe in summer are dominated by summer cold bias and negative differences in down SW.
- Negative differences in SCA in spring are dominated by high snow albedo values.

From climatological point of view, the underestimated downward radiation has no feedback on the climate over water surfaces. Over land surfaces it reduces the soil temperature and contributes to the models cold bias.

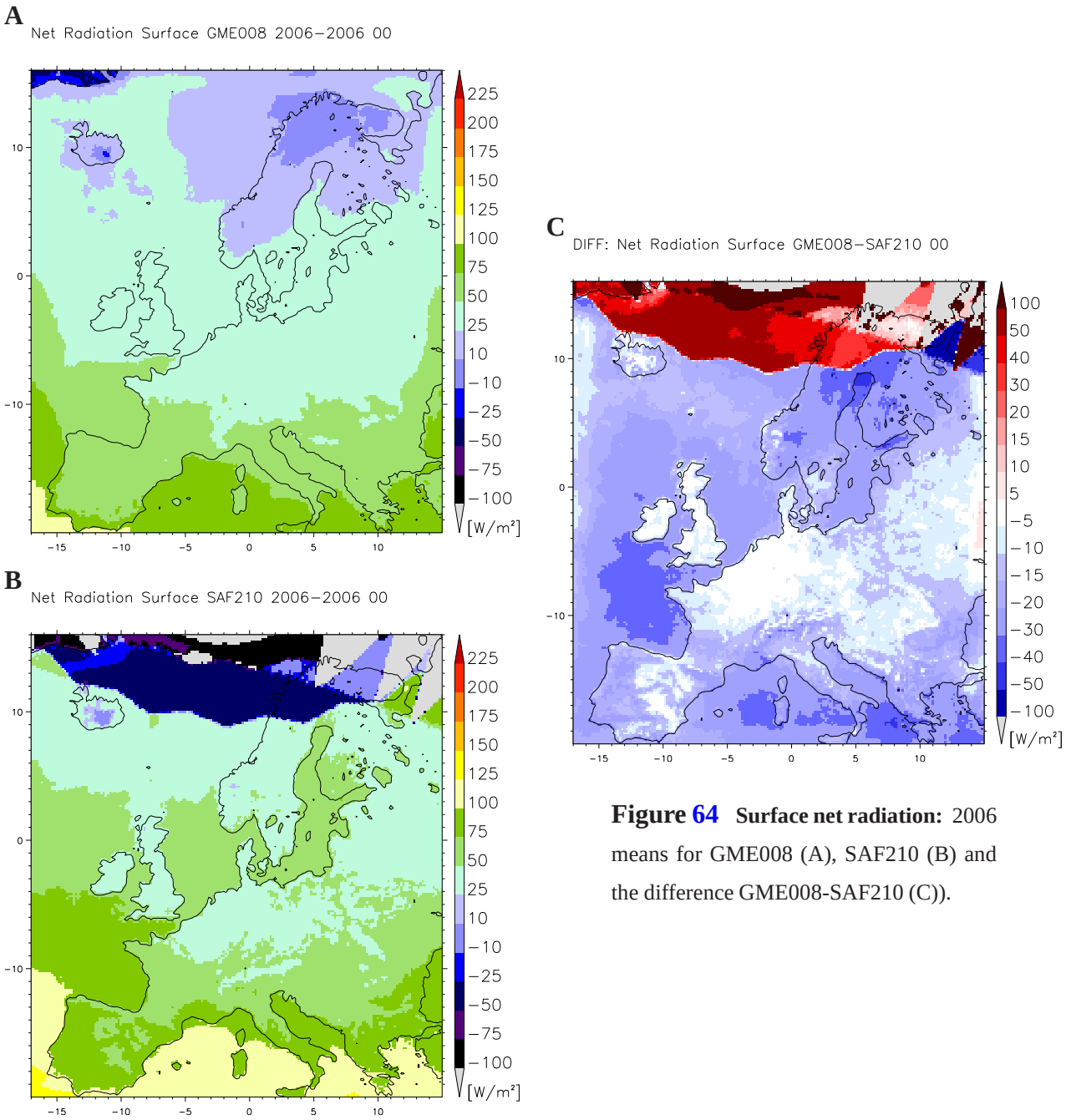

Figure 64 **Surface net radiation:** 2006 means for GME008 (A), SAF210 (B) and the difference GME008-SAF210 (C)).

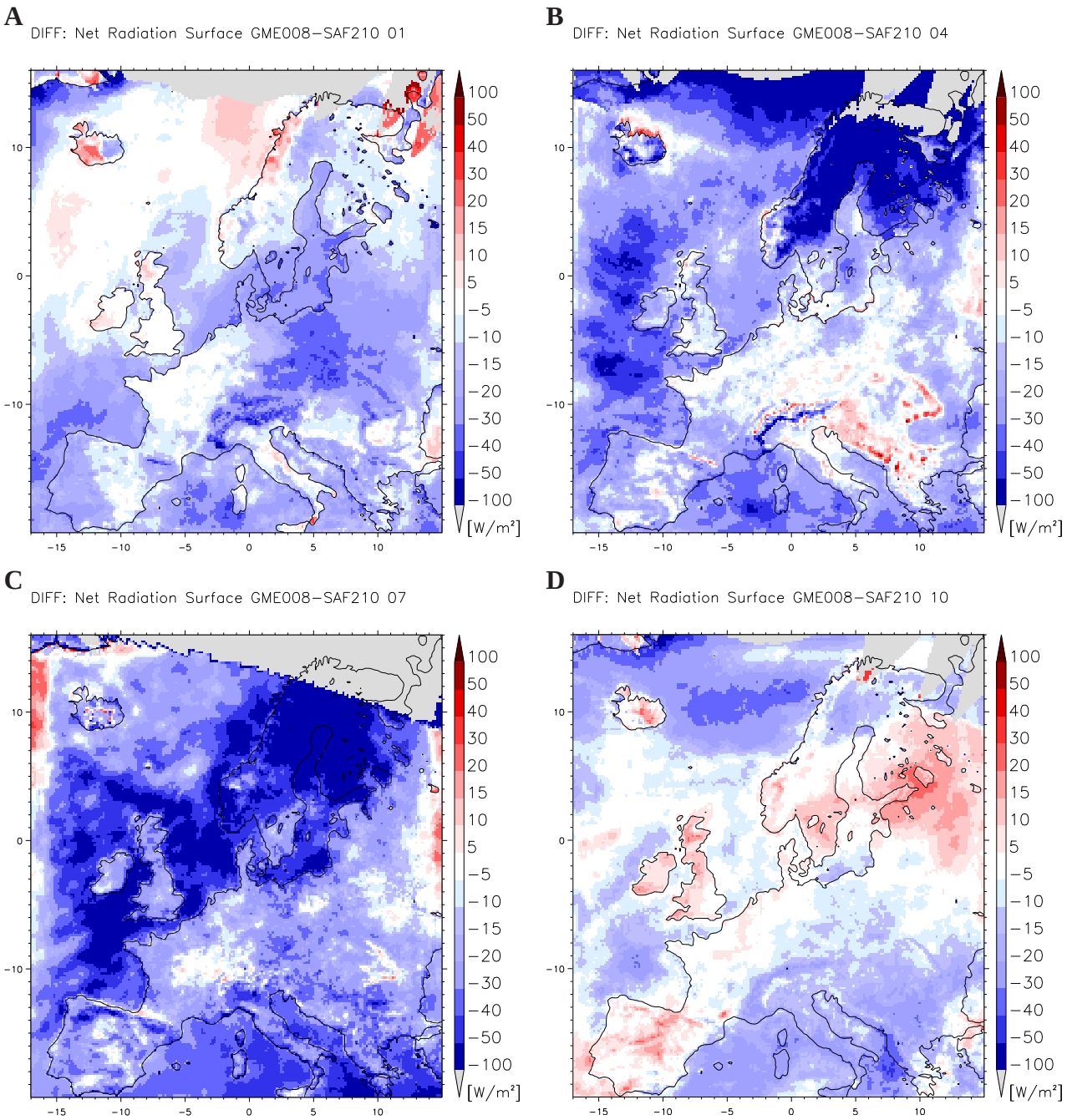

Figure 65 **Surface net radiation:** monthly means of the differences GME008-SAF210 for January (A), April (B), July (C) and October (D) of the year 2006.

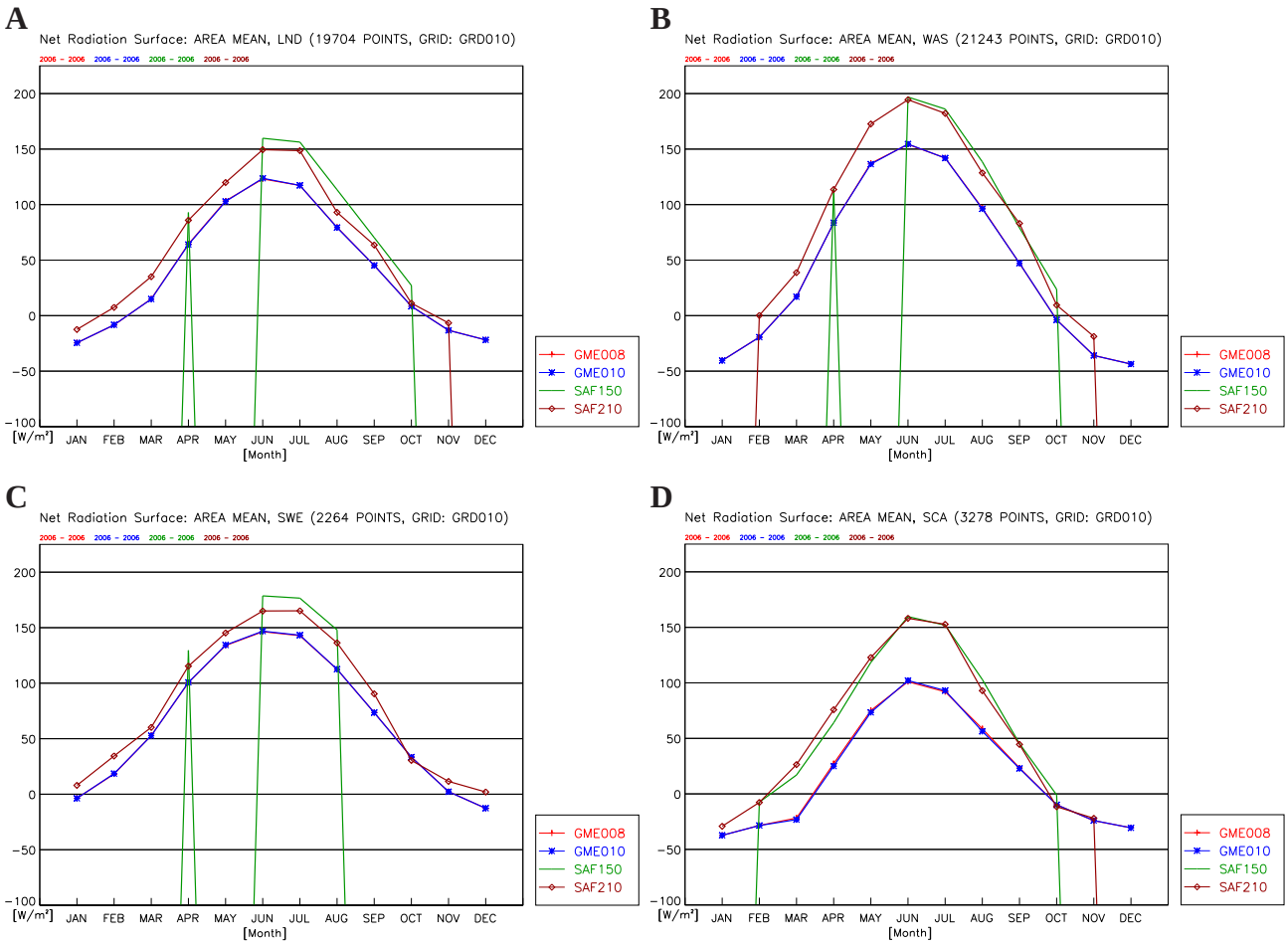

Figure 66 **Surface net radiation:** annual cycle of the monthly means GME008, GME010, SAF150 and SAF210 for LND (A), WAS (B), SWE (C) and SCA (D) for the year 2006.

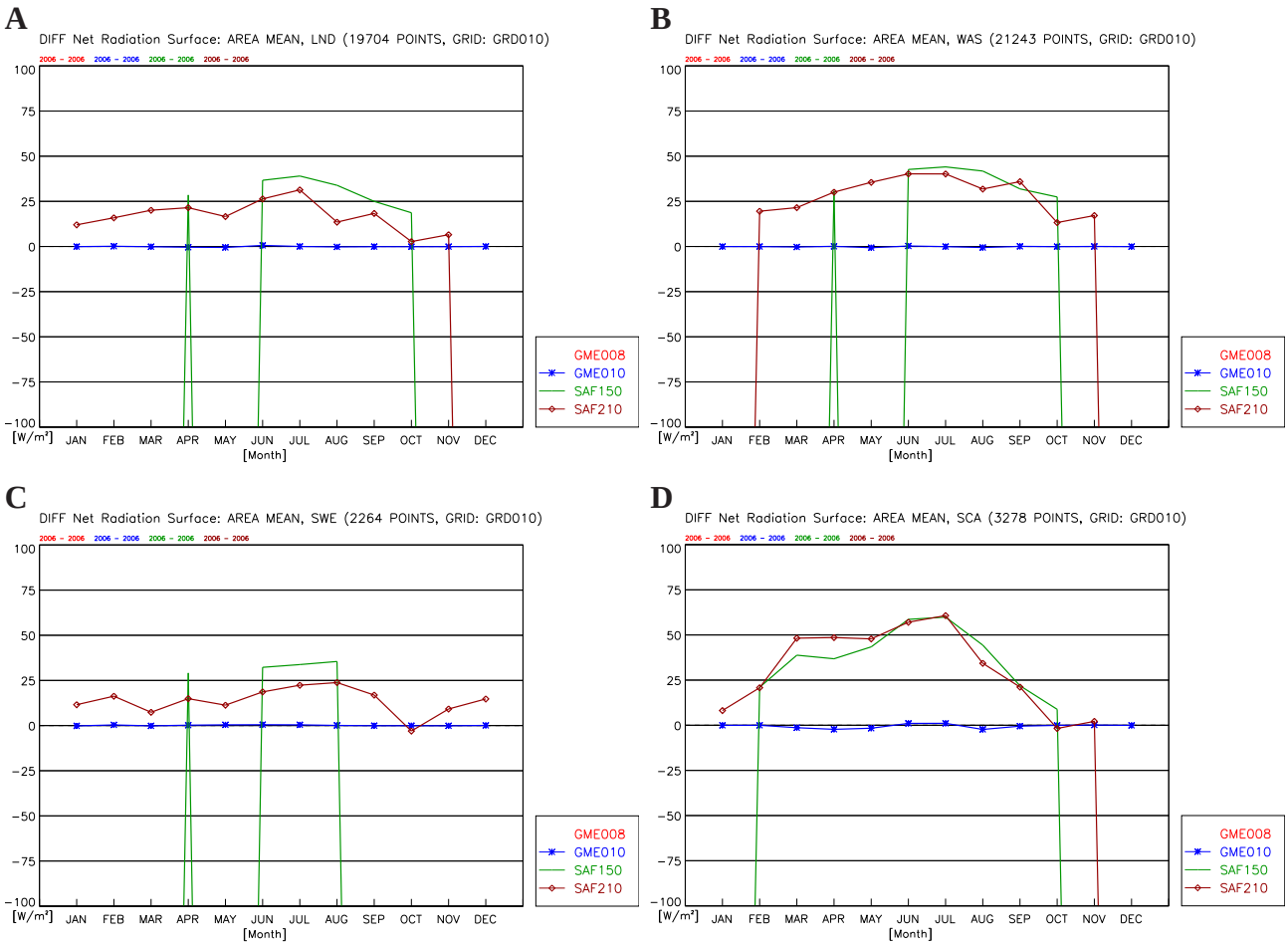

Figure 67 **Surface net radiation:** annual cycle of the monthly mean differences Data-GME008 for LND (A), WAS (B), SWE (C) and SCA (D) for the year 2006.

8 Meteorological variables

8.1 2m Temperature, 2005-2006, 2005, 2006

The reference data set (Haylock et al., 2008) used for evaluation over land areas and denoted here ECAD01 (E-OBS in other studies) has been developed within the EU-FP6 project ENSEMBLES (http://www.ensembles-eu.org/). For this study the data for the temperature 2m above ground (TEMP) on the rotated $0.22°$ grid was used. The corresponding CCLM quantity is T_2M (temperature in 2m above ground).

The accuracy of T2M is not known. It can not be derived from internal variability of different reference data sets, because no other data set for the period 2005-2006 is available at the moment. The internal CCLM variability ΔT_2M can be derived from Fig.70. It is up to $0.5\,K$ for all regions and months. The accuracy is estimated to be 1.5 K for all months.

Figure 68 A to C shows the annual mean 2005-2006 of the GME008 simulation (A), of ECAD01 (B) and their difference GME008-ECAD01 (C). The differences GME008-ECAD01 exceed the estimated accuracy $\Delta_{24}(T\_2M - T2M) \geq 0.3\,K$ over most parts of Europe. We found an annual cold bias of:

- $-1.6\,K$ over DTL and SCA,
- $-0.9\,K$ over POE and
- $-0.8\,K$ over SWE.

Figures 69 A to D exhibit the monthly mean differences GME008-ECAD01 at all grid points for January (A), April (B), July (C) and October (D) 2005-2006. Additionally Fig.70 shows the area averages of the 2005, 2006 and 2005-2006 monthly means and Fig.63 the differences for the selected regions DTL (A), POE (B), SWE (C), SCA (D) and ALP (E) for 2005-2006 in a more quantitative manner. Fig. 62 shows that the differences between these two years are small in comparison to the differences to observations and that the letter are the same for both years. On the monthly time scale the deviations GME008-ECAD01 exhibit additional spatial and temporal structures with significant deviations of $(T\_2M - T2M) \geq 1\,K$:

- Positive differences over NSK in late winter ($(T\_2M - T2M) = 1\,K$)
- Strongly significant negative differences over central Europe (MEU) and Scandinavia (SCA) in summer with peak values in July of $(T\_2M - T2M) = -3\,K$ over SCA and $(T\_2M - T2M) = -2.7\,K$ over DTL.
- Significant negative differences over ALP with peak values in March of $(T\_2M - T2M) = -3.2\,K$.

The 2m Temperature is a diagnostic variable derived from the land surface properties and the dynamical temperature field. The various potential sources of errors make it difficult to draw conclusions

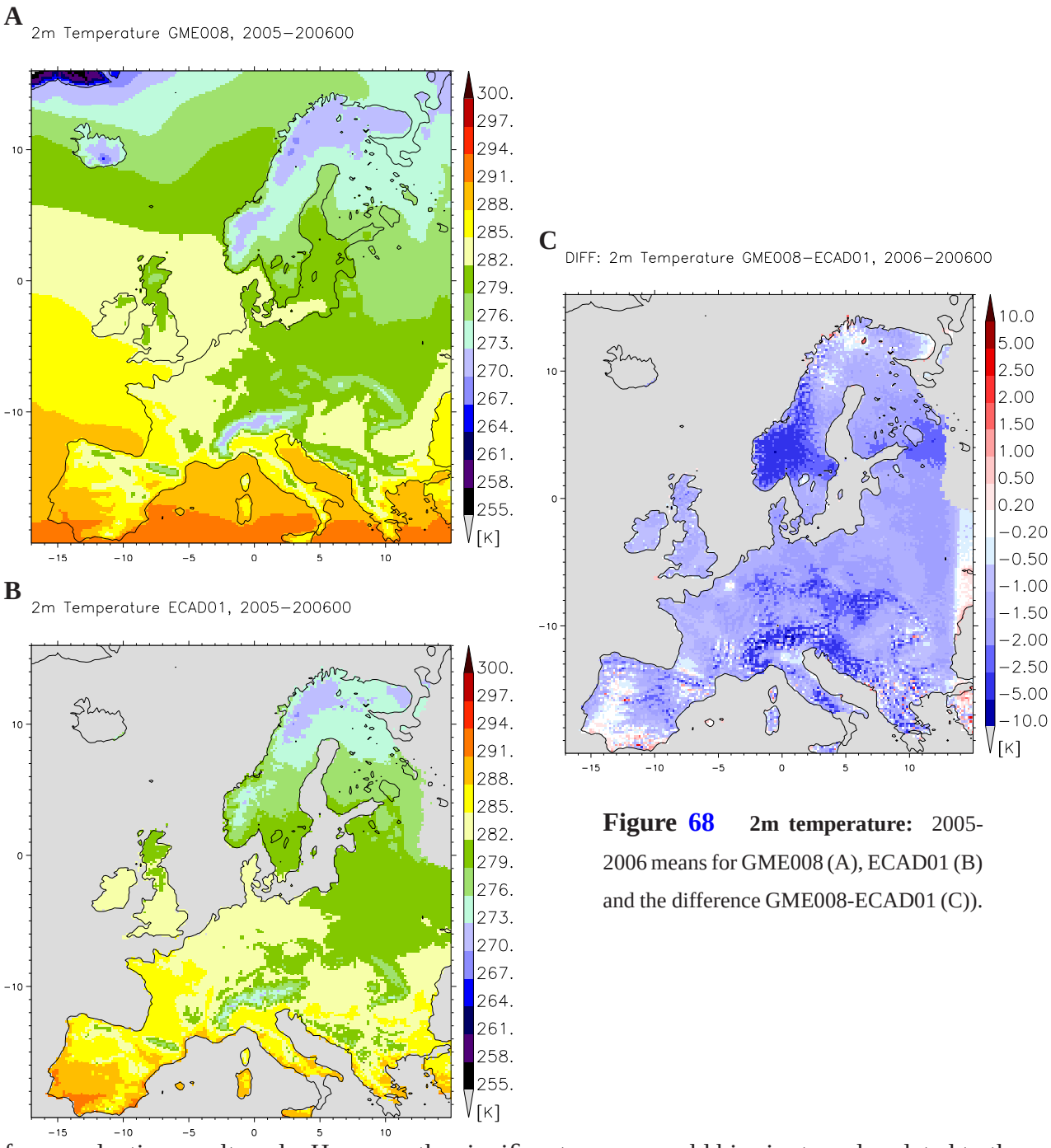

Figure 68 **2m temperature:** 2005-2006 means for GME008 (A), ECAD01 (B) and the difference GME008-ECAD01 (C)).

from evaluation results only. However, the significant summer cold bias is strongly related to the underestimation of summer outgoing long-wave radiation at the surface, higher precipitation and cloud cover. In this sense the results for the cloud cover are consistent.

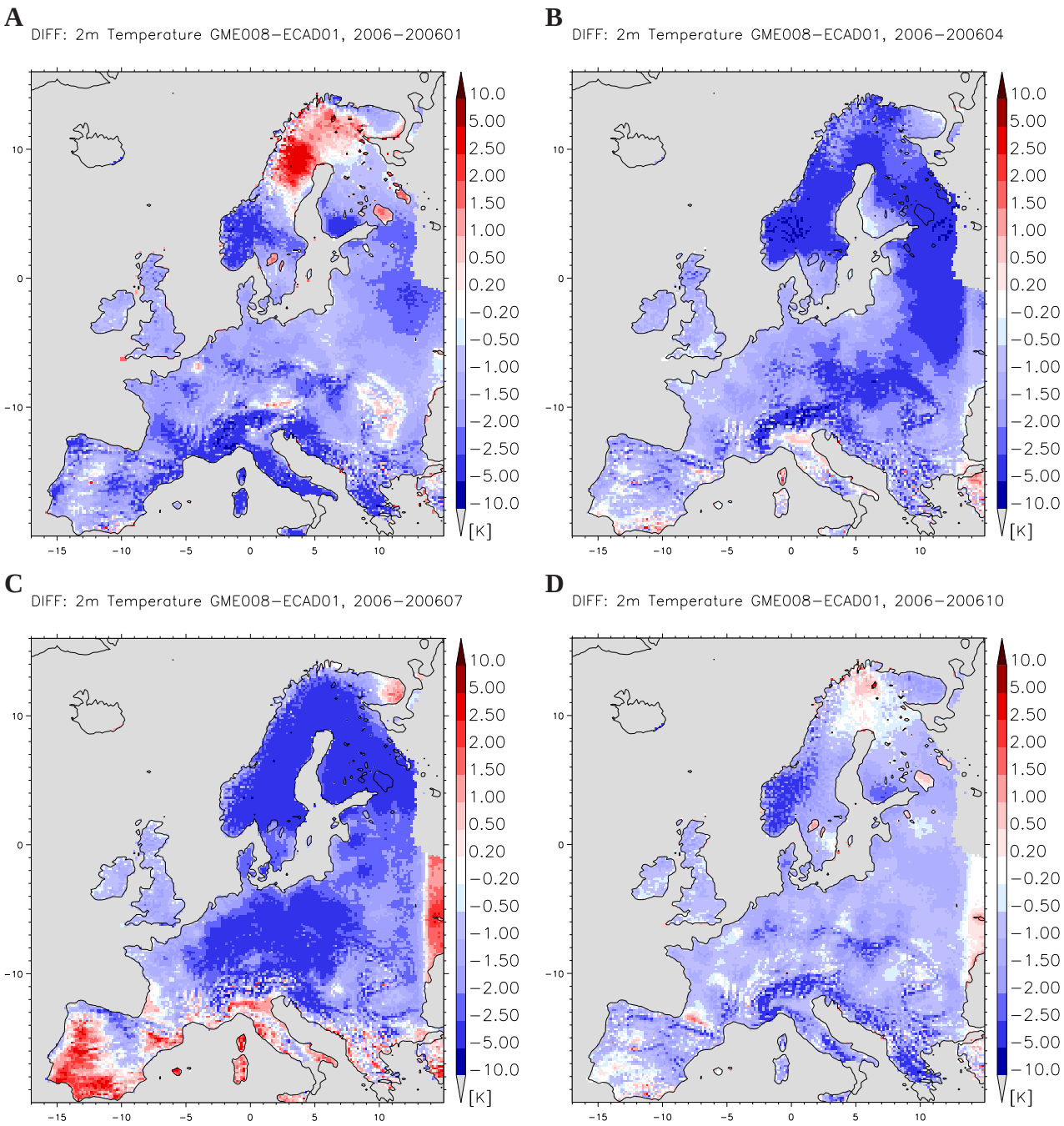

Figure 69 **2m temperature:** monthly means of the differences GME008-ECAD01 for January (A), April (B), July (C) and October (D) of the time period 2005-2006.

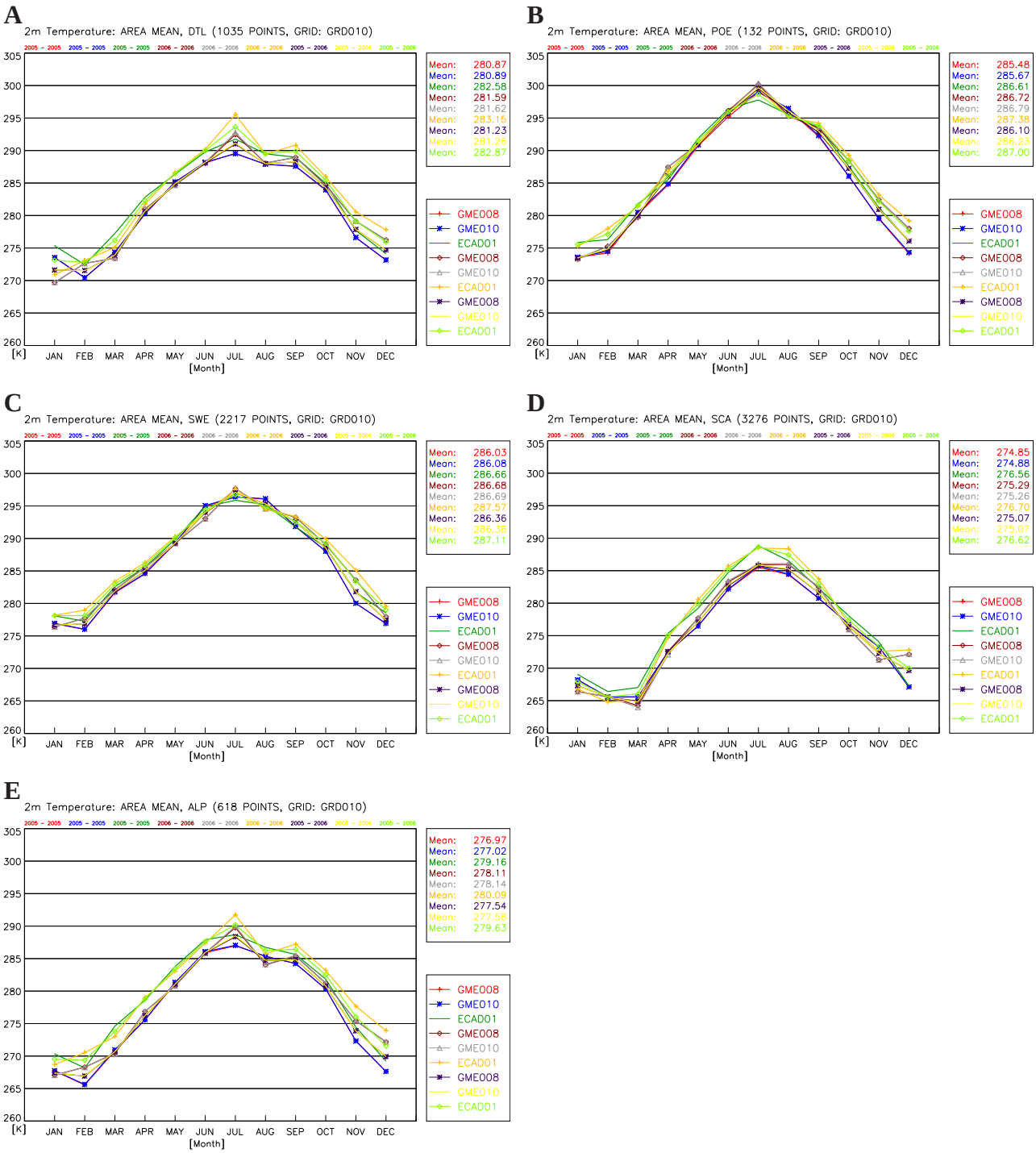

Figure 70 **2m temperature:** annual cycle of the monthly means GME008, GME010 and ECAD01 for DTL (A), POE (B), SWE (C), SCA (D) and ALP (E) for the year 2005, 2006 and 2005-2006.

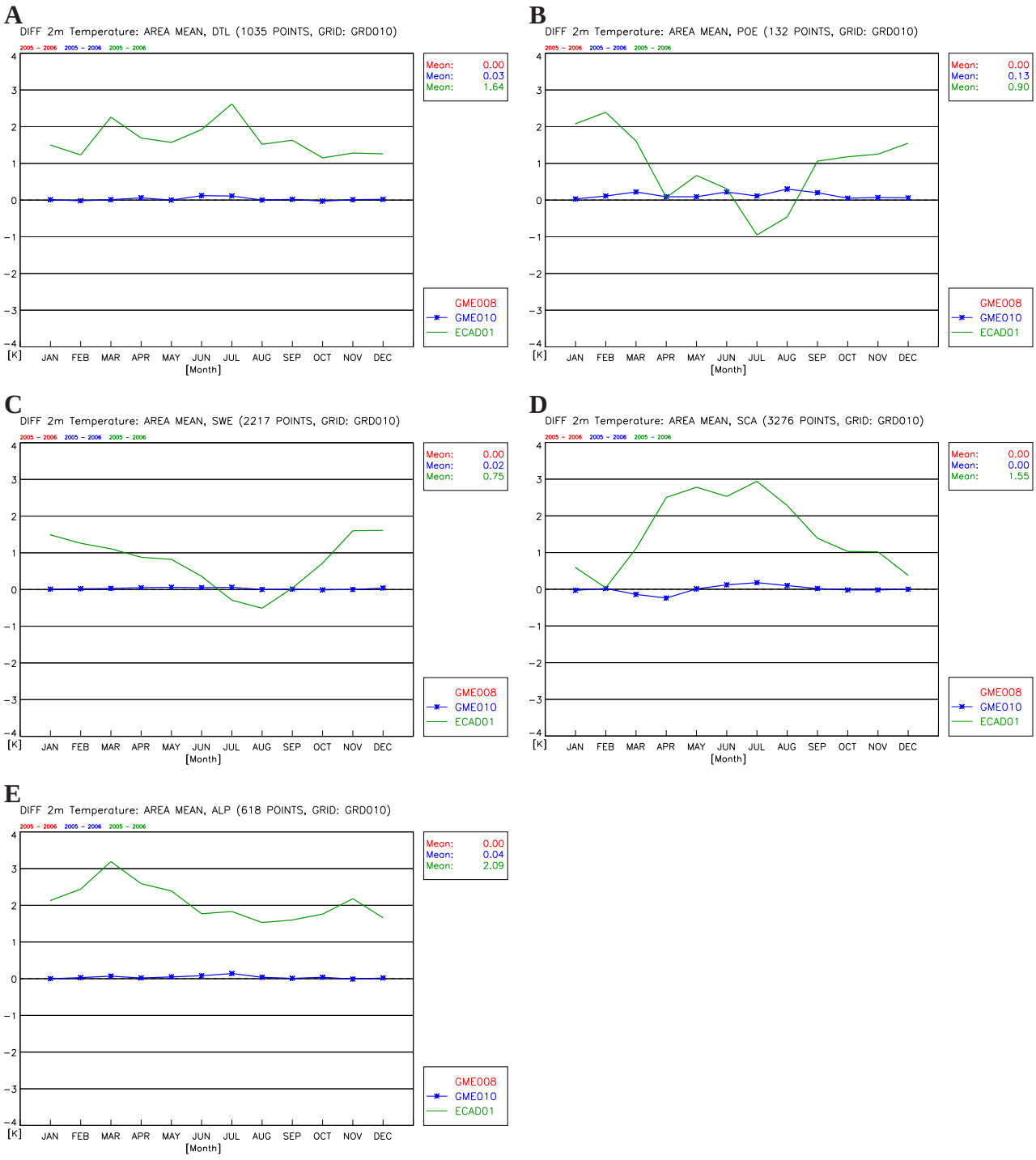

Figure 71 **2m temperature:** annual cycle of the monthly mean differences Data-GME008 for DTL (A), POE (B), SWE (C), SCA (D) and ALP (E) for the time period 2005-2006.

8.2 Total precipitation, 2005-2006. 2005, 2006

Annual mean For the Alpine region and probably also for Scandinavia the model overestimates the mean precipitation. Monthly mean All results are smaller than the uncertainty due to small disturbances of the boundary conditions.

The total precipitation is one of the most intensively investigated climatological variables. For 2006 three different data sets are available to the authors. Version 1 (GPCP01) and version 2 (GPCP02) of the GPCP data set ([*Adler et al.*(2003)]) for global precipitation (PRECIP) are available on the $0.5°$ geographical grid and PRECIP of the ECAD01 (see 8.1 for details) on the $0.22°$ rotated grid of the ENSEMBLES project. The corresponding CCLM quantity is TOT_PREC (total precipitation).

The accuracy of PRECIP is not available. It can be estimated from the internal variability of different reference data sets shown in Fig.74 to be $\Delta PRECIP = 30mm/mon$ in SWE and $\Delta PRECIP = 10mm/mon$ in SCA. It has to be mentioned that the GPCP data exhibit significantly more precipitation than all other climatological data sets and that the data sets tend to underestimate the prcipitation amounts. The internal CCLM variability ΔTOT_PREC can also be estimated from Fig.74. It is up to $10\,mm/mon$ in SCA. The resulting accuracy is therefore $\Delta(TOT\_PREC - PRECIP) = 32\,mm$ for monthly sums.

Figure 68 A to C shows the annual sum 2006 of the GME008 simulation (A), of GPCP01 (B) and their difference GME008-GPCP01 (C). The differences GME008-GPCP01 exceeds the annual accuracy $\Delta_{12}(TOT\_PREC - PRECIP) \geq 115mm/y$ over some parts of Europe. We found the following:

- Not significant positive differences $(TOT\_PREC - PRECIP) = 75\,mm/y$ over NOA.
- Not significant negative differences $(TOT\_PREC - PRECIP) = -263\,mm/y$ over MED and other water surfaces.
- Weakly significant positive differences $(TOT\_PREC - PRECIP) = 171\,mm/y$ over SCA.
- Weakly significant positive differences $(TOT\_PREC - PRECIP) = 270\,mm/y$ over ALP.
- Not significant negative differences $(TOT\_PREC - PRECIP) = -87\,mm/y$ over SWE and $(TOT\_PREC - PRECIP) = -97.5\,mm/y$ over UNG.

Figures 73 A to D show the monthly mean differences GME008-GPCP01 at all grid points for January (A), April (B), July (C) and October (D) 2006. Additionally Fig.74 shows the area average of the 2005, 2006 and 2005-2006 monthly means and Fig.63 the 2005-2006 differences for the selected regions LND (A), WAS (B), SWE (C) and SCA (D) in a more quantitative manner. On the monthly time scale the deviations GME008-GPCP01 exhibit additional spatial and temporal structures with significant deviations of $(TOT\_PREC - PRECIP) \geq 33\,mm/mon$:

- High variability over NOA up to $(TOT\_PREC - PRECIP) = 39.4\,mm/mon$ in Nov. and -45.9 in January .
- Not significant positive differences in SCA in summer with up to $(TOT\_PREC - PRECIP) = 28.4\,mm/mon$ in June.

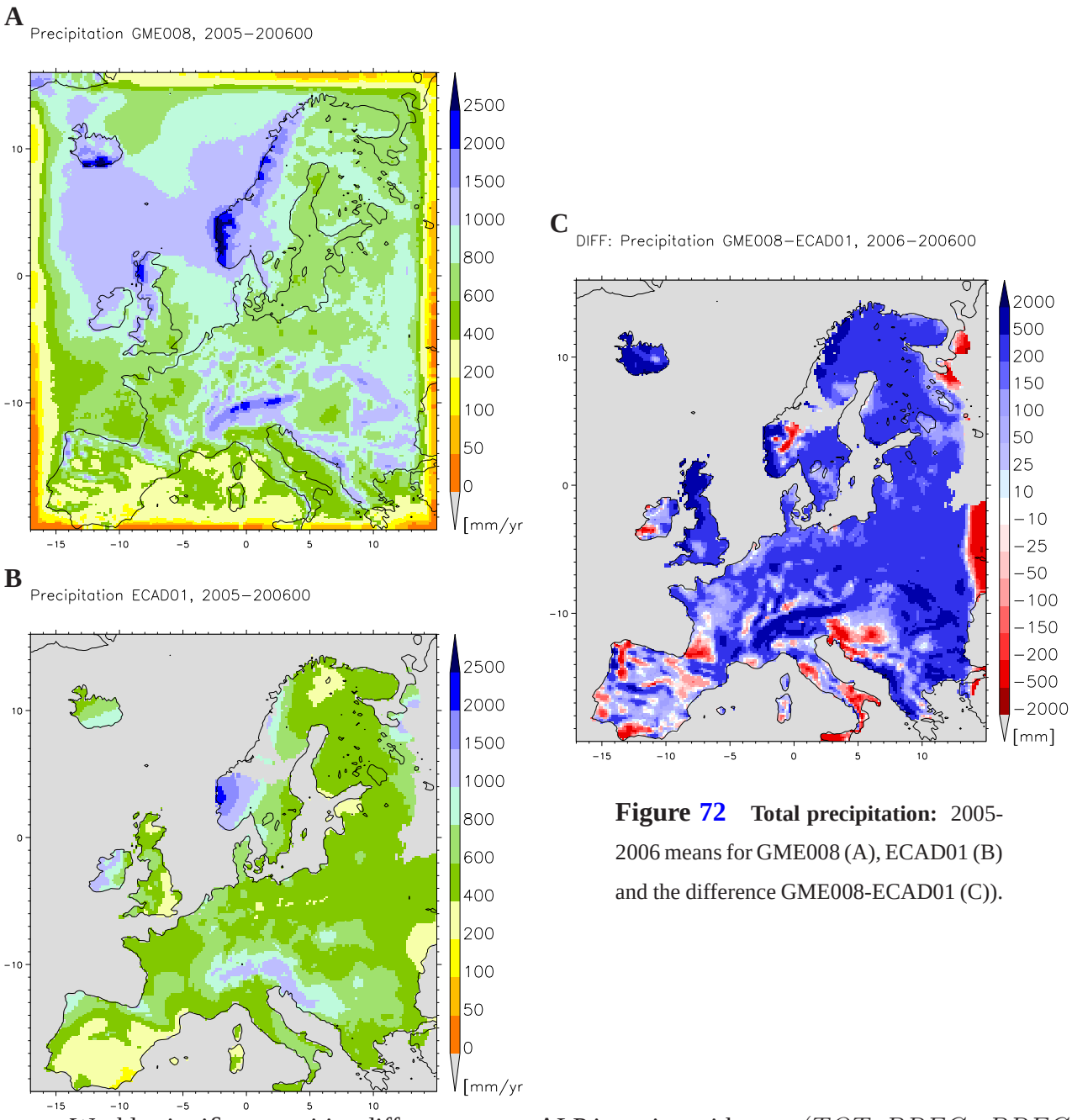

Figure 72 **Total precipitation:** 2005-2006 means for GME008 (A), ECAD01 (B) and the difference GME008-ECAD01 (C)).

- Weakly significant positive differences over ALP in spring with up to $(TOT\_PREC - PRECIP) = 45.3\,mm/mon$ in April.
- Not significant negative differences in SWE in autumn and winter with up to $(TOT\_PREC - PRECIP) = -32.3\,mm/mon$ in November and all over the year in UNG with up to -35.2 mm/mon in August.

The total precipitation is a highly stochastic variable following an extreme value distribution with high variability. Furthermore, it is difficult to observe with high accuracy due to evaporation in summer and snow in winter. All results are close to the limit of accuracy derived from internal variability of the data used and simulations conducted. Significant results can be obtained only for longer time serieses. Typical results obtained from long time evaluations are not visible in these results.

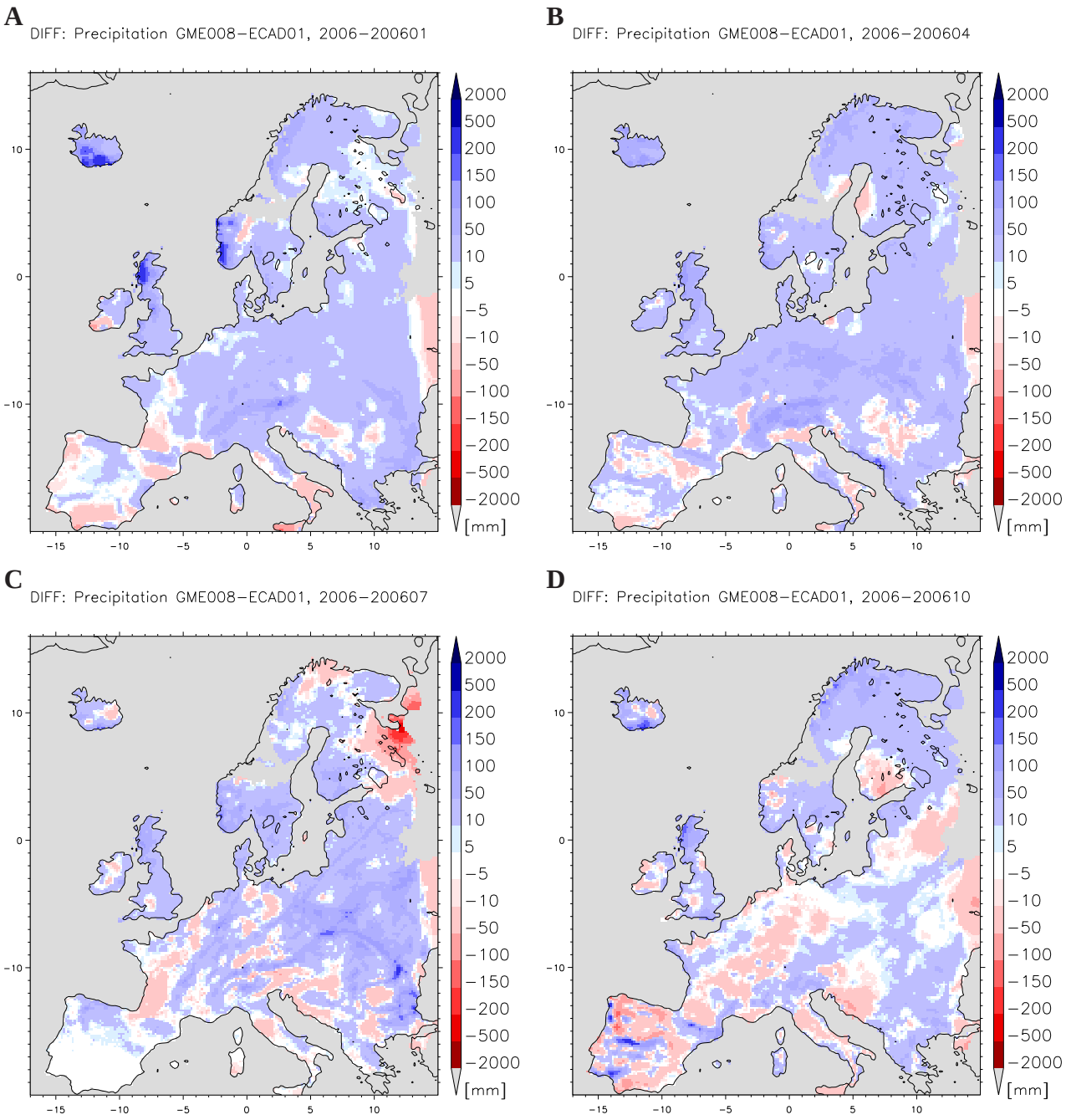

Figure 73 **Total precipitation:** monthly means of the differences GME008-ECAD01 for January (A), April (B), July (C) and October (D) of the time period 2005-2006.

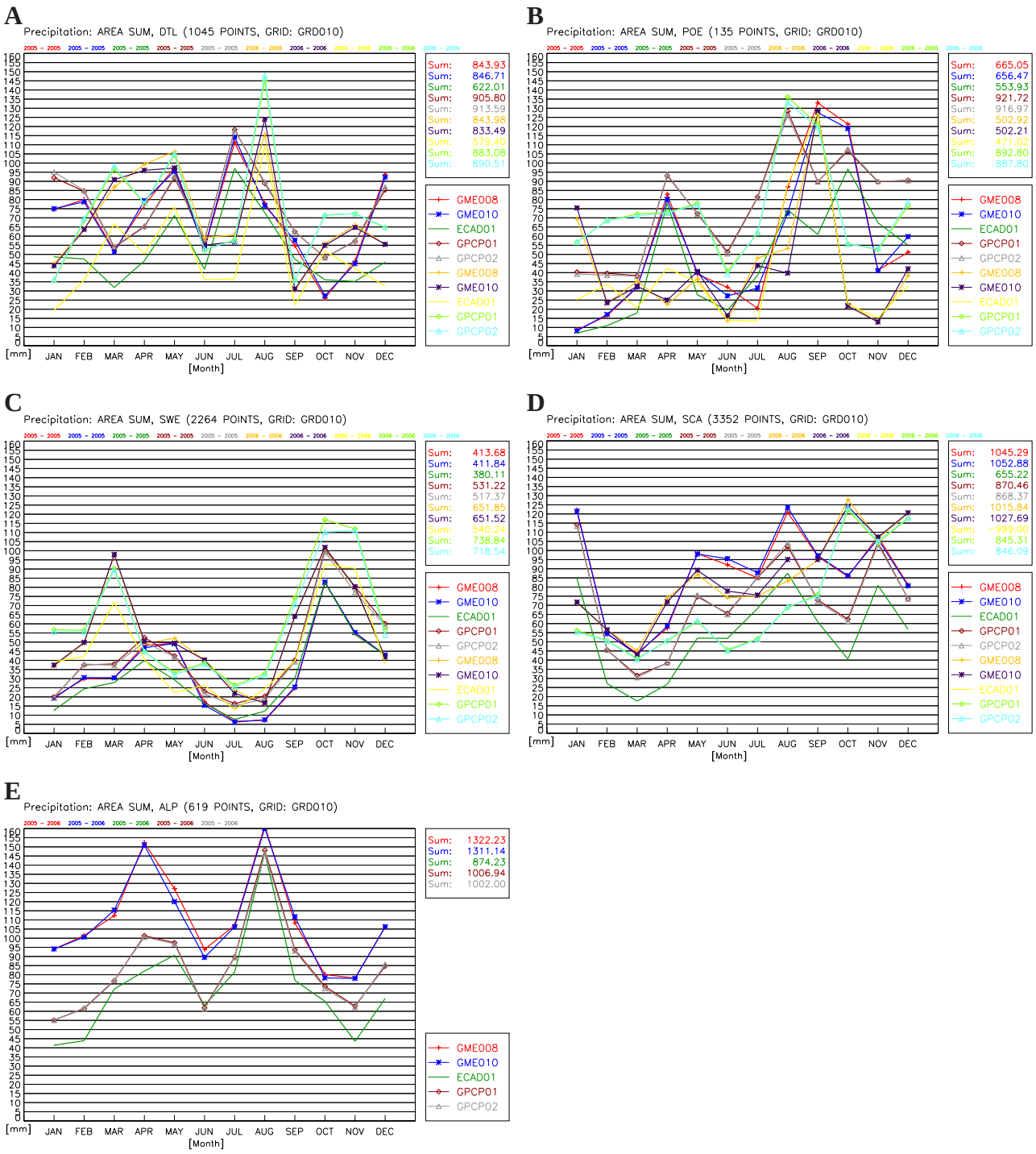

Figure 74 **Total precipitation:** annual cycle of the monthly means GME008, GME010, ECAD01, GPCP01 and GPCP02 for LND (A), WAS (B), SWE (C), SCA (D) and ALP (E) for the time periods 2005 and 2006.

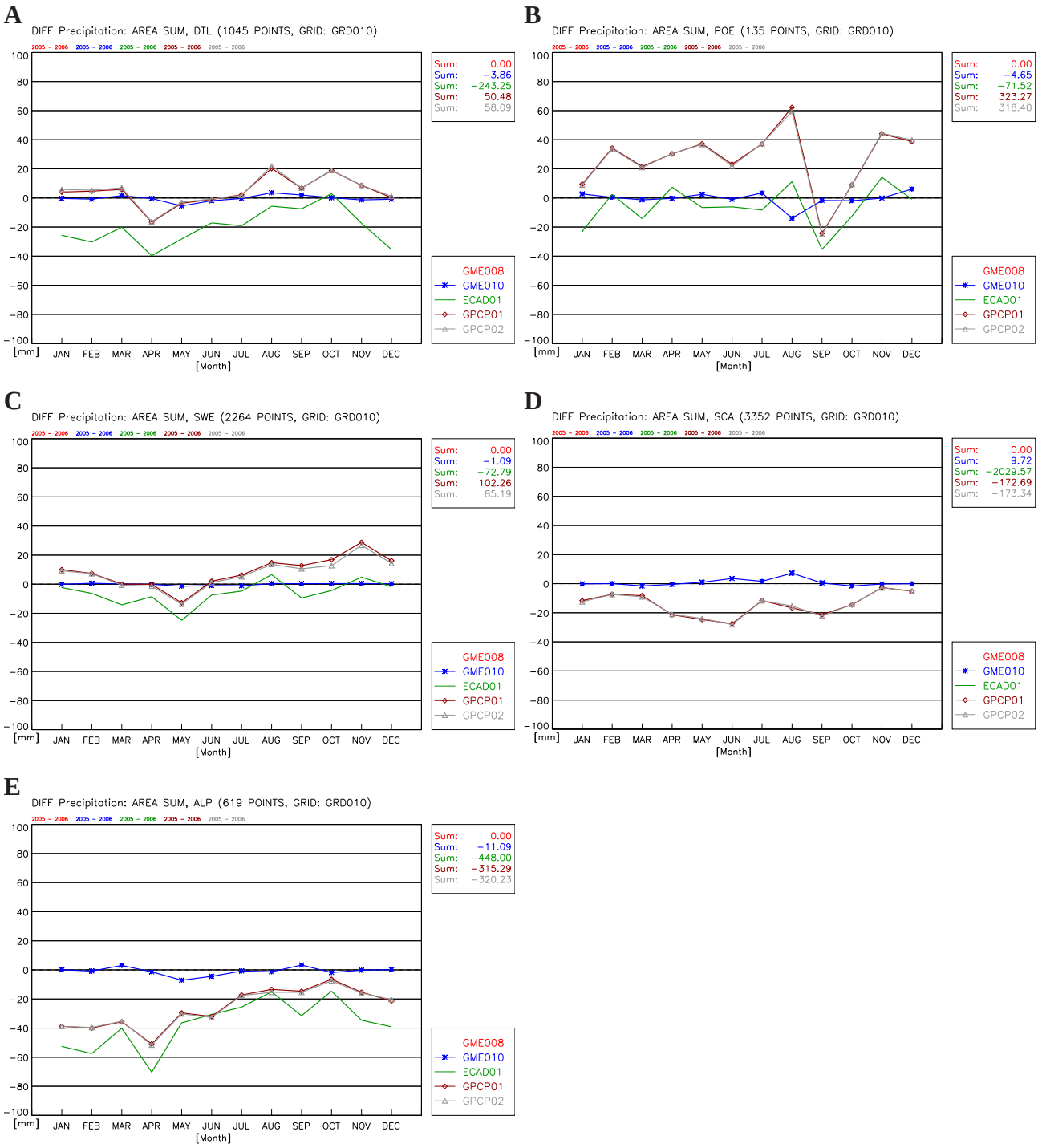

Figure 75 **Total precipitation:** annual cycle of the monthly mean differences Data-GME008 for LND (A), WAS (B), SWE (C), SCA (D) and ALP (E) for the time period 2005-2006. No differences have been calculated in the SCA for ECAD01 due to more than 5% of missing data.

9 Summary

For the first time all radiation components TOA and at the surface of the regional climate model COSMO-CLM have been systematically compared with the CMSAF products aiming to analyse the potential of such a comparison for evaluation of the model and of the CMSAF data.
The group Environmental Meteorology at BTU Cottbus conducted a systematic comparison of CM-SAF products for Europe with the model output of two regional climate model simulations with COSMO-CLM on the model grid of $0.165°$. COSMO-CLM was forced with the analysis of the global model GME provided by the German Weather Service. The discussion of the significance of the deviations between model and data for all radiation components and integral cloud properties for selected regions confirmed the potential of the method.
First, different types of differences could be identified and hypotheses on possible origins could be formulated. Second, specific properties of CMSAF variables could be identified which should be improved in order to substantially increase the relevance of the CMSAF products for climate model evaluations.

This study is based

- on the accuracy statements of the SAF data and
- on the comparisons of absolute values and differences between model results and between model results and SAF products for
  - annual means,
  - monthly means and
  - annual cycles of spatial averages for 35 selected regions.

All differences exceeding the accuracy on space scales larger than $200 \times 200\,km^2$ are regarded as significant and the systematic analysis is restricted to the significant differences. The comparison of second moments and other statistical quantities like the spatio-temporal correlations remains for future work.

The analysis of the results aims to determine the consistency of the provided SAF products with the accuracy statements, to quantify the inevitable uncertainties, and to draw conclusions about the origin of the differences between model and data taking into account the assumed typical spatial structures of the differences originating in model deficiencies and/or Satellite data bias. It is assumed that

- a SAF data bias typically exhibits
  - a North-South contrast,
  - an annual cycle,
  - a land-sea contrast,
  - a day-night contrast and/or
  - a cloud free to cloudy contrast in the differences,

- a typical model bias exhibits
  - a land-sea contrast,
  - a spatial structure defined by a typical local climate,
  - a seasonal structure,
  - a cloud free to cloudy contrast and/or
  - a model domain boundary symmetry.

However, the land-sea contrast, the annual cycle, the daily cycle and/or the cloud free to cloudy contrast may have its origin in both, the SAF data bias and/or a model deficiency. As additional informations the model evaluation results obtained from comparisons with ground station observation products are taken into account. Furthermore, the inter comparison between the results for variables, which have a direct physical relation, like e.g. the albedo the incoming and the outgoing short-wave radiation at the surface is considered.
All discussions and analyses presented in this study are restricted to a previously selected set of parameters, regions, and time periods. The conclusions drawn in this report for a certain parameter in a specific region cannot generally be assigned to other parameters, regions and model configurations. Additionally to the results presented in this report the annual cycles for the other regions are provided as a supplement.

In the following the main results of this first study are summarized.

Two model simulations have been conducted with different initial conditions for the soil variables temperature and soil moisture. The internal model variability due to this difference appeared to be of minor importance in comparison with the stated accuracy of the SAF products. It increases slightly the total accuracy and will not be discussed in the follwing (see the discussion of each variable for details). One year data over Europe appeared to be sufficient for identification of different patterns of significant differences and to make suggestions on its possible origins like model deficiencies and/or SAF-data bias exceeding the stated accuracy.

In the following the main hypotheses derived from the results are listed.

- Boundary conditions inconsistent with cloud conditions in the model causing:
  - Negative differences of CLCT in the boundary shown in 24.
  - negative differences of ASWU_T shown in 8,
  - positive differences of ASWG_S shown in 36,
  - positive differences of ASOB_S shown in 49,
  - negative differences of ATHB_S shown in 60.
- Overestimation of CLCT in the model over central to northern Europe of up to 0.3 in summer in Scandinavia causing:
  - Positive differences of ASOU_T shown in 9

  - Positive differences in ATHB_T shown in 17
  - Negative differences of ASWG_S shown in 37
  - Negative differences of ASWDIFU_S in summer shown in 45
  - Negative differences of ASOB_S shown in 49
  - Positive differences of ALWD_S in SCA shown in 53

- Overestimation of formation of clouds over land in the model or bias over land in CMSAF data causing
  - negative differences of TQV over land shown in 32
  - Neutral to positive differences in CLCT shown in 25
  - CLCT and TQV show a weak negative correlation in winter (33 and 25 Jan.) and weak positive correlation in summer (33 and 25 Jul..)

- Overestimation of deep convection in the model over land in summer or overestimated North-South gradient in CMSAF data causing
  - positive differences of HTOP_CON in summer shown in 29 and 31,

- Underestimation of formation of clouds in the model over water or CMSAF data bias over water surfaces
  - negative CLCT shown in 24 and 26
  - negative differences (downward positive!) and weaker land-sea contrast in SAF120, especially in winter in ToA LW net shown in 16 and 18
  - negative differences in ALWD_S shown in 52 and 55 especially in late winter to early spring.
  - negative differences in ATHB_S over WAS and Italy shown in 60
  - negative TOT_PREC shown in 75

- Overestimation of the model surface albedo in regions covered by snow causing:
  - Positive albedo values over ALP and SCA in winter and spring shown in 41
  - Positive ASWDIFU_S over ALP and SCA in late winter shown in 45

- Inconsistency of 2m temperature of the model and of the outgoing LW radiation in CMSAF indicating a bias in the GME analysis used in the SAF product.
  - negative differences in the 2m temperature shown in 68 and 69 all over the year and
  - neutral to positive (in SUE and POE in spring and autumn) differences of ALWU_S shown in 53

- Additional summer cold bias of GME008 configuration causing

  - negative differences in central and northern Europe in summer in T_2M shown in 69
  - negative differences in central and northern Europe in summer in ALWU_S shown in 57
  - no differences in central and northern Europe in summer in ALWD_S shown in 53
  - positive differences in central and northern Europe in summer in ATHB_S shown in 53
- Weaker variability on regional scale in CCLM in
  - monthly and annual means of ALB_RAD in 40 and 41
  - monthly and annual means of surface up SW in 44 and 45
- CMSAF data bias:
  - higher north-south gradient in SIS than in ASOG_S in January shown in 37
  - stronger land-sea contrast in CMSAF data CLC (24 and 25)
  - strong land-sea contrast in SDL shown in 52

The results show that the availability of independent SAF products for complementary variables allows to identify different space-time patterns of differences and to draw up hypotheses on its possible origins. However, the typical SAF product time scale of 1 or 2 years appears to be a limiting factor of the analysis. In this sense the results confirm the potential of the CMSAF data for model evaluation and the analysis of the quality of the CMSAF data. The availability of many variables can not replace the limited length of the time serieses.
From physical point of view the cloud cover and the atmospheric content of water vapour, liquid and ice water in dependence on the height appear as the primary variables and it is suggested to focus in the future on these variables and on the consistency of the results obtained for these variables with the results for the radiation components.

Assuming the accuracy stated for each SAF variable the provided SAF data are of satisfying quality for state of the art climate model evaluation. The SAF product accuracy values are substantially larger than the internal model variability and they are in many regions and seasons smaller than the differences between model results and SAF data.
Assuming the accuracy stated as not certain, most of the difference patterns can be attributed to SAF product bias or to a model deficiency. Additional investigations are necessary to find the right answers. In this sense this report exhibits the potential of the method and invites to make additional contributions.

Substantial progress can be expected from the analysis of the vertical structure, daily cycle and cloud free/cloudy states focussing on the cloud properties and related variables. Furthermore, a specification of the SAF accuracy limits in space and time and the extension of the time serieses are important for clarification of the applicability of the SAF products for model evaluation.

Acknowledgement

The work was funded by CM-SAF and the BMBF. The simulations were run on NEC SX-6 machines of the DKRZ (German Climate Computing Centre). We are grateful for support from the staffs. The support from the CM-SAF group at DWD Offenbach is much appreciated and the discussions with K.Keuler and E.Schaller as well. A lot of technical work on the COSMO-CLM model system was done in close cooperation with Ulrich Schättler (DWD) and the CLM Community members, in particular H.-J.Panitz (IMK-TRO). H.D.Hollweg (Model and Data Hamburg) provided the template of this report.

We also acknowledge the GME analysis data provided by the DWD-Offenbach, the E-OBS (ECAD) dataset from the EU-FP6 project ENSEMBLES (www.ensembles-eu.org) and the data providers in the ECA&D project (www.eca.knmi.nl) and the GPCC data available from WDC for Meteorology, Ashville.

References

[*Adler et al.*(2003)] Adler, R., et al., The version-2 global precipitation climatology project (GPCP) monthly precipitation analysis (1979-present), *4*, 1147–1167, 2003.

[*Doms and Schättler*(2002)] Doms, G., and U. Schättler, A Description of the nonhydrostatic regional model LM, Part I: Dynamics and Numerics, LM_F90 2.18, *Tech. rep.*, Deutscher Wetterdienst, P.O. Box 100465, 63004 Offenbach, Germany, 2002.

[*Doms et al.*(2005)] Doms, G., J. Förstner, E. Heise, H.-J. Herzog, M. Raschendorfer, R. Schrodin, T. Reinhardt, and G. Vogel, A Description of the nonhydrostatic regional model LM, Part II: Physical Parameterization, LM_F90 3.16, *Tech. rep.*, Deutscher Wetterdienst, P.O. Box 100465, 63004 Offenbach, Germany, 2005.

[*Haylock et al.*(2008)] Haylock, M. R., N. Hofstra, A. M. G. K. Tank, E. J. Klok, P. D. Jones, and M. New, A European daily high-resolution gridded data set of surface temperature and precipitation for 1950-2006, *Journal of Geophysical Research*, *113*, 2008.

[*Heise*(2002)] Heise, E., Parametrisierungen, *Promet*, *3/4*, 130–141, 2002.

[*Helmert et al.*(2008)] Helmert, J., A. Will, M. Raschendorfer, B. Ritter, and J.-P. Schulz, The extended land surface scheme TERRA of the COSMO model for operational numerical weather prediction and regional climate applications, *Meteorologische Zeitschrift, submitted*, 2008.

[*Hollweg et al.*(2008)] Hollweg, H.-D., et al., Ensemble simulations over europe with the regional climate model clm forced with ipcc ar4 global scenarios, *Technical Report 3*, Model and Data Group at the Max Planck Institute for Meteorology, Hamburg., 2008, iSSN printed: 1619-2249, ISSN electronic: 1619-2257.

[*Karlsson et al.*(2008)] Karlsson, K., U. Willen, C. Jonses, and K. Wyser, Evaluation of regional cloud climate simulations over scandinavia using a 10-year noaa advanced very high resolution radiometer cloud climatology, *Journal of Geophysical Research*, *113*, DO1203, 2008.

[*Legutke et al.*(2007)] Legutke, S., I. Fast, and V. Gayler, The prism standard compile environment, *PRISM Report Series 4*, Model and Data, MPI-M Hamburg, 2007.

[*Satellite Application Facility on Climate Monitoring*(2008)] Satellite Application Facility on Climate Monitoring, CDOP Service Specifications, *Tech. Rep. SAF/CM/DWD/SeSp/1.3*, CM-SAF, 2008.

[*Schättler*(2008)] Schättler, U., A Description of the nonhydrostatic regional COSMO-Model, Part V: Preprocessing: Initial and Boundary Data for the COSMO-Model, *Tech. rep.*, Deutscher Wetterdienst, P.O. Box 100465, 63004 Offenbach, Germany, 2008.

[*Schättler et al.*(2008)] Schättler, U., G. Doms, and C. Schraff, A Description of the nonhydrostatic regional COSMO-Model, Part VII: User's Guide, COSMO-Model 4.2, *Tech. rep.*, Deutscher Wetterdienst, P.O. Box 100465, 63004 Offenbach, Germany, 2008.

[*Smerdon and Stieglitz*(2006)] Smerdon, J. E., and M. Stieglitz, Simulating heat transport of harmonic temperature signals in the earth´s shallow subsurface: Lower-boundary sensitivities, *Geophysical Research Letters*, *33*, L14,402,1–6, 2006.

[*Will et al.*(2008)] Will, A., M. Baldauf, and A. Seifert, Physics and Dynamics of the COSMO-CLM, *Meteorologische Zeitschrift*, *submitted*, 2008.